The effects of Ethanol and *Aspalathus linearis* on immortalized mouse brain endothelial cells (bEnd5).

Kelly Angelique Thomas

A thesis submitted in partial fulfilment of the requirements for the degree of Magister Scientiae, in the Department of Medical Biosciences, University of the Western Cape.

Supervisor: Prof David Fisher

Co-supervisor: Dr Kareemah Gamieldien

September 2015

Declaration

I, **Kelly Angelique Thomas**, declare that ***The effects of Ethanol and Aspalathus linearis on immortalized mouse brain endothelial cells (bEnd5)*** is my own work, that it has not been submitted before for any degree or assessment in any university, and that all the sources that I have used or quoted have been indicated and acknowledged by means of complete references.

_____ _____

K. A. Thomas Date:

Acknowledgments

I would like to start off by thanking God for granting me the opportunity to complete my MSc degree.

I express my sincerest gratitude to my supervisor, Prof David Fisher, for granting me the opportunity to work with him, Dr Kareemah Gamieldien for assisting me academically and always motivating me, Dr Franscious Cummings from the electron microscope unit for providing assistance, and the National Research Foundation for funding me.

I wish to extend my sincerest gratitude to Mr F. Rautenbach and Prof J Marnewick, from the Oxidative Stress Research Centre at the Cape Peninsula University of Technology (CPUT) for analysing and providing us with the relevant information and data pertaining to the chemical analyses of fermented rooibos, allowing for the necessary understanding of the 20% extract, and its interaction with our BBB model.

To my neurobiology colleagues, Tarryn Prinsloo and Shireen Mentor, and the greater department of Medical Biosciences, thank you for the support.

To my mother, I am in awe of everything you did and still do for me. You have been my rock and pillar of strength, and I dedicate this manuscript to you. My sister, Vanessa for always encouraging me to do and be my best, no words can describe just how thankful I am to you. To the rest of my family and friends, thank you for your patience and supporting me through this academic chapter of my life. Finally, to my late father, Anthony Thomas, you might not be here to witness my great accomplishment, but thank you for the time I did get to spend with you, and raising me to be the person I am today.

Abstract

The blood brain barrier (BBB) is a signaling interface between the blood and the central nervous system (CNS), which prohibits the entry of harmful blood-borne substances into the brain micro-environment, thus maintaining brain homeostasis. The crucial role of the BBB is protecting the CNS, which may adversely be affected by alcohol. The central component of the BBB, endothelial cells (ECs), regulates BBB transport by regulating the permeability both transcellularly and through their paracellular junctions, by structures called tight junctions (TJs) that are composed of proteins. The aim of this study was to investigate the *in vitro* effects of ethanol (EtOH) and fermented rooibos (R_f) on a monolayer of bEnd5 mouse brain ECs, by determining the effects of EtOH and R_f on bEnd5 (i) cell viability (ii) cell proliferation (iii) rate of cell division (iv) cell toxicity (v) claudin-5 transcription (vi) permeability across a monolayer of bEnd5 ECs and (vii) morphology, for a selected experimental timeline of 24, 48, 72, and 96hrs. We then investigated if the simultaneous exposure of R_f and EtOH could reverse or alleviate the EtOH-induced effects on the bEnd5 ECs.

EtOH metabolism induces oxidative stress and results in a range of adverse physiological effects. *Aspathalus linearis* (rooibos) contains many phenolic compounds, of which the main antioxidant activity is attributed to aspalathin. Our underlining hypothesis is that the antioxidants in an aqueous rooibos extract may therefore protect against the potential oxidant damaging effects of alcohol on the BBB. Cells were exposed for 24hrs to selected concentrations of EtOH (25mM and 100mM), a concentration of R_f containing equivalent of 1.9nM aspalathin, and the combinations of EtOH and R_f. Cell viability and cell toxicity was determined, while cell proliferation and rate of cell division was estimated using the trypan blue exclusion assay. Real time quantitative PCR was implemented to quantify claudin-5 transcription, normalized against housekeeping genes, GAPDH and HPRT. Transepithelial electrical resistance (TEER) was measured using the Ohm Millicell-electrical resistance system, while bEnd5 monolayer morphology was analysed using the Zeiss scanning electron microscope.

Both concentrations of EtOH led to an overall decrease in cell viability, and a decreased number of live cells across 72hrs. Consistent with this, EtOH resulted in increased cell toxicity across the 96hr experimental timeframe and a diminished rate of cell division. The transcription of claudin-5 in bEnd5 ECs exposed to 25mM and 100mM EtOH varied dramatically across the 96hr timeframe. While 25mM EtOH resulted in an overall decrease in TEER, cells exposed to 100mM EtOH only decreased TEER between 48 and 96hrs. Morphologically, both concentrations of EtOH led to compromised paracellular spaces as endorsed by high definition SEM analysis.

The administration of Rf on its own resulted in an initial decrease in viability, followed by recovery between 72 and 96hrs. Exposure to Rf diminished live cell numbers at 72 and 96hrs, accompanied by a compromised rate of cell division and an overall increase in cell toxicity. In addition, R_f down-regulated claudin-5 transcription across the course of the experiment, particularly between 24 and 48hrs. In alignment with this, Rf also led to an increase in BBB permeability from 24 to 96hrs. However, SEM studies were not able to discriminate any differences between control and Rf treated cells.

Our study showed that the BBB could be protected against the adverse effects of EtOH, and this at the plasma concentration induced by 500ml's of Rooibos tea. The simultaneous exposure of Rf and EtOH was able to negate the effects of EtOH on cell viability, cell proliferation, and cell toxicity but exacerbated the effects of EtOH on claudin-5 transcription and paracellular permeability. Morphologically, co-exposure with Rf only reversed the effects of 25mM EtOH while exacerbating the effects of 100mM EtOH at 96hrs.

In conclusion, EtOH was shown to be detrimental to the integrity of bEnd5 ECs, and the addition of a minuscule quantity of the Rf extract was able to partially alleviate excess ROS-induced effects.

September 2015

THE EFFECTS OF ETHANOL AND *ASPALATHUS LINEARIS* ON IMMORTALIZED MOUSE BRAIN ENDOTHELIAL CELLS (bEnd5)

Kelly Angelique Thomas

KEYWORDS

Blood-Brain Barrier

Ethanol

Rooibos

Aspalathin

Claudin-5

Transepithelial electrical resistance

Scanning electron microscopy

Paracellular spaces

mRNA transcription

bEnd5 mouse brain endothelial cells

List of abbreviations

A

AA	acetaldehyde
AAE	ascorbic acid equivalents
AAPH	2,2'-Azobis (2-methylpropionamidine)
ABTS	2,2'-azino-di-3-ethylbenzthialozine sulphonate
ADH	alcohol dehydrogenase
AJ	adherens junction
ALDH	aldehyde dehydrogenase
ANS	autonomic nervous system
ATCC	American tissue culture collection
ATP	adenosine triphosphate

B

BAC	blood alcohol concentration
BBB	blood brain barrier
BRB	blood retinal barrier
BBMvEC	bovine brain microvascular endothelial cell
BEC	brain endothelial cell
bEnd5	mouse brain endothelial cell
BM	basement membrane
BMVEC	brain microvascular endothelial cell
BRCP	breast cancer resistance protein

C

$C_2OH_{10}Na_2O_5$	fluorescein sodium salt
Ca^{2+}	calcium
CAM	cell adhesion molecules
cAMP	cyclic AMP
CAT	catalase
CE	catechin equivalents
CGA	chlorogenic acid

CNS	central nervous system
CO_2	carbon dioxide
CPD	critical point dryer

D

DA	dopamine
DALYs	disability adjusted life years
dH_2O	distilled water
ddH_2O	double distilled water
DMACA	4-dimethylaminocinnamaldehyde
DMEM	Dulbecco's Modified Eagle Medium
DNA	deoxyribonucleic acid

E

EC	endothelial cell
ECACC	European collection for animal cultures
ECIS	electrical cell-substrate impedance sensing
EGCG	epigallocatechin gallate
EM	electron microscopy
ER	endoplasmic reticulum
ERS	electric resistance system
EtOH	Ethanol

F

FACS	fluorescent activated cell sorting
FAD	flavinadenine dinucleotide
FAS	fetal alcohol syndrome
FASD	fetal alcohol spectrum disorders
FBS	fetal bovine serum
FPM	first pass metabolism
FRAP	ferric reducing antioxidant power

G

GABA	gamma-aminobutyric acid
GAE	gallic acid equivalents

GAPDH	glyceraldehyde-3-phosphate dihydrogenase
GC	glucocorticoids
GSH	reduced glutathione
GSSG	oxidized glutathione
GST-a	glutathione-S-transferase
GTP	green tea polyphenols

H

H_2O	water
H_2O_2	hydrogen peroxide
HC	hydrocortisone
HCl	hydrogen chloride
hCMEC/D3	human brain microvascular endothelial cell line
HDL	high density lipoprotein
HIV	human immunodeficiency virus
HPLC	high pressure liquid chromatography
HPRT	hypoxanthine guanine phosphoribosyltransferase
HSA	human serum protein albumin

I

IP_3R	inositol 1,4,5-triphosphate
IV	intravenous

J

JAMs	junctional adhesion molecules

L

LDL	low density lipoprotein

M

MeOH	methanol
MEOS	microsomal ethanol-oxidizing system
MLC	myosin light chain
MLCK	myosin light chain kinase
MMP	matrix metalloproteinase
MRP	multidrug resistance protein

mRNA	messenger RNA
MS	multiple sclerosis
mtGSH	mitochondrial GSH
MV	microvesicle

N

$Na_2HPO_4.{}_2H_2O$	di-sodium hydrogen orthophosphate dehydrate
$NaH_2PO_4.{}_2H_20$	Sodium di-hydrogen orthophosphate-1-hydrate
NAD	nicotinamide adenine dinucleotide
NADH	nicotinamide adenine dinucleotide (reduced)
NADP	nicotinamide adenine dinucleotide phosphate
NADPH	nicotinamide adenine dinucleotide phosphate (reduced)
NEAA	non-essential amino acids
NO	nitric oxide
NOS	nitric oxide synthase
NMDA	N-methyl-D-aspartate
NVU	neurovascular unit

O

O_2	oxygen
ORAC	oxygen radical absorbance capacity

P

PBCEC	porcine brain capillary endothelial cell
PBS	phosphate buffered saline
PCR	polymerase chain reaction
P-gp	P-glycoprotein
PKA	protein kinase A
PKC	protein kinase C
PMBMEC	primary mouse brain microvascular endothelial cell
PNS	peripheral nervous system
PTK	protein tyrosine kinase

Q

QE	quercetin equivalents

R

RBE4	rat brain endothelial cell
RBC	red blood cell
R_f	fermented rooibos
ROS	reactive oxygen species
RNA	ribonucleic acid
RNS	reactive nitrogen species

S

SA	South Africa
SEM	scanning electron microscopy
Ser	serine
SOD	superoxide dismutase

T

TAC	total antioxidant capacity
TAS	total antioxidant status
TEAC	trolox equivalent antioxidant capacity
TEER	transepithelial electrical resistance
Thr	threonine
TJ	tight junction
TPTZ	2,4,6-tri[2-pyridyl]-s-triazine
TE	trolox equivalents

U

UDP-GT	UDP-glucuronosyl transferase

V

VEGF	vascular endothelial growth factor

W

WKS	Wernicke Korsakoff syndrome

Z

ZO zonula occluden

Table of Contents

		Page
Declaration		**i**
Acknowledgments		**ii**
Abstract		**iii**
Keywords		**x**
List of Abbreviations		**xi**
Table of Contents		**xvii**
List of Figures		**xxiii**
List of Tables		**xxvi**
Chapter 1: Literature Review		**1**
1.1	Alcohol	1
1.1.1	Chemistry and statistics of alcohol abuse	1
1.1.2	Socio-economic implications of alcohol	2
1.1.3	Metabolism and bioavailability of alcohol	4
1.1.4	Pathophysiology of alcohol	5
1.1.5	Reactive oxygen species	7
1.1.6	Generic effects of alcohol on the brain	8
1.1.7	Effects of alcohol on neuronal excitations	10
1.2	Blood-Brain Barrier	11
1.2.1	The BBB	11
1.2.2	Morphology of the BBB	14
1.2.3	The BBB paracellular proteins	14
1.2.4	Permeability and pathophysiology of the BBB	16
1.2.5	Effects of Ca^{2+} on BBB permeability	17
1.2.6	Other molecular mechanisms influencing permeability of the BBB	18

1.2.7 The BBB and disease 19
1.2.8 Tight junction proteins: Occludin and Claudin-5 20

1.3 Alcohol and the BBB 22
1.3.1 Mechanisms of alcohol-induced BBB damage 22
1.3.2 The effects of alcohol on the BBB and TJs 24

1.4 Rooibos 25
1.4.1 Flavonoids 25
1.4.2 Rooibos and its antioxidant potential 27
1.4.3 Fermented and unfermented rooibos 30
1.4.4 The physiological effects of rooibos 33
1.4.5 Bioavailability and metabolism of rooibos 35

1.5 Rooibos and the BBB 38
1.5.1 The effects of rooibos on the brain 38

1.6 Model 41
1.6.1 Immortalized mouse brain endothelial cells (bEnd5) 41
1.6.2 Transepithelial electrical resistance on ECs 42
1.6.3 Ultrastructure modifications on ECs investigated with scanning electron microscopy (SEM) 43

1.7 Aims and objectives 45

Chapter 2: Methods & Materials **47**
2.1.1 Experimental model: bEnd5 mouse brain endothelial cells 47
2.1.2 Concentrations of EtOH used in this study 47
2.1.3 Concentration of R_f used in this study 47

2.2 Cell culture 48
2.3 Treatment protocol 48
2.4 Trypan blue exclusion assay 49

2.5 Transcription Analysis 50
2.5.1 RNA extraction of bEnd5 cells 51
2.5.2 Gene amplification optimization 51
2.5.3 cDNA synthesis 52
2.5.4 Gene expression analysis 53

2.6 Transepithelial electrical resistance 54

2.7 Scanning electron microscopy 56
2.7.1 Preparation of the bEnd5 monolayer for SEM 56

2.8 Chemical analysis of fermented rooibos (R_f) 57

2.9 Statistical analysis 58

Chapter 3: Results **59**
3.1.1 Effects of selected concentrations of EtOH on bEnd5 cell viability 59
3.1.2 Effects of a selected concentration of R_f on bEnd5 cell viability 60
3.1.3.1 Effects of R_f on 25mM EtOH exposure on bEnd5 cell viability 61
3.1.3.2 Effects of R_f on 100mM EtOH exposure on bEnd5 cell viability 62
3.1.4 Summary: The effects of EtOH, R_f, and the combinations thereof on bEnd5 cell viability 63

3.2.1 Effects of selected concentrations of EtOH on bEnd5 live cell number 64
3.2.2 Effects of a selected concentration of R_f on bEnd5 live cell number 65
3.2.3 Effects of combinations' exposure on bEnd5 live cell number 66
3.2.4 Summary: The effects of EtOH, Rf, and combinations' exposure on bEnd5 live cell number 67

3.3.1 Effects of selected concentrations of EtOH on the rate of cell division 67
3.3.2 Effects of a selected concentration of R_f on the rate of cell division 69
3.3.3 The combinatorial effects of EtOH and R_f on the rate of cell division 70
3.4.1 Effects of EtOH, R_f, and combinations' exposure on bEnd5 cell toxicity 71

3.5.1 Effects of selected concentrations of EtOH on the relative transcription of paracellular TJ proteins in bEnd5 cells 72
3.5.2 Effects of a selected concentration of R_f on the relative transcription of paracellular TJ proteins in bEnd5 cells 74
3.5.3 Effects of the combinations' exposure on the relative transcription of claudin-5 in bEnd5 cells 75
3.5.4 Summary: Effects of selected concentrations of EtOH, R_f, and the combinations thereof on the relative transcription of paracellular TJ proteins 76

3.6.1 Effects of selected concentrations of EtOH on transepithelial electrical resistance of monolayers of bEnd5 ECs 76
3.6.2 Effects of a selected concentration of R_f on transepithelial electrical resistance of monolayers of bEnd5 ECs 77
3.6.3 Effects of combinations' exposure on transepithelial electrical resistance of monolayers of bEnd5 ECs 78
3.6.4 Summary: The effects of selected concentrations of EtOH, R_f, and the combinations' exposure on transepithelial electrical resistance of monolayers of bEnd5 ECs 79

3.7.1 Confluent monolayer of untreated bEnd5 ECs 81
3.7.2 Ultrastructure of untreated bEnd5 ECs 82
3.7.3 The effects of 25mM EtOH on the ultrastructure of bEnd5 ECs 83
3.7.4 The effects of 100mM EtOH on the ultrastructure of bEnd5 ECs 84
3.7.5 The effects of R_f on the ultrastructure of bEnd5 ECs 85
3.7.6 The effects of R_f on the ultrastructure of bEnd5 ECs at 5000X magnification 86
3.7.7 The simultaneous effects of 25mM EtOH and R_f on the ultrastructure of bEnd5 ECs 87
3.7.8 The simultaneous effects of 100mM EtOH and R_f on the ultrastructure of bEnd5 ECs 88
3.7.9 The simultaneous effects of 100mM EtOH and R_f on the ultrastructure of bEnd5 ECs at 5000X magnification 89

3.7.10 The simultaneous effects of 100mM EtOH and R_f on the ultrastructure of bEnd5 ECs at 10000X magnification 90

3.8 Chemical analysis of R_f 91

Chapter 4: Discussion **94**

4.1.1 Introduction 94

4.1.2 Chemical analysis 95

4.1.3 Rationale: EtOH and R_f concentrations 96

4.1.4 Viability 98

4.1.4.1 The effect of EtOH treatment on cell viability 98

4.1.4.2 The effect of R_f treatment on cell viability 99

4.1.4.3 The effect of EtOH and R_f treatment on cell viability 99

4.1.5 Cell proliferation 100

4.1.5.1 The effect of EtOH treatment on cell proliferation 100

4.1.5.2 The effect of R_f treatment on cell proliferation 101

4.1.5.3 The effect of EtOH and Rf treatment on cell proliferation 101

4.1.6 Cell toxicity 102

4.1.6.1 The effect of EtOH treatment on cell toxicity 102

4.1.6.2 The effect of R_f treatment on cell toxicity 103

4.1.6.3 The effect of EtOH and R_f treatment on cell toxicity 103

4.1.7 Transcription 103

4.1.7.1 The effect of EtOH treatment on claudin-5 transcription 103

4.1.7.2 The effect of R_f treatment on claudin-5 transcription 104

4.1.7.3 The effect of EtOH and R_f treatment on claudin-5 transcription 104

4.1.8 Permeability 105

4.1.8.1 The effect of EtOH treatment on bEnd5 permeability 105

4.1.8.2 The effect of R_f treatment on bEnd5 permeability 106
4.1.8.3 The effect of EtOH and R_f treatment on bEnd5 permeability 106

4.1.9 Morphology of a monolayer of bEnd5 cells 107
4.1.9.1 Cultural monolayers 107
4.1.9.2 The effect of EtOH treatment on the ultrastructure of bEnd5 cells 108
4.1.9.3 The effect of R_f treatment on the ultrastructure of bEnd5 cells 108
4.1.9.4 The effect of EtOH and R_f treatment on the ultrastructure of bEnd5 cells 108

Chapter 5: Conclusion **110**

References **112**

Appendices **129**

List of Figures

Chapter 1 Page

Figure 1.1: Schematic illustration demonstrating the metabolic pathway of EtOH metabolism. 7

Figure 1.2: Diagram illustrating the relationship between EtOH and ROS. 8

Figure 1.3: Schematic representation of the neurovascular unit (NVU) and the BBB. 12

Figure 1.4: Schematic illustration of the junctional molecules in the BBB. 16

Figure 1.5: Schematic illustration of the molecular arrangement of paracellular space proteins between adjacent ECs. 22

Figure 1.6: Structures of the different classes of flavonoids. 26

Figure 1.7: Flavonoids present in rooibos tea. 32

Chapter 2 Page

Figure 2.1: A schematic diagram of the bicameral chamber for TEER analysis of a bEnd5 monolayer. 55

Figure 2.2: A graphical representation of how critical point drying achieved. 57

Chapter 3 Page

Figure 3.1.1: The effects of EtOH on bEnd5 EC viability as ascertained using the Trypan Blue Assay following a 24hr incubation period. 60

Figure 3.1.2: The effects of R_f on bEnd5 EC viability following a 24hr incubation period. 61

Figure 3.1.3.1: The effects of the simultaneous exposure of 25mM EtOH and R_f on bEnd5 EC viability following 24hr exposure. 62

Figure 3.1.3.2: The effects of 100mM EtOH and R_f on bEnd5 EC viability following 24hr exposure. 63

Figure 3.2.1: The effects of selected concentrations of EtOH on bEnd5 EC live cell number following 24hr exposure. 64

Figure 3.2.2: The effects of a selected concentration of R_f on bEnd5 live cell number following a 24hr incubation period. 65

Figure 3.2.3: The effects of selected concentrations of 25mM and R_f and 100mM and R_f on bEnd5 live cell number following a 24hr incubation period. 66

Figure 3.3.1: The graph represents a regression analysis on the effects of selected concentrations of EtOH on bEnd5 live cell number following 24hr exposure. 68

Figure 3.3.2: The graph represents a regression analysis on the effects of a selected concentration of R_f exposure on bEnd5 live cell number following 24hr exposure. 69

Figure 3.3.3: The graph represents a regression analysis on the effects of selected concentrations of 25mM and R_f and 100mM and R_f on bEnd5 live cell number following a 24hr incubation period. 70

Figure 3.4.1: The graph represents the effects of selected concentrations of EtOH, R_f, and the combinations thereof, respectively on bEnd5 EC toxicity following 24hr exposure. 72

Figure 3.5.1: The graph represents the effects of 25 and 100mM EtOH following 24hr exposure, respectively, on the relative mRNA transcription of claudin-5 after normalization with HPRT and GAPDH. 73

Figure 3.5.2: The graph represents the effects of R_f following 24hr exposure on the relative mRNA transcription of claudin-5 after normalization with HPRT and GAPDH. 74

Figure 3.5.3: The graph represents the effects of 24hr combinations' exposure on the relative mRNA transcription of claudin-5 after normalization with HPRT and GAPDH. 75

Figure 3.6.1: The graph represents the effects of 25mM and 100mM EtOH, respectively, on TEER following a 24hr exposure. 77

Figure 3.6.2: The graph represents the effects of R_f on TEER following 24hr exposure. 78

Figure 3.6.3: The graph represents the effects of 25mM EtOH and R_f, and 100mM EtOH and R_f, respectively, on TEER following 24hr exposure. 79

Figure 3.7.1: Ultrastructure of a monolayer of confluent bEnd5 cells at 1000X magnification (96hrs representation). 81

Figure 3.7.2: Ultrastructure of untreated bEnd5 cells at 10000X magnification. 82

Figure 3.7.3: Ultrastructure of bEnd5 ECs exposed to 25mM EtOH at 1000X magnification. 83

Figure 3.7.4: Ultrastructure of bEnd5 ECs exposed to 100mM EtOH at 1000X magnification. 84

Figure 3.7.5: Ultrastructure of bEnd5 ECs exposed to R_f at 1000X magnification. 85

Figure 3.7.6: Ultrastructure of bEnd5 ECs exposed to R_f at 5000X magnification. 86

Figure 3.7.7: Ultrastructure of bEnd5 ECs exposed to 25mM EtOH and R_f at 1000X magnification. 87

Figure 3.7.8: Ultrastructure of bEnd5 ECs exposed to 100mM EtOH and R_f at 1000X magnification. 88

Figure 3.7.9: Ultrastructure of bEnd5 ECs exposed to 100mM EtOH and R_f at 5000X magnification. 89

Figure 3.7.10: Ultrastructure of bEnd5 ECs exposed to 100mM EtOH and R_f at 10000X magnification. 90

Figure 3.8: Illustration of HPLC (High Pressure Liquid Chromatography) results illustrating polyphenols present in an R_f sample. 92

List of Tables

Chapter 2 Page

Table 1: qPCR amplification efficiency for target genes. 52

Table 2: cDNA synthesis cycling parameters. 53

Table 3: qPCR cycling parameters. 53

Chapter 3 Page

Table 4: The effects of selected concentrations of EtOH on the rate of cell division. 68

Table 5: The effects of a selected concentration of R_f on the rate of cell division. 69

Table 6: The effects of combinations' exposure on the rate of cell division. 70

Table 7: Chemical analysis of R_f sample. 91

CHAPTER ONE

Literature Review

1.1 Alcohol

1.1.1 Chemistry and statistics of alcohol abuse

Alcoholic drinks are generally either classified as beer, wine, or spirits. They may comprise of volatile and non-volatile flavour compounds. Volatile compounds may include aliphatic carbonyl compounds, alcohols, monocarboxylic acids and their esters, nitrogen- and sulphur-containing compounds, hydrocarbons, and heterocyclic and aromatic compounds; whereas non-volatile would refer to the alcoholic beverages containing unfermented sugars, di- and tribasic carboxylic acids, colouring substances, tannic and polyphenolic compounds, as well as inorganic salts (Anon, 1988). Ethanol (EtOH) which is grain alcohol is a clear, transparent liquid with a characteristic smell. It is produced by fermenting carbohydrates with yeast. EtOH, CH_3CH_2OH, forms part of a group of chemical compounds in which the molecules consist of a hydroxyl group that is bonded to a carbon atom. EtOH has a melting point of -114.1^{o}C and a boiling point of 78.5^{o}C. Acetaldehyde (AA), which is a by-product of EtOH metabolism, constitutes greater than 90% of the overall aldehyde content in wines (WHO, 2011).

Alcohol has been a social beverage for centuries. The distillation of alcohol began in the Far East and moved to Europe more than a thousand years ago (Anon, 1988). Alcohol serves various functions in humans, such as satiate thirst, or in some countries it is perceived more hygienic than the local water present. It has also been employed medicinally in some cultures and may be used in pharmaceutical preparations (Anon, 1988; WHO, 2011).

Consequences of alcohol consumption pose a severe health risk globally, with an approximate 3.8% mortality rate and 4.6% of disability-adjusted life-years

(DALYs). In particular, excessive alcohol use poses a daunting threat to the age-groups 15 - 29 years, with 9% of deaths in this age group (WHO, 2011). This occurs since alcohol is generally more acceptable in society when compared to methamphetamine or other drugs and is commonly abused by all age groups.

In South Africa (SA), alcohol-induced diseases are thought to account for 7.1% of all deaths and 7% of DALYs. Furthermore, due to alcohol abuse, 44.6% resulted in alcohol use disorders, 23.2% in interpersonal violence, and 18.1% in fetal alcohol syndrome (FAS). Studies show that in the Western Cape, a province in SA (2002-2004), alcohol was the most widely abused narcotic. The Western Cape also has the most frequent occurrence of risky drinking (16%), and a staggering prevalence of fetal alcohol spectrum disorders (FASD) in the world with 75/1000 children suffering from FASD. However, despite worrisome statistics illustrating the detrimental effects of alcohol, it remains the substance most widely used by South Africans (38.7%) (Van Heerden et al., 2009).

1.1.2 Socio-economic implications of alcohol

Alcohol is the one of the most common and widely used drugs worldwide (Boé et al., 2009) accounting for approximately 100,000 deaths each year (Abdul Muneer et al., 2011). An average of two glasses of alcohol or more per day is suggested to induce harmful effects on one's health, including those associated with increased mortality (Boé et al., 2009). Alcohol is also implicated as being an economic burden. It contributes to the harmful effects on patient outcomes, such as increased occurrence of ICU admission, prolonged hospital stay, augmented sepsis, as well as a greater necessity for mechanical ventilation (Boé et al., 2009). Peripheral nervous system (PNS) and central nervous system (CNS) toxicity is commonly caused by EtOH consumption. In the US, alcohol dependence affects more than 14% of its population and is one of the leading causes of dementia with more than half of sober, detoxified former alcoholics having cognitive impairments. In India

the stats show that alcohol-related dementia is 3.3% more than malnutrition-related dementia and 5.7% more than Alzheimer's disease (Tiwari et al., 2009).

Generally, people react differently to alcohol, especially since the neurobiological mechanisms underlying these are not the ones causing addiction. The term alcoholism or alcohol dependence refers to the chronic relapsing course and the subsequent occurrence of a constant negative state when access to alcohol is prevented (Koob, 2013; Sommer and Spanagel, 2013). Relapse occurs due to potent impulses and cravings which in turn initiate changes in behaviour (Tiffany et al., 2000; Sommer and Spanagel, 2013). The maximum legal limit for EtOH-induced inebriation in several countries is 0.05% or 11mM EtOH in the blood, while 100mM EtOH is regarded as the deadening concentration in humans (Sommer and Spanagel, 2013). Most people consume alcohol to perceive feelings of relaxation and delight, in addition to relieving stress or anxiety. However, there is variation among different persons in response to alcohol, such as the respective person's alcohol history, conditions of ingestion, and general wellbeing (Sommer and Spanagel, 2013). Generally stimulatory or sedating effects tend to occur, which can be experienced simultaneously or alone. Fast increasing blood levels following consumption will be indicative of stimulation whereas sedation will occur steadily during the latter part of the blood alcohol elimination curve. According to Sommer and Spanagel (2013), no definite treatment exists to cure alcohol addiction.

Alcohol is effortlessly obtainable in nearly all communities, and the licensed and unlicensed outlets are prevalent in many areas. The alcohol control legislation differs between provinces and countries (Prevention Symposium, 2008), however, although there is enough legislation to ensure the prevention of alcohol abuse in pregnant woman and children, insufficient strategy is employed (Prevention Symposium, 2008).

The term FASD is used to include the various permanent conditions that arise from exposure to alcohol *in utero*, the most common being FAS. Children with FAS display impairments that are usually associated with brain damage inheriting brain disorders, low intelligence, impaired social judgment, and a general complexity in performing everyday tasks. Infants that are born with FAS have an increased risk of developing mental health problems later in life (Prevention Symposium, 2008).

1.1.3 Metabolism and bioavailability of alcohol

Primary alcohol, EtOH, may be absorbed alongside the whole length of the digestive tract, following oral administration (Manzo-Avalos and Saavedra-Molina, 2010), which happens rapidly from the stomach (20%) and the small gut (80%) (Mallikarjuna et al., 2010). The eradication of absorbed EtOH occurs mostly through metabolism (95-98%), while approximately 0.7% is excreted in the breath, 0.1% in sweat, and 0.3% in urine (Manzo-Avalos and Saavedra-Molina, 2010). The post drinking rate of alcohol absorption is exaggerated by numerous factors such as volume, concentration, the nature of the alcoholic drink, the presence or absence of food in the stomach, rate of gastric emptying, pylorospasms, permeability of the gastric and intestinal tissues and individual variations. Alcohol is immediately distributed throughout the total body water after it gets absorbed into the bloodstream and with effect it gets metabolized at a steady rate (Mallikarjuna et al., 2010).

The liver is the major site for the metabolism of EtOH. Two leading factors that are associated with the decrease in the hepatic antioxidant enzyme activities are ageing and chronic alcohol consumption. Alcohol liver disease is notoriously associated with reduced antioxidant enzyme status. More specifically, chronic EtOH exposure may lead to a decrease in the major antioxidant enzymes in the liver, including superoxide dismutase (SOD), catalase (CAT), as well as glutathione family enzymes (Mallikarjuna et al., 2010). It is proposed that the rate-limiting step in the metabolism of alcohol is its switch to AA, a reaction that is catalyzed through the zinc-containing

enzyme, alcohol dehydrogenase (ADH). Factors influencing the rate of metabolism include the B vitamins, nicotinamide and riboflavin, which assist in the metabolism of alcohol, and vitamin C and E, which may be implicated in the oxidation-reduction reactions (Pawan, 1972). In alcoholics, EtOH may also be oxidized by means of the peroxidase-xanthine oxidase-catalase system. Small quantities of alcohol may also be converted to ethyl glucuronide, ethyl sulphate and other esters that are generally released in the urine. Other tissues such as the kidney, muscle, lung, intestine, and most likely even the brain may metabolize smaller quantities (Pawan, 1972).

Studies have showed that females have greater EtOH serum concentrations following oral administration than males, which may most likely be attributed to the enhanced activity of gastric ADH in males and the subsequent higher first-pass metabolism (FPM) of EtOH. It has been established that this increased activity of ADH and FPM was significantly reduced in non-alcoholic men by approximately 50% (Cobaugh et al., 1999). FPM of alcohol is validated by reduced blood alcohol concentrations (BAC) following oral administration of the same dose of alcohol than that of intravenous (IV) administration. FPM takes place mainly in the stomach, and has been attributed to the activity of ADH in the gastric mucosa (Sharma et al., 1995). In addition, there is no variation in the bioavailability of EtOH following oral or IV administration (Cobaugh et al., 1999), since the quantity of alcohol reaching the systemic circulation is similar in both oral and IV administration (Sharma et al., 1995). Furthermore, it has been established that the precise time of day is not a major aspect in the FPM of alcohol (Sharma et al., 1995).

1.1.4 Pathophysiology of alcohol

The mitochondrion, a membrane-enclosed organelle established in eukaryotic cells, which generates most of the cells adenosine triphosphate (ATP), serves a key role in alcohol metabolism via the enzyme, aldehyde dehydrogenase (ALDH), which catalyzes the conversion of AA into acetate, and

simultaneously produces large quantities of nicotinamide adenine dinucleotide (NADH) (Manzo-Avalos and Saavedra-Molina, 2010).

In individuals who drink moderate amounts of alcohol, EtOH is oxidized to AA, in a rescindable reaction, catalyzed by class I ADH. However, this enzyme becomes saturated following a few drinks. The AA becomes subsequently oxidized to acetate through the mitochondrial isoform of ALDH. Acetyl CoA, which is the actuated form of acetate, could be further metabolized, contributing to the formation of amino acids, ketone bodies, steroids, and fatty acids. When oxidized in the Krebs cycle, carbon dioxide (CO_2) and water (H_2O) result as the final products of EtOH oxidation. Once AA accumulates, it enters the blood stream and results in the damage of plasma based lipids, proteins, and nucleic acids, causing the harsh effects experienced with alcohol consumption (Manzo-Avalos and Saavedra-Molina, 2010). In chronic alcohol drinkers, the microsomal ethanol-oxidizing system (MEOS), which serves a role in the smooth endoplasmic reticulum (ER) of hepatocytes, contributes to the removal of noxious compounds through cytochrome P450 (CYP2E1), by converting alcohol to AA. Nicotinamide adenine dinucleotide phosphate (NADP) and H_20 is then also subsequently formed in the reaction from oxygen and reduced nicotinamide adenine dinucleotide phosphate (NADPH) (Manzo-Avalos and Saavedra-Molina, 2010).

A large amount of acetate ensuing from alcohol metabolism leaves the liver and enters the blood, and ultimately gets metabolized to CO_2 in the heart, skeletal muscle and brain cells. Acetate also diminishes the integrity of the CNS. It is been suggested that instead of using glucose as a source of energy, the brain utilizes acetate following chronic alcohol consumption, resulting in the inhibition of mitochondrial functions which is caused by an AA build-up. Several studies have showed that the mitochondrial levels of reactive oxygen species (ROS) have been exacerbated following chronic alcohol intake, which may be due to the increased CYP2E1 levels (Manzo-Avalos and Saavedra-Molina, 2010). CYP2E1 belongs to the cytochrome P450

superfamily (Sameer et al., 2011), and its activity increases in both moderate and excessive alcohol consumers (Manzo-Avalos and Saavedra-Molina, 2010). It is an important enzyme involved in the metabolism and bioactivation of low molecular weight compounds, especially EtOH and acetone (Sameer et al., 2011).

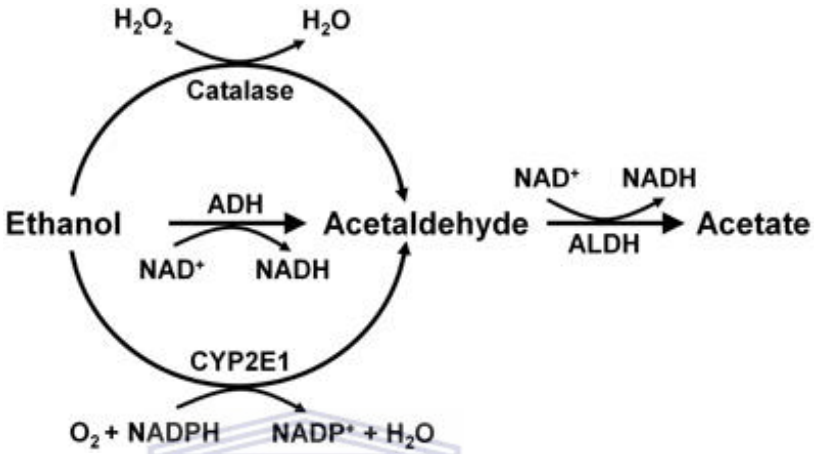

Figure 1.1: Schematic illustration demonstrating the metabolic pathway of EtOH metabolism. Taken from Israel et al (2013).

1.1.5 Reactive oxygen species

ROS are small, extremely reactive, oxygen-containing molecules, naturally produced in minute quantities during metabolic reactions in the body. Alcohol results in excess ROS production which interferes in the body's homeostatic mechanisms. The major site for these processes is the liver. Alcohol stimulates the enzymatic activity of cytochrome P450, which influences ROS production, as well as diminishes the levels of agents such as antioxidants which may reduce ROS (Wu and Cederbaum, 2003). Furthermore, it has been established that EtOH not only increases the production of ROS, but reactive nitrogen species (RNS) also, which may sequentially ensue in mitochondrial dysfunction and decreased energy conservation. Chronic alcohol consumption also decreases mitochondrial GSH (mtGSH), predisposing these organelles to oxidative damage and lipid peroxidation (Manzo-Avalos and Saavedra-Molina, 2010). Alcohol

metabolism produces nitric oxide (NO), along with ROS by induction of NADPH/xanthine oxidase and nitric oxide synthase (NOS) in human neurons adding to oxidative and nitrosative stress.

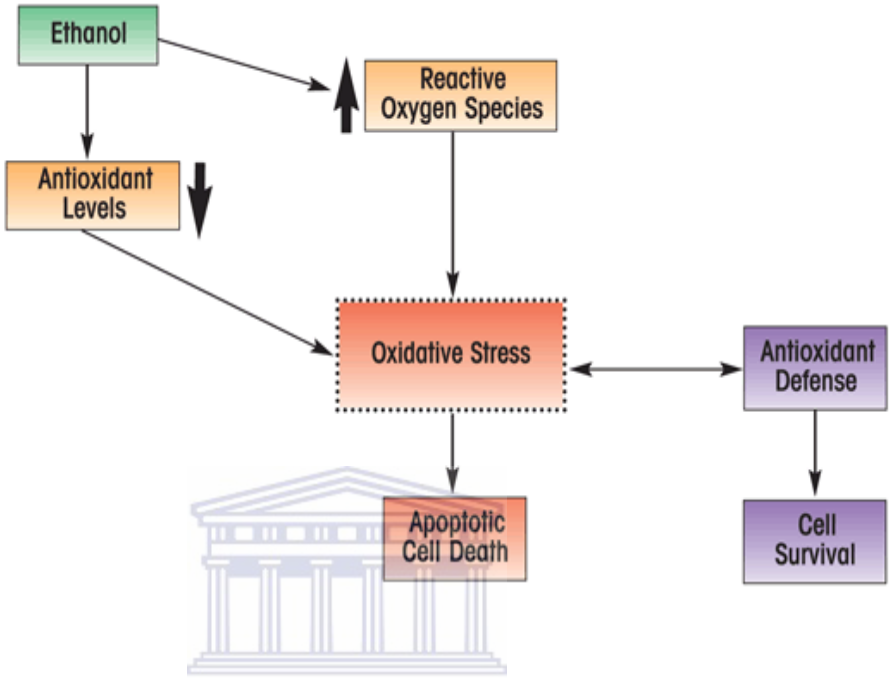

Figure 1.2: Diagram illustrating the relationship between EtOH and ROS.

1.1.6 Generic effects of alcohol on the brain

The effect of alcohol on the brain extends from slight memory loss to permanent conditions that may require lifelong custodial care. Alcohol has various and diverse effects on the brain, which is influenced by a wide range of variables (Parsons, 1996; Oscar-Berman and Marinkovic, 2003), such as the amount of alcohol consumed, the age at which the person started consuming alcohol and the period of alcohol consumption. People that chronically consume alcohol are faced with the risk of developing serious and permanent changes in the brain and its function. Harmful alcohol associated effects include permanent brain tissue injury (Harper and Matsumoto, 2005; Haorah et al., 2008), with neuro-degeneration being a prominent characteristic in brain tissue of chronic alcoholics (Harper, 1998; Haorah et al., 2008). White matter aberrations noted in persons excessively consuming

alcohol (Haorah et al., 2008) may perhaps be correlated with blood-brain barrier (BBB) dysfunction identified in alcoholics (Haorah et al., 2008) as well as in animal models chronically treated with alcohol (Haorah et al., 2008).

Alcohol exposure affects the entire brain and increases the chances of cerebral atrophy. If the limbic system, thalamus or hypothalamus is affected, the person is more vulnerable to Wernicke-Korsakoff syndrome (WKS). The frontal lobe system is more vulnerable to the effects of alcohol and results in more harmful effects as opposed to other brain regions. Several monoaminergic systems (gamma-aminobutyric acid, glutamate, dopamine, acetylcholine and serotonin) are sensitive to the effects of alcohol (Oscar-Berman and Marinkovic, 2003). It has been reported that neurological diseases such as Alzheimer's, Parkinson's, and stroke arise due to mitochondrial oxidative damage (Abdul Muneer et al., 2011), and it is evident that alcohol intake negatively contributes to the mitochondrial oxidative damage (Abdul Muneer et al., 2011) and neuronal degeneration (Haorah et al., 2008; Abdul Muneer et al., 2011). Chronic alcohol exposure may stimulate selective neuronal damage related to an increase in oxidative-nitrosative stress and the activation of an inflammatory cascade which consequently results in neuronal apoptosis and dementia (Tiwari et al., 2009). EtOH-induced selective neuronal damage is not yet been investigated fully, hence various hypothesis has been suggested including excitotoxicity linked to excessive neurotransmitter release, oxidative stress leading to free radical damage and edema resulting from alterations in cellular control of ion transport (Tiwari et al., 2009). Modulation of the pituitary-adrenal and pituitary-gonadal axes as a result of systemic alcohol is mostly arbitrated through its central actions at the level of the hypothalamus (Pruznak et al., 2013). Remarkably, this proves to be consistent as the properties of EtOH includes the aptitude of it to readily diffuse into all body compartments and tissues, and of particular importance here, the CNS (Gill et al., 1986; Pruznak et al., 2013).

Studies focusing on the effects of alcohol on the brain revealed that male and female alcoholics had significantly larger amounts of intracranial cerebrospinal fluid opposed to non-alcohol-drinking people, thus indicating greater brain shrinkage. The CNS of women has proved to be more vulnerable to the effects of alcohol than damage in the CNS of men (Hommer, 2003). Furthermore, alcohol-related brain atrophy is believed to result from the neurotoxic effects of alcohol (Oscar-Berman and Marinkovic, 2003).

1.1.7 Effects of alcohol on neuronal excitations

Alcohol-induced effects on the brain diminish neuronal excitability in different regions and reduce most forms of synaptic plasticity, particularly the establishment of drug memories. Possibly clarifying the reason as to why alcohol addiction is lower than other drugs and why alcohol addiction progresses over a lengthier period of time. However, this is likely to differ between individuals (Sommer and Spanagel, 2013). The interactions of EtOH and the binding of it to its specific proteins varies markedly from the manner in which most other psychoactive drugs interact with their respective neurochemical targets (Sommer and Spanagel, 2013). EtOH binding positions at the ligand-gated ion channels such as glutamate receptors of the N-methyl-D-aspartate (NMDA) type results in increased sensitivity to alcohol responses at these receptors from the mid to low millimolar range; ultimately, signifying significant cellular and synaptic consequences.

In the CNS, excitation and inhibition processes is governed by the synaptic inputs from the chief excitatory and inhibitory neurotransmitters, glutamate and gamma-aminobutyric acid (GABA), respectively. Acute exposure to alcohol stimulates the GABA-ergic neurotransmission, while inhibiting the glutamatergic neurotransmission by precisely acting on neurotransmitter receptors, in addition to intracellular signaling cascades. Moreover, acute exposure to 1-100mM alcohol disturbs both input and output synapses. With regard to chronic exposure, after a certain amount of alcohol, the response

differs as there is a different pharmacological interaction of EtOH with its targets, making it functionally tolerant. In particular, creating anxiolytic, sedative and ataxic effects via the GABA-ergic neurotransmission, while augmenting the function of NMDA receptors (Ron and Messing, 2013; Lovinger and Roberto, 2013; Sommer and Spanagel, 2013). Initially, the subjective effects felt as intoxication signal is set off at the synapses, followed by implications of the various neurotransmitter and neuromodulator systems, such as the monoamines (i.e. dopamine (DA), serotonin, and noradrenalin) (Vengeliene et al., 2008; Sommer and Spanagel, 2013). Following adequate amounts and time, neuroadaptations at both the cellular and synaptic levels are likely to trigger dependence and bring about specific withdrawal symptoms, such as increased extracellular glutamate levels at the NMDA receptors (Sommer and Spanagel, 2013).

1.2 Blood-brain Barrier (BBB)

1.2.1 The BBB

The BBB is an active and complex signaling interface between the blood and the CNS. It prohibits the entry of harmful blood-borne substances into the brain micro-environment (Colgan et al., 2008) and controls the exchanges that take place between the blood and the brain compartments. It plays a pivotal role in brain homeostasis and provides significant protection against numerous toxic compounds and pathogens. In contrast to blood vessels external of the CNS, tight junctions (TJ) which are responsible for closing the endothelial cell layer, are well established in the endothelium of the BBB (Fig 1.3) (Förster et al., 2008). The BBB which is developed by brain capillary endothelial cells (ECs) is indicative of a barrier that demonstrates exceptionally significant epithelial and endothelial properties. The maturation of the BBB is believed to occur following the formation of cerebral microvasculature during early embryonic development, and is functionally existent in early fetal life (Malaeb et al., 2012).

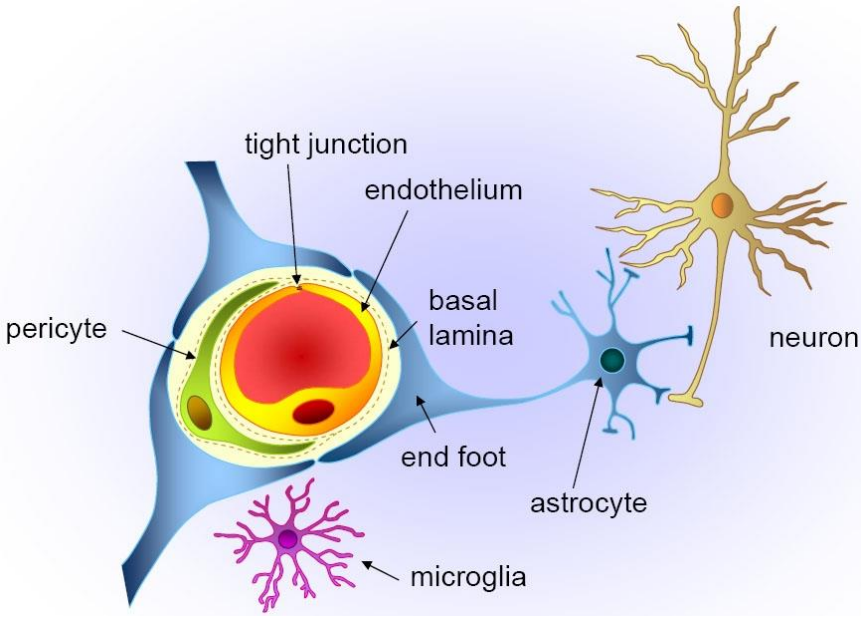

Figure 1.3: Schematic representation of the neurovascular unit (NVU) and BBB. Taken from Abbott et al (2006).

The BBB restricts the bidirectional movement of big molecules, in addition to minute polar particles (Dziegielewska et al., 1979; Malaeb et al., 2012), which traverse the microvascular endothelium of capillaries in the peripheral passage by means of the paracellular or transcellular pathway. However, the paracellular transmission of polar compounds along with electrolytes between neighboring ECs of the BBB is rather restricted by TJs found in paracellular spaces (Malaeb et al., 2012).

The BBB exists in all brain regions, excluding the cirumventricular organs. These include the postrema, median eminence, neurohypophysis, pineal gland, subfornical organ, and lamina terminalis. The reason for this is that the blood vessels in these regions of the brain possess fenestrations which allow for the diffusion of blood-borne substances across the vessel wall. The areas of the brain lacking a barrier are responsible for the regulation of the autonomic nervous system (ANS) and endocrine glands (Ballabh et al., 2004; Cardoso et al., 2010).

The nature of the BBB is formed by the cellular basis of the brain capillary endothelium combined with other cell types of the NVU such as the astrocytes, pericytes and neurons (Fig 1.3) (Yang et al., 2007). The BBB surrounds the pericytes, holding the cells in place and establishes a relation with the surrounding resident brain cells. The involvement of the pericytes to blood vessels has been suggested to normalize the EC proliferation, migration and differentiation, and evidence has been provided that pericytes are involved in the regulation of transport across the BBB (Cardoso et al., 2010). Astrocytes are glial cells which develop extensions commonly referred to as "endfeet", which forms a structure of fine lamellae that are closely contacted with the exterior surface of the basement membrane of the BBB endothelium. The basolateral condition of the brain microvascular endothelium impacts BBB phenotype. The basolateral surface of the blood-brain endothelium *in vivo*, is immersed in serum-free interstitial fluid, covered by astrocytic end feet. *In vivo*, the endothelial BBB is comprised of a luminal plasma membrane, the cytosol, and the abluminal membrane of the EC (Grant et al., 1998). ECs are the most important component of the BBB (Enciu et al., 2013). They are responsible for regulating the release of glucose into the brain and maintaining homeostatic regulation of the brain microenvironment (Lund-Anderson et al., 1976; Abbott, 2002; Abdul Muneer et al., 2011).

Lipophilic solutes can cross the BBB, as a result of their membrane solubility, despite its barrier properties (Schrot et al., 2005). Oxygen (O_2), CO_2, and EtOH diffuse across the endothelium with ease as a result of their lipid soluble properties. Other essential solutes necessary for brain function, such as glucose and amino acids, are transported by aid of carriers specific for them, namely: Glut-1 and L-system carriers, respectively. Transport pathways, for example, transendothelial channels and/ or pinocytotic vesicles are associated with ECs, which are in turn capable of expressing high levels of active efflux transport proteins such as P-glycoprotein (P-gp), Multidrug Resistance Protein (MRP)-1 (MRP-1), and Breast Cancer Resistance Protein (BRCP). Certain molecular compounds with suitable molecular weight, charge, as well as lipophilicity may diffuse from the blood into the CNS

(Gabathuler, 2010). Various compounds associated with opening of the BBB are suggested to emerge as a result of receptor mediated processes, by activating the signal transduction pathways within the endothelium. Augmented intracellular calcium (Ca^{2+}) concentration may possibly be a chief factor in the opening of the TJ's (Abbott, 2002).

1.2.2 Morphology of the BBB

The BBB constitutes brain capillaries, choroid plexus cuboidal epithelium, and the arachnoid membrane. The BBB is distinguished by the presence of TJs, the absence of endothelial pores, and a lack of pinocytic vesicles (Burns et al., 1981). Early studies have showed the absence of a restraining barrier in the pineal body, the neurohypophysis and adjacent ventral portion of the median eminence, the area postrema, and the intercolumnar tubercle (Burns et al., 1981).

In terms of morphology, adaptation of the BBB may occur, apparent by the opening of TJs following hyperosmolar insults, weakening of capillary walls, and increased pinocytosis by noxious compounds. A change in the physiological systems will ensue if the morphological substrates in which they reside undergo alterations. As a result, many substances and compounds will easily diffuse into and out of the CNS (Burns et al., 1981).

1.2.3 The BBB paracellular proteins

The BBB consists of both TJs and adherens junctions (AJs) (Fig 1.4) (Furuse et al., 1999; Ballabh et al., 2004). The BBB elicits homeostatic effects is through its permeability of the EC and the presence of TJs across paracellular spaces. Transport through the paracellular spaces are regulated by TJs that form rows of extensive, coinciding occlusions that inhibit the leakage of blood-borne substances (Grant et al., 1998) and block the intercellular route of solute entry into the CNS (Yang et al., 2007). TJs consist of protein molecules which include the occludins, claudins, cingulins, and the zonula occludens (ZO-1/2/3) family members; all of which are significantly

important for exhibiting barrier properties. TJs function to regulate paracellular diffusion between the lateral plasma membranes of adjacent ECs by acting as a seal, to limit paracellular permeability (Cardoso et al., 2010). Disrupted TJ's could result in the uncontrolled entry of potentially damaging agents and transmit toxic effects to remote sites in the body. Studies have established that intracellular signaling mechanisms which channel cell proliferation, differentiation, as well as the development of polarity are associated with TJ's (Sambuy, 2009). TJs consist of two important processes associated with signal transduction. These involve signals transduced from the inside of the cell outward towards the TJ to regulate paracellular permeability, as well as signals conveyed from the TJ to the cell interior, to control and regulate gene expression, cell proliferation, and differentiation (Matter and Balda, 2003; Ballabh et al., 2004).

AJs are comprised of two fundamental adhesive units, the cadherin/catenin, and nectin/afadin complexes. These complexes have a significant task in stabilizing the epithelium, by promoting TJ development and epithelial cell polarity. However, they do not form a physical fence to macromolecules, but in some way regulate the integrity of TJ's as well as the role of the epithelial barrier (Sambuy, 2009).

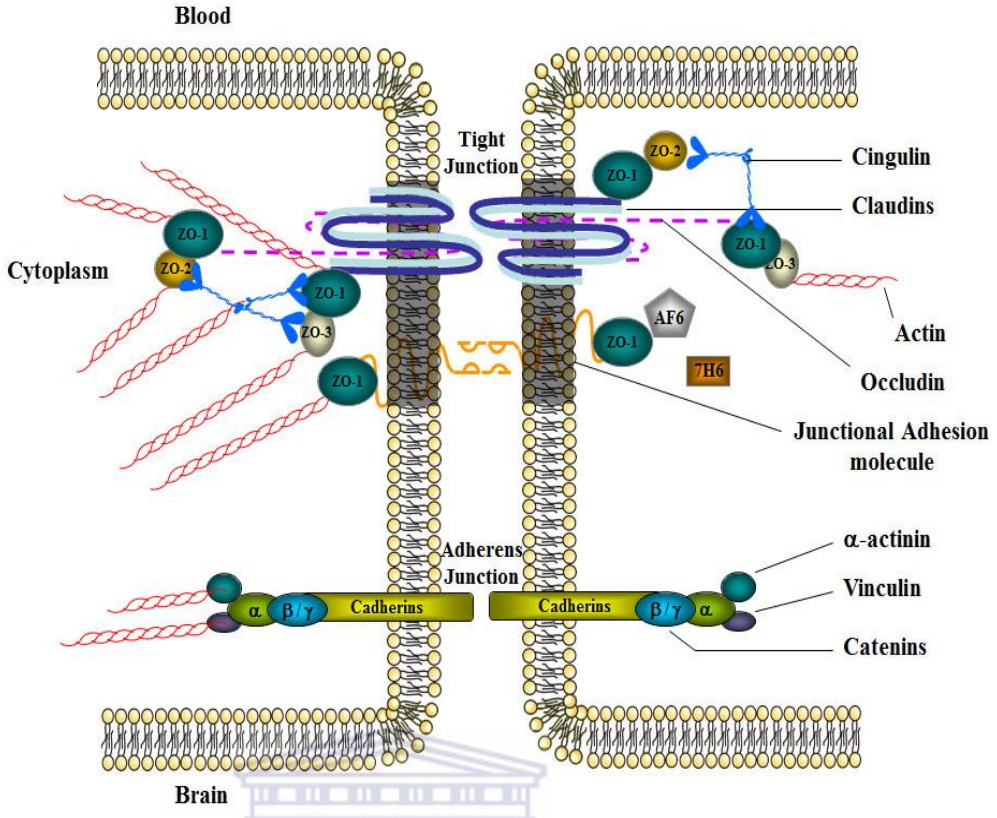

Figure 1.4: Schematic illustration of the junctional molecules in the BBB. (http://www.marshall.edu/bms/2012/08/30/richard-egleton-ph-d/)

1.2.4 Permeability and Pathophysiology of the BBB

ROS contributes to the disruption of the BBB as well as inflammation in the brain by enhancing cellular migration. It affects BBB integrity, causes cytoskeleton rearrangements, in addition to the modifications of claudin-5 and occludin. The carboxyterminal parts of occludin and claudins work together with the membrane-related recruiting proteins of the ZO protein family. The proposed function of the ZO proteins is to connect transmembrane proteins to the actin cytoskeleton and may also be involved in cellular signaling. During its contact with TJ molecules, the actin cytoskeleton plays a significant role in maintaining TJ integrity. Protein tyrosine kinases (PTKs) may possibly be activated in brain endothelial cells (BECs) which could progress to tyrosine phosphorylation of TJ proteins as a result of ROS (Schreibelt et al., 2007). In a previous study it was hypothesized that Rho and other small GTPases influence the expression of

TJ proteins, occludin and claudin-1 in various epithelial models (Enciu et al., 2013).

Studies have shown that a chief mechanism influencing BBB permeability is the ROS-induced redistribution and disappearance of claudin-5 (Schreibelt et al., 2007). The organization of occludin and ZO-1 is transformed by exogenous ROS in epithelial and BECs (Schreibelt et al., 2007). There are several mechanisms used to diffuse across the BBB. Small hydrophilic molecules, essential for the survival of brain cells implement transporters which are expressed at the luminal and basolateral side of the ECs, whereas, larger and/or hydrophilic essential molecules make use of specific receptors which are greatly expressed on the luminal side (Gabathuler, 2010). Some molecules, such as alcohol and nicotine can without restrictions diffuse across the brain. This ability to freely diffuse is governed by the molecular size, charge, and lipophilicity (Pardridge, 1995; Gabathuler, 2010).

Experimentally-generated peripheral inflammation enhances BBB permeability and results in decreased occludin expression (Huber et al., 2001; Enciu et al., 2013) and augmented expression of claudin-3, and -5 (Brooks et al., 2005; Enciu et al., 2013). The extravasation of plasma proteins associated with BBB dysfunction could occur through transcellular or paracellular routes, including TJs, induction of fluid-phase or nonspecific pinocytosis and transcytosis, formation of transendothelial channels, or disruption of the EC membrane (Grant et al., 1998). Efflux transporters, such as P-glycoprotein, are of particular importance as they enhance barrier properties. They do this by restoring the small lipophilic molecules that disseminate into the brain microvascular endothelial cells (BMVECs), back to the bloodstream (Pardridge, 2003; Lippmann et al., 2012).

1.2.5 Effects of Ca^{2+} on BBB permeability

Several signaling pathways and proteins are involved in the regulation of TJ association such as, Ca^{2+}, protein kinase A (PKA), protein kinase C (PKC), G

protein, calmodulin, cyclic AMP (cAMP), and phospholipase C (Ballabh et al., 2004). Ca^{2+} functions both intracellularly and extracellularly to modulate TJ activity. Numerous molecules implicated in regulating BBB permeability appear to act by way of altering intracellular Ca^{2+}.

Intracellular Ca^{2+} increases transepithelial electrical resistance (TEER), and is involved in ZO-1 migration from intracellular sites to plasma membrane, eventually reestablishing the TJ complex (Stevenson and Begg, 1994; Ballabh et al., 2004). An increase in extracellular Ca^{2+} initiates a cascade of molecular events, whereby the resistance across the membrane is increased, followed by a decrease in permeability (Stevenson and Begg, 1994; Ballabh et al., 2004).

Modifications in BBB permeability triggered by rapid changes in extracellular Ca^{2+} occur as consequence of the disruption in the AJ between microvessel ECs. Sequentially, this may cause the disruption of the TJ, by removing the extracellular Ca^{2+}, and possibly also by eliminating the supporting structure of the AJ, which may result in increased permeability due to the tension on the TJ strand (Brown and Davis, 2002).

1.2.6 Other molecular mechanisms influencing permeability of the BBB

Numerous molecular mechanisms are associated with the disruption of TJ's. These include serine/ threonine (Ser/Thr) and tyrosine (Tyr) phosphorylation. Furthermore, the degradation of translocation of proteins is also involved. The RhoA GTPase signaling pathway has been found to induce actin cytoskeleton rearrangements in several cell types and is also associated with cell migration and proliferation. Activated RhoA increased permeability in BECs as recorded by Luissint et al. (2012). This increase in permeability occurred in response to chemokines, such as MCP-1/ CCL2, whereby acting by means of their seven transmembrane domain receptors, are identified to initiate the RhoA pathway in mouse BECs, ultimately inducing occludin, claudin-5 and ZO-1 Ser/Thr-phosphorylation. This is then in due course

followed by increased barrier permeability. Changes in the expression and localization of TJ proteins, following exposure to several pathological stimuli, may be a contributing factor in the disruption of TJ's as well as augmented BBB permeability (Luissint et al., 2012).

1.2.7 The BBB and disease

Disrupted BBB integrity may possibly result in vascular leakage, the chief pathophysiological mechanism of most diseases, such as ischemic injury and stroke (Brown and Davis, 2002; Colgan et al., 2008), multiple sclerosis (MS), meningitis/encephalitis, and neurodegenerative diseases (Colgan et al., 2008).

BBB function may be compromised by toxic agents and pathological conditions through early changes in its function, which are mediated through direct effects on the ECs and associated with morphological changes in astrocytes. Various neurological diseases as a result of BBB degradation has been described as delayed but generally implicated in the early steps of disease progression. Thus injury to the BBB may begin and/or contribute to progressive nerve cell dysfunction in disorders such as Alzheimer's and Parkinson's (Cardoso et al., 2010). In pathological illnesses like this, there is a disturbance in BBB integrity, with interference in ion homeostasis and transporter function (Brown and Davis, 2002).

When signaling from the brain to the periphery, the brain undergoes regular, but restricted immune surveillance, thus the exudation of blood leukocytes into the brain is critical for brain protection. This process is signaled by pro-inflammatory mediators including cytokines, which have the ability to set off ECs at post capillary venules to which countless properties of the BBB extend. Two pathways are available for the transmigration of cells, namely, the paracellular and transcellular pathway. The paracellular pathway occurs through the interendothelial junctions, whereas the transcellular pathway refers to movement through single ECs (Wilhelm et al., 2013).

1.2.8 Tight Junction Proteins: Occludin and Claudin-5

The most important components of TJ strands are the transmembrane proteins, claudin and occludin. Claudins are responsible for the seal formation of the TJs, and regulate the specificity of TJ permeability. Their key function is to regulate the paracellular selectivity to small ions. Occludin functions as an active regulatory protein, and has been assumed to be the physical basis of the TJ barrier, but has since been disputed. However, occludin-deficient mice are viable and exhibit normal barrier function (Findley and Koval, 2009).

The presence of occludin in the membrane is associated with augmented TEER across the membrane and diminished paracellular permeability (Huber et al., 2002), and therefore is imperative for regulating ionic permeability across the paracellular cytoplasmic shunts (Ballabh et al., 2004). Occludin is characteristic of being a 522-amino acid phosphoprotein, determined in humans through the OCLN gene (Furuse et al., 1993; Malaeb et al., 2012). The expression of occludin is greater in BECs in contrast to non-neural tissues (Ballabh et al., 2004). When non-phosphorylated, it serves as a 60 kDa protein in comparison to 65 kDa when phosphorylated. It is a fundamental plasma membrane protein which extends over the plasma membrane four times; creating two extracellular loops with both COOH and NH_2 terminal endings in the cytosol (Furuse et al., 1993; Schreibelt et al., 2007; Malaeb et al., 2012). Occludin may be linked with ZO proteins through its binding domains, thus performing a vital function in regulating TJs (Malaeb et al., 2012). Previous studies reveal that several phosphorylation sites have been recognized on occludin serine and threonine residues, therefore post-translational modifications of this protein involves phosphorylation events (Tong et al., 2013).

Claudins are transmembrane proteins, which measure 20 to 27 kDa, and are genetically encoded for, by a multigene family of 24 distinct affiliates (Furuse and Tsukira, 2006; Malaeb et al., 2012). Claudins, as with occludins

extends over the plasma membrane four times, by which two extracellular loops are established with both NH_2 and COOH terminals in the cytosol. The transmembrane domains interact in both homophilic and heterophilic manners with claudins of neighboring cells (Schreibelt et al., 2007). Claudins are homotypically bound to other claudins on adjacent ECs, which establishes the seal function of the TJs (Ballabh et al., 2004). Claudins exhibit tissue specific expression patterns in addition to the formation of the aqueous pores which permit selective paracellular diffusion based on size and charge. More specifically, claudins-5 has proved to display endothelial cell-specific properties of the TJ strands, which also occurs in the BBB TJ's (Pfeiffer et al., 2011). Claudin-5 is fundamental to the BBB as it seals the BBB for molecules smaller than 800 Da (Nitta et al., 2003; Schreibelt et al., 2007), and this seal function is also critical as it is involved in the production of the high electrical resistance of the TJ at the BBB (Furuse and Tsukira, 2006; Malaeb et al., 2012).

Phosphorylation stimulates an increase in BBB permeability, and numerous phosphorylation sites may be found in the C-terminus sequence of occludin and claudins, and the phosphate in these areas enhances protein internalization (Capaldo and Nusrat, 2009; Enciu et al., 2013). With regard to *in vivo* studies, an augmented permeability of TJ's in blood vessels was observed as result of the removal of claudin-5 (Nitta et al., 2003; Anderson and Van Itallie, 2009). Therefore, it is emphasized that there is not inevitably a relation between the level of permeability for non-charged and charged solutes, and subsequently as a consequence, a contradiction may be noted in which solute permeability could increase while ion permeability decreases, with the subsequent result of an increase in TEER (Anderson and Van Itallie, 2009). The well characterized barrier function exhibited by the TJ's is accomplished as a result of paracellular pore formation displayed by claudins, thus, it may very well be that TJ's are in fact the targets for signaling pathways controlling cell growth and differentiation through various mechanisms. These mechanisms include, controlling the movement of growth factors throughout the paracellular pathway, and the relationship of TJ

proteins with transcription factors and signaling molecules (Citi et al., 2009). A possible mechanism causative to the disruption of the BBB may perhaps be the posttranslational modifications of occludin and claudin-5. The homophilic and heterophilic relationship amid the extracellular loops of claudins warrant tight contacts of the cell monolayers. TJ formation does not depend on occludin expression, irrespective of whether overexpression of claudins may prompt the establishment of TJ-like structures (Yamamoto et al., 2008).

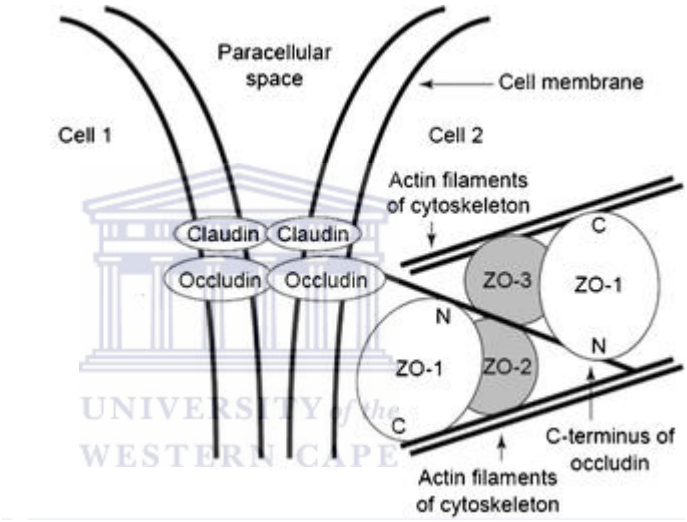

Figure 1.5: Schematic illustration of the molecular arrangement of paracellular space proteins between adjacent ECs. Taken from Perez et al. (2014).

1.3 Alcohol and the BBB

1.3.1 Mechanisms of alcohol-induced BBB damage

Matrix metalloproteinases (MMPs) are a family of secreted and membrane associated zinc-dependent extracellular endopeptidases (Taraboletti et al., 2002). They are produced by activated microglia and function to disassemble the endothelial basal lamina of the BBB (Enciu et al., 2013). The activation

of matrix MMPs and the change in the basement membrane (BM) accompanying BBB injury has been illustrated in stroke patients, and although further study is required it has been revealed that chronic alcoholism is indeed a risk factor for developing stroke (Haorah et al., 2008). With regard to the BBB, MMP-2 and -9 are of particular importance as they were the first expressed in the CNS and are used as markers in neuroinflammation (Enciu et al., 2013). EtOH-induced PTK signaling is proposed to induce a decrease in BBB integrity through the activation of MMPs and the dilapidation of the BM component, collagen-IV. Interestingly, the stimulation of MMP activities and protein contents corresponded with a decrease in collagen-IV content. Chronic alcohol exposure has triggered activation of MMP-2, and -9 *in vitro* and *in vivo* (Haorah et al., 2008); however, mechanisms leading to such effects still need to be elucidated. PTK activation as a result of EtOH also caused phosphorylation of occludin, claudin-5, and ZO-1 at tyrosine residues, instigating BBB disruption (Haorah et al., 2008).

Lipid peroxidation activates MMP-2 and -9, which sequentially activates RhoA, which is known for its phosphorylation properties with regard to TJs (ElAli et al., 2011; Enciu et al., 2013). Furthermore, *In vitro* studies suggested that EtOH activated myosin light chain (MLC) kinase (MLCK), resulting in phosphorylation of numerous TJ proteins which ultimately results in BBB impairment (Singh et al., 2007) as well as enhances the monocyte migration across the BBB (Haorah et al., 2005).

Another factor that plays a role in the EtOH-induced BBB impairment is the formation of the free radicals. The adverse effects of alcohol may be mediated through an alteration in the TJ protein architecture (Singh et al., 2007). EtOH augments the activity and content of EtOH-metabolizing enzymes, and thereby directing the production of AA and ROS in brain endothelium (Haorah et al., 2005). AA and ROS stimulates MLCK (Haorah et al., 2005) by triggering the inositol 1,4,5-triphosphate (IP_3R)-gated intracellular Ca^{2+} release signaling pathway (Haorah et al., 2008) ensuing the phosphorylation of cytoskeletal TJ proteins and BBB disruption and injury

(Haorah et al., 2005). EtOH also activates MLCK3 and ultimately stimulates production of nitric oxide (NO) (Tong et al., 2013). This generation of NO changes the actin and microtubule cytoskeletal structures, thereby permitting various mechanisms to synergistically diminish barrier function (Tong et al., 2013).

The production of AA by ADH in epithelial and ECs is the most probable explanation for the toxic effects of EtOH. AA is an extremely mutagenic and carcinogenic molecule, which has been reported to generate numerous excess ROS species, disrupting TJ's, and ultimately amplifying paracellular permeability through various mechanisms (Sambuy, 2009). Enhanced endothelial TJ permeability has shown in the study led by Sambuy. (2009), to show a relationship with decreased mRNA expression and increased phosphorylation of junctional proteins.

1.3.2 The effects of alcohol on the BBB and TJs

Alcohol impairs BBB TJ proteins, occludin, ZO-1, and claudin-5 in the brain's microvasculature (Haorah et al., 2005). The phosphorylation of claudins may regulate paracellular permeability, by increasing or decreasing TJ association and function. Phosphorylation by MLCK and rho kinase is concomitant with redistribution of TJs and amplified paracellular permeability, noted following excessive alcohol consumption (Findley and Koval, 2009). Chronic alcohol exposure in particular, resulted in altered TJ expression exhibited by a decrease in claudin-1 and -7, as well as an increase in claudin-5 expression (Koval et al., 2008).

Exposure to 217mM EtOH and above has reportedly resulted in intestinal barrier dysfunction, in particular by decreasing the paracellular barrier function in Caco-2 cells. It is proposed that these concentrations can only be located in the lumen of the small intestine, subsequent to what is commonly referred to as "binge drinking", also described as drinking approximately 160 g/day (Elamin et al., 2012). The EtOH serum concentration of 10-40mM is

proposed to occur following moderate EtOH consumption (Elamin et al., 2012). Moderate EtOH drinking, which is defined as one standard drink (12g of EtOH) a day for women and two standard drinks a day for men, has shown to increase paracellular permeability in a dose dependent manner. Despite EtOH resulting in the redistribution and intracellular mislocalization of occludin and ZO-1, it had no effect on cell viability or TJ encoding gene expression, possibly suggesting that EtOH or its metabolite alters the molecular composition of TJs (Elamin et al., 2012).

1.4 Rooibos

1.4.1 Flavonoids

Flavonoids, a set of poly-phenolic compounds are extensively distributed throughout the plant kingdom, and are found in fruit, vegetables, grains, bark, roots, stems, flowers, tea, and wine (Raj Narayana et al., 2001). Most of them exhibit low toxicity in mammals, and generally exhibit anti-inflammatory, anti-hepatotoxic, anti-ulcer actions and antioxidant display with its free radical scavenging abilities (Raj Narayana et al., 2001). Flavonoids have also been reported to suppress the growth of numerous cancer cell lines *in vitro* and depress tumour development (Raj Narayana et al., 2001). Flavonoids contribute significantly to the colour (Dai and Mumper, 2010) and taste of fruits and vegetables (Ross and Kasum, 2002). They may be classified as aglycones, glycosides, and methylated derivatives. Aglycones encompass a benzene ring condensed with a six-membered ring, which in the 2-position carts a phenyl ring as a substituent (Raj Narayana et al., 2001). Six-member ring condensed with the benzene ring is either α-pyrone (flavonols and flavonones) or its dihydroderivative. The location of the benzenoid substituent determines whether the flavonoid will fall in the 2-position (flavonoids) or the 3-position (isoflavonoids) (Raj Narayana et al., 2001). The presence of the hydroxyl group at the 3-position and the C2-C3 double bond differentiates flavonols from flavonones (Fig 1.6) (Raj Narayana et al., 2001).

Flavonoids are generally divided into different classes based on their molecular structure. There are four principle groups of flavonoids, namely, flavones, flavanones, catechins, and anthocyanins (Ross and Kasum, 2002). Flavones are categorised due to the double bond in the central aromatic ring.

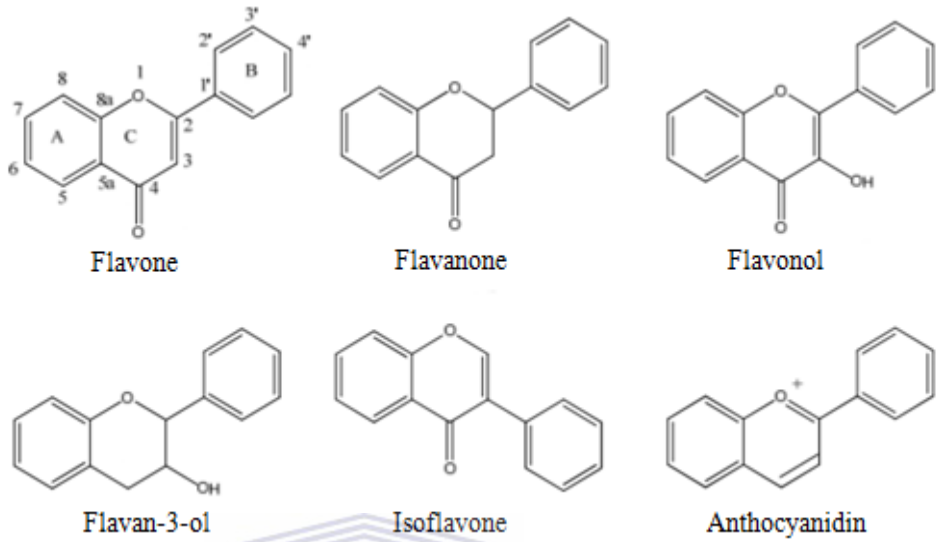

Figure 1.6: Structures of the different classes of flavonoids. Taken from Jäger and Saaby (2011).

Quercetin, an important and popular flavonoid found in rooibos herbal tea belongs to this group, whereas naringin, popular in citrus fruit is found in flavanones (Raj Narayana et al., 2001). Red wine, and green and black teas belong to the catechins group and anthocyanins are found in strawberries, grapes, wine, and tea as well. Flavones and catechins are reported to exhibit the most protection against ROS in the body (Nijveldt et al., 2001). One cup of rooibos tea has been approximated to contain 1.5mg of quercetin (Joubert and Ferreira, 1996). Rooibos has also been reported to contain aspalathin, a unique flavonoid found only in rooibos tea, and nothofagin. Aspalathin and nothofagin constitute 0.55% and 0.19%, respectively, of the soluble solids of the processed tea. Furthermore, the flavonoid fraction of rooibos tea contains the flavones: orientin, iso-orientin, vitexin, iso-vitexin, chrysoeriol, 5,7,4'-trihydroxy-3-methoxyflavone, luteolin, and the flavonols, iso-quercetin, rutin, and quercetin (Joubert and Ferreira, 1996).

Antioxidant and free-radical scavenging are just some of the properties exhibited by flavonoids *in vitro* (Ross and Kasum, 2002). They are suggested to decrease incidences of cancer, as well as heart and other chronic diseases, and believed to do this by means of their potent antioxidant capacity (Breiter et al., 2011), but this isn't endorsed completely, as it is suggested to potentially generate harm as well. Therefore, it is imperative that additional research in the laboratory as well as with populations be conducted (Ross and Kasum, 2002). Flavonoids may influence the actions of endogenous scavenging compounds, by interfering with different free radical producing systems, or they may augment the function of the endogenous antioxidants. They stabilize ROS by reacting with the reactive compound of the radical (Nijveldt et al., 2001).

1.4.2 Rooibos and its antioxidant potential

Rooibos herbal tea, indigenous to the Cederberg region of the Western Cape, is made from the South African fynbos plant, and is one of six floral kingdoms, *Aspalathus linearis* spp. *Linearis* (Joubert and Schulz, 2012; Standley et al., 2001; Krafczyk and Glomb, 2008; Pengilly et al., 2008; Snijman et al., 2009). It has been around for approximately 230 years and is being consumed by a growing market (Joubert and Schulz, 2012). *Aspalathus linearis* are vertical or flat plants, growing up to 2m tall in length, possessing yellow flowers and needle-like leaves; however, the size, density of branching, leave size, and flowering time of the plant may differ noticeably (Joubert and Schulz, 2012). The plants grow in subterranean, well-drained, sandy, acid soil, and have a well-nodulated root system for fixing elemental nitrogen from soil water (Joubert and Schulz, 2012). Furthermore, rooibos extracts could also be found in iced teas, yoghurts as well as cosmetic products (Joubert and Schulz, 2012; Joubert et al., 2010).

Aspalathus linearis is the only species in the genus *Aspalathus* which is fit for human consumption. The stems and leaves are used for the production of the tea, which is rich in flavonoids and C-glycosides. Rooibos is one of the few

beverages that are caffeine-free. It also contains low levels of tannin and is enriched with minerals (Krafczyk and Glomb, 2008).

Antioxidants are substances capable of quenching excessive quantities of ROS or RNS during oxidative stress situations (Dai and Mumper, 2010; Berker et al., 2013). They are radical scavengers that disrupt and inhibit radical chain reactions (Huang et al., 2005). Antioxidant compounds such as phenolic compounds are the most active and widely occurring hydrophilic antioxidants, particularly in the diet, such as fruits and vegetables, capable of promoting cellular defenses and inhibiting oxidative damage (Dudonne et al., 2009). Dietary antioxidants are suggested to comprise of radical chain reaction inhibitors, metal chelators, oxidative enzyme inhibitors, and antioxidant enzyme cofactors (Huang et al., 2005). Antioxidants have been proposed to delay or inhibit diseases such as Alzheimer's disease, cancer, and coronary heart failure (Berker et al., 2013).

Aspalathin is an effective antioxidant possessing anti-mutagenic and antispasmodic characteristics and has shown to have a glucose-lowering ability, further validating aspalathin as a neutraceutical ingredient in teas and other food or beverage products (Standley et al., 2001; Joubert et al., 2010). The anti-allergic effects in infants displayed by rooibos, as seen with colic babies are ascribed to the antispasmodic properties of quercetin and luteolin, found in rooibos (Standley et al., 2001), which is proposed to exhibit a calming effect on the stomach. While skin problems such as eczema and nappy rash, has shown to be combatted with topical applications of the rooibos extract (Joubert and Schulz, 2012). The consumption of rooibos tea has in addition been proposed to accompany the liberation of insomnia, stomach cramps, constipation, nervous tension, allergic symptoms, and even mild depression (Pengilly et al., 2008).

The antioxidant nature of phenolic compounds occurs as a result of their structure (Dudonne et al., 2009), just right for free radical scavenging activities, since they possess phenolic hydroxyl groups inclined to donate a

hydrogen atom or electron to a free radical, as well as an extended conjugated aromatic system to delocalize an unpaired electron (Dai and Mumper, 2010). Phenolics constitute one or more aromatic rings yielding one or more hydroxyl groups resulting in the formation of resonance-stabilized phenoxyl radicals, allowing the quenching of free radicals (Dudonne et al., 2009).

Certain phenolic compounds with dihydroxy groups may conjugate transition metals, thereby impeding the formation of metal-induced free radicals. Hydroxyl radicals, the most combative type of ROS, occurs when reactive metals such as Cu^{+} or Fe^{2+} interact with hydrogen peroxide (H_2O_2) during the Fenton reaction. This results in free radical chain reactions through removal of hydrogen from nearly any molecule (Dai and Mumper, 2010). Metal-induced oxygen radical formation may be prevented by phenolic compounds consisting of gallate and catecholate groups, by increasing autoxidation of Fe^{2+} or the establishment of inactive complex with Cu^{2+}, Fe^{2+}, or Cu^{+} with relatively weaker interaction (Dai and Mumper, 2010).

Phenolic antioxidants may also perform as prooxidants under certain circumstances, when the phenoxy radical interacts with oxygen, generating quinones and superoxide anion, instead of reacting with a second radical (Dai and Mumper, 2010). Phenolics, such as quercetin and gallic acid, which are effortlessly oxidized, may display prooxidant action, while tannins or phenolics with larger molecular weights exhibit little to no prooxidant activity (Dai and Mumper, 2010). It is imperative to know the oxidative status of a cell, since flavonoids may exhibit antioxidant or prooxidant properties, which could influence the biological response (Joubert et al., 2005). It has been said that the different phases in which polyphenols interact with free radical species determines their antioxidant or prooxidant properties (Joubert et al., 2005). Antioxidants such as epigallocatechin gallate (EGCG) and gallic acid exhibit effective prooxidant activity in the deoxyribose degradation assay, as they are capable of reducing Fe^{3+} to Fe^{2+}. It has been hypothesized that aspalathin may present prooxidant activity as it is a strong antioxidant similar to EGCG. However, in the presence of a transition metal,

the structural aspects of a dihydrochalcone may also give rise to prooxidant action (Joubert et al., 2005).

1.4.3 Fermented and Unfermented Rooibos

There are two categories of rooibos teas presented. The unfermented (green) and fermented rooibos (red-brown) tea. Fermentation is a chemical oxidation process which converts the green grassy-smelling tea to the sweet-smelling red-brown tea (Krafczyk and Glomb, 2008). It has been widely shown that fermentation diminishes the antioxidant activity of rooibos, with less than 7% of aspalathin present following fermentation. Aqueous extracts of unfermented rooibos is proposed to possess greater antioxidant activity than fermented, since aspalathin contributes to 43% of the total antioxidant capacity (TAC) (Joubert et al., 2005).

A study conducted by Villaño et al. (2010) showed that plasma antioxidant defences in humans can be amplified by consumption of both fermented and unfermented rooibos tea, despite unfermented rooibos tea having greater antioxidant properties than its fermented counterpart. Therefore, acute ingestion of both fermented and unfermented rooibos tea generated increased plasma antioxidant defences, measured as TAC.

Fermentation of rooibos reduces the aspalathin content significantly and consequently results in the formation of the flavones, iso-orientin and orientin as products. Furthermore, aqueous spray-dried extracts of fermented rooibos is suggested to comprise approximately somewhat less than 0.5% aspalathin, while green aqueous rooibos extracts is presumed to contain an estimated 7% aspalathin (Joubert et al., 2010). A study conducted by Stalmach et al. (2009), corroborated previous literature, that unfermented rooibos tea comprised more aspalathin and nothofagin than fermented tea. The complete flavonoid contents in 500 ml tea servings were 84 μmol for fermented and 159 μmol for unfermented. Furthermore, eight metabolites were distinguished, namely, the O-linked methyl, sulfate, and glucuronide metabolites of aspalathin and an eriodictyol- O-sulfate. According to literature, variation in the aspalathin and

nothofagin contents between rooibos bushes may occur, which may be accredited to genetic modification of the individual plants (Joubert and Schulz, 2006).

The leading dihydrochalcones aspalathin and nothofagin, the flavones, orientin, isoorientin, vitexin, isovitexin, chrysoeriol and luteolin, the flavonols, rutin, isoquercitrin, quercetin, hyperoside, and luteolin-7-*O*-glucoside, and the flavanol, (+)-catechin have all been detected in rooibos (Fig 1.7). The existence of the novel compound, 5,7-dihydroxy-6-C-β-D-glucopyranosylchromone, proposes oxidative conversion of dihydro-isoorientin during fermentation. Phenolic acids, secluded from fermented rooibos contain the benzoic acids, *p*hydroxybenzoic acid, protocatechuic acid, vanillic acid and syringic acid, as well as the cinnamic acids, *p*-coumaric, ferulic and caffeic acid (Joubert and Schulz, 2006; Snijman et al., 2009).

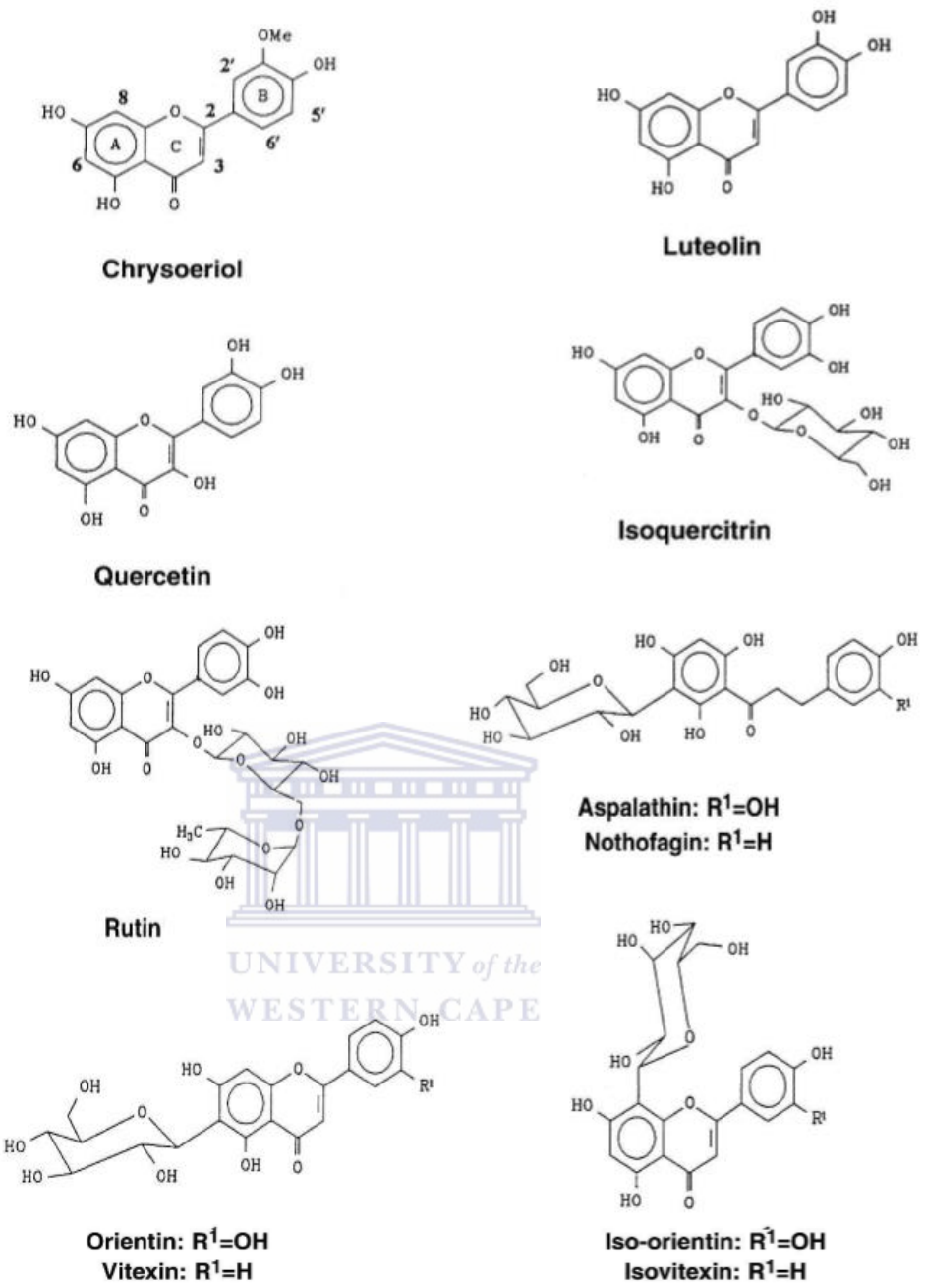

Figure 1.7: Flavonoids present in rooibos tea. Taken from Joubert and Ferreira (1996).

Flavonoids present is rooibos tea have been reported to possess antioxidant and free radical scavenging abilities. As the main reason for the consumption of rooibos tea is for its acclaimed antioxidant properties, the low levels of aspalathin in fermented rooibos led to the production of green or unfermented rooibos tea and the inclusion of green rooibos extracts in products, as it is

noted to contain more aspalathin than its fermented counterpart (Standley et al., 2001; Pengilly et al., 2008). However, the colour and smell of green rooibos tea is not perceived appealing as that of fermented rooibos, therefore a need exists to create a rooibos tea with enhanced colour as well as increased aspalathin (Pengilly et al., 2008).

1.4.4 The physiological effects of rooibos

It has been proposed that plant polyphenols deliver protection against neurodegenerative alterations related to cerebral ischemia, particularly in the hippocampal and cerebral cortex areas. A possible mechanism resulting in the neuroprotective properties of polyphenols is through its effects on decreasing the levels of apoptotic markers (Panickar and Anderson, 2011). In order for flavonoids to exhibit an effect on the CNS, they need to be absorbed in the digestive tract, transported via the circulatory system to the brain, and traverse the BBB, thus it is necessary that flavonoids and their conjugates are able to cross the BBB and enter the CNS to display an effect. Studies have shown that flavonoids can be absorbed following oral administration and are capable of crossing the BBB, resulting in numerous effects on the CNS, such as memory, cognition, and neurodegeneration (Jäger and Saaby, 2011). In addition, flavonoids are suggested to exhibit protective properties in neurons against injury induced by neurotoxins and neuroinflammation, as well as influencing endothelial function and peripheral blood flow (Jäger and Saaby, 2011).

Flavonoids such as epicatechin, 3'-*O*-methyl-epicatechin and hesperetin, have been reported to protect against neuronal damage, while naringenin, a flavanone, is proposed to prevent inflammatory processes causing neuronal cell injury. Quercetin, catechin, and epigallocatechin have also been suggested to have an effect on neuroinflammation (Jäger and Saaby, 2011).
Rooibos tea has been commended for its beneficial influences in numerous health conditions such as digestive and stomach problems, nervous tension and allergies (Kreuz et al., 2008; Kawano et al., 2009). Rooibos has also been

reported to decrease the number and volume of skin tumours, which is believed to be attributed to aspalathin, the chief flavonoid in rooibos (Marnewick et al., 2005). A study by Uličná et al. (2003) elucidated that ingestion of rooibos tea inhibited large-scale fibrosis in the liver as well as cirrhosis. Furthermore, it has displayed anti-mutagenic activity in Chinese hamster ovary cells (Marnewick et al., 2003). It is suggested that the mechanisms involved in the anti-mutagenic effects could be the decline in the generation of the genotoxic intermediate by affecting the cytochrome P450-mediated metabolic activation of mutagens as well as the interaction of nucleophilic tea components with the genotoxic intermediates (Marnewick et al., 2003).

With regard to reproduction, rooibos is proposed to enhance sperm motility and function, attributed to its eminent antioxidant properties (Opuwari and Monsees, 2014). Consequently, extended administration of rooibos tea has been reported to contribute to slight structural modifications in the male reproductive system, while excessive quantities of *Aspalathus linearis* could disrupt kidney and liver function (Opuwari and Monsees, 2014). However, Marnewick et al. (2003) stated that ingestion of aqueous extracts of rooibos tea resulted in no harmful effects in the kidney and liver of rats, and also showed no interference in iron uptake.

Aqueous extracts of fermented and unfermented rooibos resulted in a substantial increase in the antioxidant capacity in the liver of rats, through stabilization of GSH, as well as the activity of hepatic phase II metabolising enzymes, glutathione-S transferase (GST-a) and UDP-glucuronosyl transferase (UDP-GT), suggesting that rooibos modified the metabolic fate of carcinogens and oxidative status of cells, providing a defence mechanism against the harmful effects of oxidative damage generated by carcinogens (Marnewick et al., 2005). Glutathione, in a normal cell, exists as the reduced form (GSH), but this reduced form is transformed to its oxidized form (GSSG) when cells are subjected to high levels of oxidative stress. Consequently, the GSH: GSSG ratio is employed as a sensitive index of

oxidative stress in biological systems (Hong et al., 2014). Marnewick et al. (2011) reported that rooibos regulated the serum lipid profile in human participants by notably reducing triacylglycerol and low density lipoprotein (LDL)-cholesterol levels and augmenting the high density lipoprotein (HDL)-cholesterol level, in addition to enhancing the redox status exhibited by the increased GSH: GSSG ratio and diminished lipid peroxidation. Reduced glutathione is a potent intracellular antioxidant involved in stabilizing numerous enzymes and acclaimed to be a worthy marker for tissue antioxidant capacity. The diminished lipid peroxidation may be an indication of the enhanced thiol status resulting from the rooibos-induced improvement of the GSH: GSSG ratio (Marnewick et al., 2011). This is in accordance with Hong et al. (2014) who reported that rooibos tea reinstated the oxidative stress-induced reduction of GSH levels and the GSH: GSSG ratio. This was supported by a study done by Marnewick et al. (2011), who indicated that rooibos elicited no adverse effects.

1.4.5 Bioavailability and metabolism of rooibos

Polyphenolic compounds signify one of the most abundant and diverse groups of substances in the plant kingdom which arise from the secondary metabolism of plants (Dai and Mumper, 2010). They may be attached to sugars (glycosides) (Ross and Kasum, 2002), predisposing them to be water-soluble.

Since the majority of flavonoids found in foods or beverages are attached glycosides, it was proposed that the absorption of the compound was insignificant. This was concurrent with the hypothesis that the passage of aglycones from the gut wall into the blood stream was without restrictions, since there are no enzymes secreted in the gut which may cleave the glycosidic bonds. However, since then it has been established that the bioavailability of certain flavonoids are higher. A study conducted indicated that the absorption of orally administered quercetin aglycone was approximately 24% while the absorption of quercetin glycosides derived from

onions appeared to be an estimated 52%, signifying that the glycoside moiety increased absorption (Ross and Kasum, 2002). It is believed that glycosidation diminishes the antioxidant activity of flavonoids, which could result by more blocking of the phenolic compounds which controls radical scavenging and metal chelation (Ross and Kasum, 2002).

The bioavailability of flavonoids determines their activity *in vivo*, however additional human research is required to investigate the bioavailability of flavonoids and the biomarkers of antioxidant effects (Ross and Kasum, 2002). Studies have indicated that the daily intake of flavonoids have been well categorized in certain countries (Ross and Kasum, 2002).

According to Breiter et al. (2011), the dose dependent antioxidant function of aqueous rooibos extracts indicated by *in vitro* measurements could not be confirmed by *ex vivo* measurements. It has been suggested in previous literature that binding of consumed flavonoids to the antioxidant human serum protein albumin (HSA) resulted in a decrease in the antioxidant capacity by concealing the anti-oxidative activity of the flavonoids (Breiter et al., 2011). This was disproved by Breiter et al. (2011), who maintains that flavonoids are able to augment the antioxidant capacity of blood *in vitro*. Furthermore, they propose that rooibos flavonoids retain diminished bioavailability, as a result reaching the blood circulation with insignificant amounts (Breiter et al., 2011).

Administration of rooibos tea equivalent to approximately 0.76 nmol of aspalathin, resulted in increased levels of flavonoids in comparison to the isolated active fraction (0.41 nmol), which may be attributed to matrix and synergetic effects (Breiter et al., 2011). Rooibos needs to reach the target specific sites to demonstrate favourable effects, which occurs following its absorption and metabolism (Stalmach et al., 2009). Studies indicate that rooibos may result in either an increase or decrease in plasma antioxidant activity, however to determine the bioavailability and metabolism of

flavonoids from rooibos *in vivo*, it is imperative to identify the metabolites (Breiter et al., 2011).

Unchanged aspalathin and nothofagin was discovered in urine samples, while eriodictyol-C-glucosides were detected in some plasma samples following ingestion of rooibos tea as well as the isolated active form. Eriodictyol-C-glucosides are suggested to occur following the oxidative cyclisation of aspalathin during fermentation. It was not found to be present in the isolated active fraction, suggesting that the body does in fact oxidize aspalathin (Breiter et al., 2011). The plasma however, revealed a scarcity of flavonoid metabolites. Additionally, most of the aspalathin metabolites (80-90%) were excreted in a 5 hour window following the administration of tea, implicating the small intestine for absorption, while eriodictyol-O-sulfate is suggested to be absorbed in the large intestine since urinary excretion occurred within 5 to 12 hrs following ingestion (Stalmach et al., 2009). It is suggested that the dihydrochalcone-, flavone-C-, and flavonol-O-glycosides present in unfermented rooibos tea and the isolated active fraction are bioavailable to some degree, thus it can be anticipated that a relevant quantity of flavonoids directly move to the large intestine (Breiter et al., 2011). The dihydrochalcone and flavanone C-glucosides in rooibos tea have weak bioavailability with small amounts of metabolites present in the urine following 24 hour consumption. This diminished bioavailability of these compounds is further substantiated by the lack of metabolites in the plasma. A study exposing aspalathin to artificial gastric juice validated the hypothesis that aspalathin is not degraded in the stomach. It is proposed that the flavonoids present in rooibos move from the small to the large intestine, where it undergoes cleavage of the sugar moiety and ring fission, a result of the colonic microflora, generating low molecular weight phenolic acids (Stalmach et al., 2009).

Most dietary polyphenols are metabolized by colonic flora prior to absorption, a pre-requisite for absorption. Hydrolysis, reduction, ring-cleavage, decarboxylation and demethylation are the mechanisms by which

bacteria may modulate polyphenols. Synergistic activity of polyphenols following entry into circulation is suggested to influence their systemic effects as well as endogenous factors (Hanhineva et al., 2010). In addition, flavonoids are suggested to undergo at least three modes of intracellular metabolism, namely, oxidative metabolism, P450-related metabolism and conjugation with thiols, particularly GSH (Vauzour et al., 2008).

While measurements of the administered dosage of aspalathin ranging between 0.1% and 0.9% were found in the urine, no metabolites were detected in the plasma. This may be attributed to the metabolism in the colon causing the generation of breakdown products, forming lower molecular weight phenolics. The liver is believed to be another site at which metabolization of breakdown products can occur (Kreuz et al., 2008). Furthermore, the absence of aspalathin in the plasma may be attributed to its aromatic nucleus and hydroxyl substituents which may influence its affinity for proteins, such as quercetin which is bound to albumin (Kreuz et al., 2008).

1.5 Rooibos and the brain

1.5.1 The effects of rooibos on the brain

The brain is amongst the most susceptible target tissues to oxidative stress due to its substantiated level of ROS and diminished level of antioxidants. The brain possesses astronomical levels of unsaturated fatty acids, which are proposed to be principle targets of free radicals and cellular lipid peroxidation thus have increased susceptibility to ROS (Hong et al., 2014). As a result, terminally differentiated neuronal cells, present in a post-mitotic state, unlike skin, blood, or connective tissue cells, are affected by ROS. With regard to excessive quantities of ROS, endogenous defense mechanisms against ROS may be inadequate to control ROS-associated oxidative damage (Hong et al., 2014). According to literature, diets abundant in polyphenols are proposed to enhance brain function in humans (Schaffer and Halliwell, 2012). In addition, isolated polyphenols and plant extracts are reported to better memory and

cognition (Schaffer and Halliwell, 2012). These advantageous effects have been attributed to the metal chelation, free radical scavenging, and modulation of enzyme activities of polyphenols (Schaffer et al., 2006; Schaffer and Halliwell, 2012). Polyphenols are suggested to modify brain function at three sites, namely, outside the CNS, at the BBB, and inside the CNS (Schaffer and Halliwell, 2012). However, flavonoids need to traverse the BBB before they are able to enter the brain (Vauzour et al., 2008). Outside the CNS, polyphenols are proposed to enhance cerebral blood flow or control signalling pathways from peripheral organs to the brain, while inside the CNS, they may directly alter the activity of neurons and glial cells.

More importantly, at the BBB, they are suggested to modify multidrug resistant protein-dependent influx and efflux processes of numerous biomolecules (Schaffer and Halliwell, 2012).

EGCG, an acclaimed natural antioxidant and free radical scavenger, a well-known catechin/polyphenol in green tea, was shown to enhance focal ischemia/reperfusion-induced brain injury *in vivo*. Furthermore, the multi-targeted and multi-directional beneficial properties on the neuronal injury and BBB leakage, designates EGCG as an optimal neuroprotective agent against brain ischemia (Li et al., 2012; Liu et al., 2013). It has been proposed that EGCG, epicatechin, and anthocyanins are present in the brain following oral administration (Vauzour et al., 2008). Chlorogenic acid (CGA), a polyphenol originating from agricultural products (coffee, beans, potatoes, apples), established during esterification of caffeic and quinic acids is proposed to possess antibacterial, anti-inflammatory, antioxidant, and anti-carcinogenic properties (Shin et al., 2013). Shin et al. (2013) has also reported that CGA down-regulates vascular endothelial growth factor (VEGF) expression and re-establishes the decrease of occludin, decreasing the blood retinal barrier (BRB). Since there is a scarcity of literature explaining the effects of rooibos herbal tea on the blood brain barrier and tight junctions, the possibility that it may display similar effects to other well-known polyphenols is plausible since it also possesses potent antioxidant properties.

Youdim et al. (2003) illustrated the uptake of flavonoids and their respective metabolites into BECs using cell lines, mouse brain endothelial cells (bEND5) and rat brain endothelial cell (RBE4). The main pathway by which flavonoids intersect the BBB is supposedly through transcellular diffusion and is suggested to be influenced by the charged state and lipophilicity properties of flavonoids (Youdim et al., 2004). Flavanones, hesperetin, naringenin, and their glucuronidated conjugates displayed noticeable permeability across the *in vitro* BBB model, signifying transcellular flux. This is of particular interest since it has been rumoured that the physicochemical properties of glucuronides are unsuited with passage across the BBB (Youdim et al., 2003; Vauzour et al., 2008).

A few flavonoids have shown capability of entering the CNS, leading to the likelihood that the advantages correspond to systemic modifications (i.e. cerebral blood flow or immune system) (Youdim et al., 2003). The drug efflux transporter P-gp, a functional constituent of the BBB, regulates the movement of structurally diverse compounds through the BBB. Aglycones traverse the BBB by means of passive transcellular diffusion, as anticipated from their lipophilicity, while the mechanisms responsible for the movement of anionic glucuronide conjugates across the BBB remains to be elucidated as their lower lipophilicity limits transcellular diffusion. The extent of BBB permeation is determined by compound lipophilicity, as less polar O-methylated metabolites may possible result in greater brain uptake opposed to more polar flavonoid glucuronides. According to literature, there are suggestions that particular drug glucuronides are able to cross the BBB and in so doing exercising their pharmacological effects (Vauzour et al., 2008). Consequently, the mechanisms underlying their neuroprotective properties need further study and clarification (Youdim et al., 2003).

1.6 **Model**

1.6.1 Immortalized mouse brain endothelial cells (bEnd5)

An important aspect of BBB research is the scarcity of reliable *in vitro* models to study the cellular and molecular mechanisms of BBB function under both normal and pathological conditions (Yang et al., 2007). Significant advantages of using *in vitro* BBB models include diminished variability as well as possible high throughput of experimental conditions (Coisne et al., 2013). The introduction of immortalized cell lines has proved to be a successful alternative approach; most displaying the imperative *in vivo* barrier characteristics.

Generally, it is proposed that immortalized brain EC lines lack the important BBB-specific property of establishing a tight permeability barrier, whereas BBB models encompassing primary brain ECs are more suited for studying transport mechanisms across the BBB *in vitro* (Deli et al., 2005; Steiner et al., 2011). Primary or low passage brain capillary ECs displays the closest phenotypic similarity to an *in vivo* cell. Furthermore, the cultured monolayers resulting from them produce a restrictive paracellular barrier to solute permeability.

Numerous *in vitro* BBB models which exist utilizes primary brain ECs from diverse sources, namely, bovine, porcine, rat, and even human brain tissues (Deli et al., 2005; Steiner et al., 2011), yet up to now, only a handful of *in vitro* BBB models using primary brain ECs have been established. Several studies have suggested that commercially available EC lines may function as reliable BBB models.

The bEnd5 cell line is one of two commercially available cell lines which are obtainable from commercial cell banks such as the European Collection of Animal Cell Cultures (ECACC) (www.ecacc.org) or the American Type Culture Collection (ATCC) (www.atcc.org) (Gumbleton and Audus, 2001).

The bEnd5 is established from brain endothelial cells of Balb/c mice. Immortalization has been carried out by infection of primary cells with retrovirus coding for the Polyoma virus middle T-antigen. The bEnd5 cells possess an endothelial-like morphology, and as tested by fluorescent activated cell sorting (FACS), are positive for endothelial specific proteins (PECAM-1, Endoglin, MECA- 32, Flk-1) (Yang et al., 2007). bEnd5's are well distinguished for its expression of EC specific proteins, such as the vascular endothelial-cadherin (VE-cadherin), von Willebrand factor, platelet endothelial cell adhesion molecule-1, endoglin, ICAM-2, and claudin-5. Nonetheless, despite previous studies indicating the expression of occludin in brain ECs (Yang et al., 2007), it is still in question since a study by Steiner et al. (2011) found a significant decrease in occludin mRNA expression in bEnd5's when compared to primary mouse brain microvascular endothelial cells (pMBMECs).

Mouse models are expedient to use in experimental analysis because of the availability of transgenic and gene-targeted animals, however immortalized cell lines are easily available in suitable and useful quantities minus the lengthy time-consuming isolation protocols (Steiner et al., 2011).

1.6.2 Transepithelial electrical resistance on ECs

A significant feature of the BBB is its highly regulated and restrictive permeability barrier to cells and molecules (Deli et al., 2005). As present in brain microvascular endothelial cells (BMVEC), TEER is used as an indicator of paracellular ion flux, defined as the frequency domain ratio of the voltage to the current, to the transport of small ions through a physiological barrier. TEER is denoted as being a physical parameter to quantify the barrier function of a given cell layer, and is calculated by Ohm's law, including a correction for the resistance of the empty filter insert and the bulk electrolyte (Wegener et al., 1996). *In vivo,* TEER is high due to this barrier which is resistant to charged particles, proteins, ions, and hormones that has the potential to act as neurotransmitters (Tanobe et al., 2003; Colgan et al., 2008).

BMVECs are characterized by the presence of an increased amount of TEER, intercellular TJs, minimal pinocytic activity, and lack of fenestrations (Grant et al., 1998). Colgan et al. (2008) suggested that serum-contact with the basolateral surface of the BBB endothelium could possibly increase the permeability directly by means of down-regulation of expression, association and membrane localization of TJs. Astrocytic components have the ability to up-regulate barrier function through alterations in occludin and ZO-1.

1.6.3 Ultrastructural modifications on ECs investigated with scanning electron microscopy (SEM)

Electron microscopy (EM), an essential tool in science has long been used to analyse structures as close to its native state as possible (Thiberge et al., 2004). Since its inception and as of late, SEM is generally used to investigate the ultrastructure of cell surfaces using high resolution. In SEM, electron beams scan surfaces, illuminating morphological and topographical changes on cell monolayers (von Wedel-Parlow and Galla, 2010). SEM is advantageous in the sense that the surface of a specimen is accessible for experimentation at a resolution and depth of field greater than that of the optical microscope (Nixon, 1971).

Cultured ECs, when viewed ultrastructurally, encompass numerous organelles needed for the synthesis of secretory proteins and glycoproteins (Maccallum et al., 1982). In addition, an extensive juxtanuclear Golgi complex comprising several arrays of flattened lamellae and a multiplicity of vesicles are also present. These vesicles are reported to occasionally contain granular or flocculent material (Maccallum et al., 1982). After attaining confluence, bovine ECs have been reported to establish a well-arranged monolayer similar to the arrangement of the innate endothelium when looked at in SEM. They exhibit the hexagonal shape and close apposition to one another (Maccallum et al., 1982). In a study by Jaffe et al. (1973), ECs appeared homogenous, when investigated with SEM. They were large, flat cells which grew in a monolayer with well-defined cell boundaries and

outstanding nuclei. Furthermore, ECs enclose less rigidly organized junctions and displayed a considerable amount of overlap between cells (Dejana, 2004).

A study by Taraboletti et al. (2002) using ultrastructural analysis, reported that HUVECS shed vesicles from localized regions of the plasma membrane. These vesicles have been described to contain two gelatinases, MMP-2 and -9, in the active and proenzyme forms. Taraboletti et al. (2002) further explained that the protease-containing vesicles shed by ECs may be involved in endothelial proteolytic activity during angiogenesis. Cellular activation and transformation activities are also suggested to regularly result in shedding of microvesicles (MVs) from the plasma membrane, and are referred to as ectosomes, exosomes, or microparticles, subject to their nature, size, and origin (Al-Nedawi et al., 2009). MVs have been reportedly associated with secretory processes, immunomodulation, inflammation, coagulation, and intercellular communication, possibly credited to the transfer of MV-mediated intercellular exchange amid adjacent or remote cells. The MV-mediated intercellular exchange may possibly comprise of transmembrane proteins, lipids, nucleic acids, soluble proteins, chemokine receptors, and receptor tyrosine kinases (Al-Nedawi et al., 2009).

Shedding from the cell surface is an essential communication process between eukaryotic cells and their environment. Shedding is explained as the discharge of soluble or vesicle-related cell surface constituents, without influencing cell viability. Shedding of vesicles from the cell surface is suggested to be a selective procedure and occurs in endothelial and tumor cells *in vivo* and *in vitro*, however the processes between the two types of cells differ (Taraboletti et al., 2002). In ECs, shedding is limited to distinct areas of the plasma membrane, while in tumor cells vesicle shedding implicates the entire plasma membrane. Furthermore, it appears that vesicle shedding in ECs is triggered by specific stimuli. In particular, Taraboletti et al. (2002) found that vesicle shedding was regulated by serum and angiogenic factors.

1.7 Aims and objectives

The aim of this study was to investigate the *in vitro* effects of EtOH and fermented rooibos (R_f) on a monolayer of bEnd5 mouse brain ECs. In order to evaluate the ameliorating effect of drinking approximately 500ml of R_f tea on our *in vitro* model of brain endothelial cells (bEnd5) exposed to alcohol, we propose to utilize the novel approach in using Breiter et al. (2011) estimation of the bioavailability of plasma aspalathin following the consumption of 500ml R_f tea.

The scope of the proposed study, was therefore to establish if the simultaneous exposure of 0.08% R_f equivalent to the plasma concentration of aspalathin, after consuming 500ml R_f, was able to negate the EtOH-induced adverse effects on the bEnd5 monolayers. The concentration of R_f used in this study (0.08%) would be the plasma concentration of aspalathin present in the rooibos which was equivalent to 500ml of R_f tea.

The objectives are to determine:

- The effects of selected concentrations of EtOH (25mM and 100mM) on bEnd5 ECs for a selected experimental timeline of 24, 48, 72, and 96 hrs. The 25mM EtOH represents the average plasma concentration after alcohol consumption, whereas the 100mM represents the supraphysiological concentration.

- The effects of 0. 08% R_f (≡ 1.9nM Aspalathin) on bEnd5 ECs for the selected experimental timeline of 24, 48, 72, and 96 hrs.

- The effects of the simultaneous exposure of EtOH and R_f on bEnd5 ECs for the selected experimental timeline of 24, 48, 72, and 96 hrs.

Parameters monitored with the trypan blue exclusion assay included cell viability, cell toxicity, cell proliferation, and rate of cell division. Furthermore, occludin, and claudin-5 mRNA transcription was investigated with real-time PCR, and paracellular permeability was measured using

TEER. Ultrastructural modifications elicited on the surface of bEnd5 cells in response to the experimental compounds was analysed at 96hrs, using SEM. Objectives were conducted to establish the mechanism/s by which EtOH induces its adverse effects, and if administration of R_f could reverse the EtOH-induced effects.

CHAPTER TWO

Methods and Materials

2.1.1 Experimental Model: bEnd5 mouse brain endothelial cells

The bEnd5 is established from brain endothelial cells of Balb/c mice and possess an endothelial-like morphology. It is positive for endothelial specific proteins (PECAM-1, Endoglin, MECA- 32, Flk-1) (Yang et al., 2007). bEnd5's are well distinguished for its expression of EC specific proteins, such as the vascular endothelial-cadherin (VE-cadherin), von Willebrand factor, platelet endothelial cell adhesion molecule-1, endoglin, ICAM-2, and claudin-5.

2.1.2 Concentrations of EtOH used in this study

It is suggested that the EtOH serum concentrations of 10-40mM EtOH is proposed to occur following moderate EtOH consumption (Elamin et al., 2012). The maximum legal limit for EtOH-induced inebriation in several countries is 0.05% or 11mM EtOH in the blood, while 100mM EtOH is regarded as the lethal concentration in humans (Sommer and Spanagel, 2013). The objective for our study was to look at the effects induced by a physiological and supraphysiological concentration of EtOH. We therefore used two concentrations of EtOH in our study, 25mM EtOH and 100mM EtOH.

2.1.3 Concentration of R_f used in this study

A study done by Breiter et al. (2011) has shown that following the consumption of 500ml of R_f, the plasma concentrations of the individuals contained approximately 1.9nM aspalathin. As aspalathin is the most prominent antioxidant present in R_f, this serves as the rationale for the usage

of 0.08% R_f containing equivalent of 1.9nM aspalathin (See chapter four for rationale).

A.linearis is harvested in the Cederberg region of Clanwilliam. The aqueous infusion of *A. linearis* was concocted by soaking the parched leaves in boiling water for 30 min. Thereafter, a 20% aqueous extract was strained through cheesecloth, followed by whatman no.4 and no.1 filter paper (Sigma, South Africa), in that order. The filtered extract was stored with minimal to no light exposure at -20˚C. The R_f extract was diluted with dH_20 to a final concentration of 20%, after which it was used directly. Centrifugation was utilized to eliminate any sample precipitates (4000rpm, 3 min), while the supernatant was used for the chemical analysis. The concentration of R_f used to expose the cells was 0.08% which was equivalent to 1.9nM aspalathin.

2.2 Cell Culture

Mouse brain endothelial cells (bEnd5) (Sigma, 96091930), were grown in sterile tissue culture treated flasks until 70-80% confluence in Dulbecco's Modified Eagle Medium (DMEM) (Whitehead Scientific, 12-719F) supplemented with 10% Fetal Bovine Serum (FBS) (Separations, SV30160.02), 1% non-essential amino acids (NEAA) (Lasec, 13-114E), 1% sodium pyruvate (Whitehead Scientific, 13-115E), and 1% antibiotic (penstrep) (Whitehead Scientific, 17-745E). At confluence, cells were trypsinated using 0.25% EDTA-trypsin (Whitehead Scientific, BE02-007E). bEnd5 culture conditions for cell growth was 37^oC with 95% humidity and 5% CO_2.

2.3 Treatment Protocol

For the trypan blue assay, bEnd5 ECs were seeded at a density of 50 000 cells in clear 6-well tissue culture plates (n=6), and were incubated for 24hrs to allow for attachment. For RNA extraction and subsequent PCR analysis, bEnd5 ECs were seeded at a density of 150 000 cells in clear 90mm tissue

culture treated petri dishes (n=6). Thereafter the ECs were exposed to 25mM and 100mM EtOH (Sigma, E7023); R_f containing equivalent of 1.9nM aspalathin (South African Rooibos Council, Batch no. P06/02KK), as well as combinations of 25mM EtOH and R_f and 100mM EtOH and R_f, respectively. After 24hrs, all media was replaced with untreated DMEM. The cells were then incubated for the selected time intervals of 24, 48, 72, and 96hrs.

2.4 Trypan Blue Exclusion Assay

Trypan Blue is a dye used to identify the amount of viable cells present in a sample. Non-viable cells absorb the trypan blue dye via a non-selective process whereas viable cells do not absorb the dye, thus when viewed under a light microscope; dead cells stain blue while unstained cells will indicate viable cells (Mascotti et al., 2000, Strober, 2001). An established ratio was used (10µl of cell suspension, 30µl trypan blue dye, and 60µl complete DMEM). 10µl was then added to the haemocytometer and observed under an inverted phase contrast microscope for cell counts. Live cell number (Cadena-Herrera et al., 2015) and subsequent rate of cell division was established using the live cell number; whereas % cell viability and % cell toxicity (Masters and Stacey, 2007) was determined using the following equations:

$$\text{Cell Viability (\%)} = \frac{\text{Number of unstained (live) cells}}{\text{Total number of cells}} \text{ X } 100$$

$$\text{Cell Toxicity (\%)} = \frac{\text{Number of stained (dead) cells}}{\text{Total number of cells}} \text{ X } 100$$

2.5 Transcription analysis

2.5.1 Ribonucleic acid (RNA) Extraction of bEnd5 cells

Phenol-chloroform extraction is a liquid-liquid extraction. A liquid-liquid extraction is a method that separates mixtures of molecules based on the differential solubility's of the individual molecules in two different immiscible liquids. Liquid-liquid extractions are widely used to isolate RNA, deoxyribonucleic acid (DNA), or proteins (Stenesh, 1989). bEnd5 cells exposed to the above conditions were rinsed twice with 1ml phosphate buffer serum (PBS) (Lonza, Whitehead Scientific, BE17-516F). 1ml of cold Tripure (Roche, 11667165001) was then added to each petri dish plated with exposed cells at the respective time interval and homogenized. Each ml of homogenate was transferred to a 2ml eppendorf and incubated for 5min at room temperature. Tripure disrupts the cell wall and releases the content of the cell. 0.2ml of chloroform (Kimix, SA, chl001) was added to the homogenate and vortexed for 15sec. This was then incubated for 5-10 minutes at room temperature. The solution was separated into three phases by centrifuging at 12 000g for 15min. 400µl of the upper aqueous phase was transferred to a 1.5ml eppendorf. Subsequently, 0.5ml of isopropanol (Kimix, SA, ipr001) was added to the solution, and mixed thoroughly. RNA precipitated overnight at -20ºC. RNA was then centrifuged at 12 000g for 10min and the supernatant removed. Following this, 1ml of 75-80% molecular EtOH was added to the RNA pellet, vortexed and centrifuged at 7500g for 5min. The supernatant was aspirated and the pellet was re-suspended in 100µl DEPC-treated water (Invitrogen, AM 9916). The quality of the RNA samples was interrogated using the Nanodrop ND-1000 (Thermo Scientific, ND1000).

2.5.2 Gene amplification Optimization

An aliquot of cDNA synthesized from all RNA samples was pooled and used to generate an 8-point, 2-fold serial dilution series in order to determine the efficiency of the primer sets. The dilution series was used as qPCR template and the reference and target genes were assayed using 125nM of each primer set. All three genes (β-actin, occludin, and claudin-5) failed to amplify. A serial dilution was then generated using only 12 control bEnd5 samples in case gene expression is diluted when using all samples. *Mus musculus* Occludin (Whitehead Scientific, forward primer: 5'- GTT GAA CTG TGG ATT GG - 3', reverse primer: 5'- ATT GGG TTT GAA TTC ATC AG - 3') failed to amplify once again, and *Mus musculus* Claudin-5 (Whitehead Scientific, forward primer: 5'- GGG TGA GCA TTC AGT CTT TA - 3', reverse primer: 5'- CAG CAC AGA TTC ATA CAC CT - 3') showed very low expression. PCR inhibition was suspected and the 12 control samples were cleaned-up using NaOAc/ethanol precipitation (Ambion AM9740, Kimix, SA, UN1170). New reference gene primers, *Mus musculus* hypoxanthine guanine phosphoribosyltransferase (HPRT) (Whitehead Scientific, sequence ID: NM 013556.2, forward primer: 5'- AGT CCC AGC GTC GTG ATT AG - 3', reverse primer: 5'- TCC AAA TCC TCG GCA TAA TG - 3') and *Mus musculus* glyceraldehyde-3-phosphate dehydrogenase (GAPDH) (Whitehead Scientific, sequence ID: NM 001289726.1, forward primer: 5'- GTC GGT GTG AAC GGA TTT G - 3', reverse primer: 5'- TGG CAA CAA TCT CCA CTT TG - 3'), were then used. GAPDH and HPRT amplified in the bEnd5 control samples indicating that the RNA was intact and functional. No amplification was observed for β-actin in the bEnd5 control samples, and the use of the primers were therefore discontinued and replaced by GAPDH and HPRT primer sets. *Mus musculus* spleen RNA samples were used as an external control to generate an 8-point, 2-fold serial dilution series. A standard curve was generated by plotting the Ct value of each serial dilution point against the known quantity of cDNA in each serial dilution. Each standard curve was generated in triplicate for each data point. The calculated polymerase chain reaction (PCR) efficiency, slopes and

R^2values are detailed in Table 1. All amplification curves were submitted for a melt-curve analysis to evaluate primer specificity. No primer-dimers or non-specificity was observed in HPRT, GAPDH or Claudin-5.

Table 1: qPCR amplification efficiency for target genes.

Gene name	**Slope**	**R^2 value**	**PCR efficiency (%)**
β-actin	N/A	N/A	N/A
HPRT	-3.2	0.975	105%
GAPDH	-3.8	0.99	83%
Claudin-5	-3.14	0.987	110%
Occludin	N/A	N/A	N/A

2.5.3 cDNA synthesis

A starting concentration of 2µg RNA was used for cDNA synthesis. For each sample, two reactions were carried out. A reverse transcriptase buffer, random primers, dNTP mix, MultiScribe™ reverse transcriptase (High Capacity cDNA synthesis Kit) (Life Technologies, 4368814) and nuclease-free water (BIO-37080 Bioline Water, 18.2MΩ PCR Grade) were added to 10µl of RNA sample up to a total reaction volume of 20µl. The components were thoroughly mixed and spun down using a bench top centrifuge to collect all the liquid. Cycling was performed on the GeneAmp® PCR System 9700 (Life Technologies) using the cycling parameters tabulated in table 2.

Table 2: cDNA synthesis cycling parameters.

	Step 1	**Step 2**	**Step 3**	**Step 4**
Temperature (°C)	25	37	85	4
Time	10 min	120 min	5 min	∞

The synthesized cDNA was stored at -20 °C until further processing. Before expression analysis, each experimental sample was diluted 1:5 with nuclease-free water (BIO-37080 Bioline Water, 18.2MΩ PCR Grade).

2.5.4 Gene expression analysis

For gene expression analysis, each reaction (for standard curves and samples) consisted of 1µl cDNA template (equivalent to approx. 200ng RNA); 0.125µl of each of the primers (final concentration of 125nM); 5µl Power Sybr® Green PCR Master Mix (Life Technologies, 4367659) and nuclease-free water. Expression analysis was performed on the ABI 7900HT Fast Real Time PCR system using the cycling parameters listed in table 3, followed by a dissociation (melt) curve analysis.

Table 3: qPCR cycling parameters.

Step	**Temperature (°C)**	**Time**	**Number of cycles**
Hold	95	10 min	1
Denature	95	15 sec	40
Anneal/Extend	60	60 sec	

Post cycling, the data was analysed using the SDS v2.3 software (Life Technologies) and relative expression analysis performed using qBase+(BioGazelle).

2.6 Transepithelial electrical resistance

Across the *in vitro* blood brain barrier, TEER was measured using an Ohm Millicell-ERS (Electrical Resistance System) (Millipore, MERS 000 01), which measures the membrane potential and resistance of the epithelial cells in culture. TEER is employed to evaluate integrity and permeability of epithelial monolayers, as it is an instant measure of ion flux and an indirect measurement of the formation of TJs (Derk et al., 2015). The TEER measurements of the blank inserts were subtracted from the readings that were obtained from the inserts with confluent endothelial monolayers so that the true resistance could be determined. The blank inserts consisted of media with and without the respective experimental compounds, respectively. More importantly, no cells were present in the blank inserts. Furthermore, the resistance between the blank inserts containing only media and the blank inserts containing media with the respective experimental compounds were similar. The controls were implemented by growing confluent endothelial monolayers. These monolayers were not exposed to any of the experimental compounds. The culture media was supplemented with 10% FBS, as TEER values using this concentration of FBS, remained consistent for longer in addition to aiding the proliferation of cells. An article by Derk et al. (2015) has confirmed that 10% FBS is the optimal concentration to use in culture media.

$$R_{sample}-R_{blank}=R_{cell\ monolayer}$$

$R_{cell\ monolayer}\ (\Omega) \times 0.6cm^2$ = Resistance normalized per square cm ($\Omega.cm^2$)

(Nb.: 0.6cm = surface area of insert use to grow monolayer of cells)

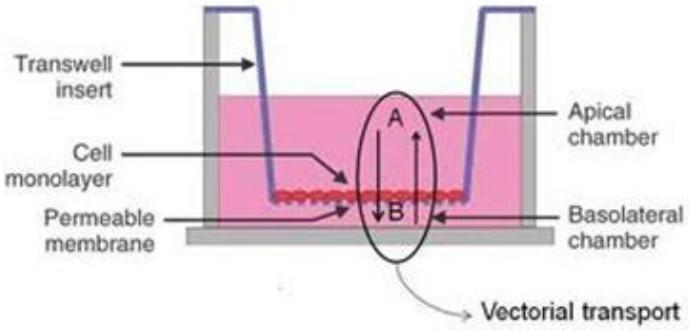

Figure 2.1: A schematic diagram of the bicameral chamber for TEER analysis of a bEnd5 EC monolayer. (http://www.pharmadirections.com/_blog/Formulation_Development_Blog/post/Biopharmaceutics_Classification_System_and_In-vitro_membrane_models/)

1×10^6 bEnd5 cells (Sigma, 96091930) were seeded per well on sterile inserts (Microsep, PIHA012) and grown to confluence for 24hrs in clear 24-well tissue culture plates (n=6). Samples were then exposed to 25 and 100mM EtOH (Sigma, E7023), R_f containing equivalent of 1.9nM aspalathin and combinations of 25 and 100mM EtOH together with R_f respectively for 24hrs. Following the 24hr exposure to the compounds, the various compounds were removed from the cells and replaced with untreated DMEM (Whitehead Scientific, 12-719F) and incubated for 24, 48, 72, and 96hrs. The blanks used contained 10% FBS-supplemented media, 10% FBS-supplemented media with 100mM EtOH, and 10% FBS-supplemented media with R_f. The controls contained 10% FBS.

The electrodes were immersed in the wells with the shorter electrode placed in the insert containing the media and the longer electrode was inserted through the basolateral access in the media within the growth well. The shorter electrode did not make contact with the cells growing on the membrane since it could pierce the monolayer, which could have resulted in a short circuit, hence the electrical current would not flow. Once stable, resistance readings were observed and the TEER values were recorded. Readings were taken in duplicate every 2hrs at three time intervals.

2.7 Scanning electron microscopy

High resolution scanning electron microscopy (SEM) was employed to visualize the fine detail of the cells growing on cellulose covered inserts to compare the morphological effects of alcohol, R_f, and the combinations on bEnd5 ECs. SEM was performed following TEER analysis.

2.7.1 Preparation of the bEnd5 monolayer for SEM

A 2.5% glutaraldehyde (Biochemica, Sigma, 49626) solution was prepared in a PBS solution. The mixed cellulose membranes containing the cells which were exposed to 25mM and 100mM EtOH, respectively, R_f equivalent to 1.9nM aspalathin, and the combinations thereof was placed in the 2.5% solution. After 1hr, the membranes were removed from the glutaraldehyde and washed twice in PBS (without glutaraldehyde) for 5min, followed by distilled water.

The cells were subsequently submitted for a dehydration procedure in ascending EtOH concentrations. The membranes encompassing the cells were removed from the distilled water and placed in a 50% EtOH solution (diluted with distilled water) for 10min. This was followed by a 70% EtOH solution, 90% EtOH solution, 95% EtOH solution, and 100% EtOH solution for 10min. The membranes with cells were removed from the 100% EtOH solution after 10min, and placed in a fresh solution of 100% EtOH for an additional 10min (Faso et al., 1994). The membranes with cells were removed from the 100% EtOH solution, and placed in a Hitachi critical point dryer (CPD) (Hitachi-HCP-2). CPD dehydrates biological samples preceding analysis in the scanning electron microscope (Zeiss). CPD is dependent on the principle referred to as the continuity of state whereby there is no noticeable modification between the liquid and gas state of a medium, ultimately resulting in the surface tension between this interface being reduced to zero. This event occurs at a specific pressure and temperature (Fig 2.2), and is established as the critical point (Bozzola and Russel, 1999).

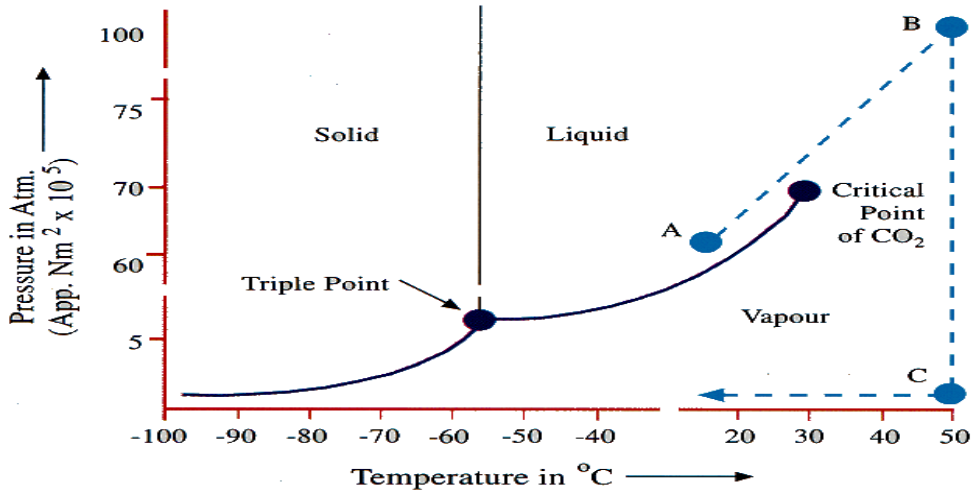

Figure 2.2: A graphical representation of how critical point drying is achieved.

Following CPD, the samples which were dried and rid of any fluids, was placed on double coated carbon conductive support (PELCO Tabs ™, 16084-01) on an aluminum stub (Agar Scientific, AGG301, 12.5mm diameter, 8mm pin). The sample was then sputter-coated with gold palladium (Quorum-Q1SOT ES), to insure that the specimens were electrically conductive, and electrically grounded to avoid the accretion of electrostatic charges at the surface the specimen. SEM was carried out on samples using a Zeiss scanning electron microscope.

2.8 Chemical Analysis of fermented rooibos (R_f) (Analysed by the Oxidative Stress Research Centre at CPUT)

The R_f (batch no. P06-02KK) extract utilized in this study was obtained from South African Rooibos Council and analysed by the Oxidative Stress Research Centre at the Cape Peninsula University of Technology (CPUT), Bellville, Cape Town. Furthermore the analyses conducted included the ferric reducing antioxidant power (FRAP), oxygen radical absorbance capacity, and ABTS (TEAC) assay, while the flavanol, flavonal, and total polyphenol content was also determined. In addition, the methodology used for the

respective chemical analysis (see Appendix A-F, page 129-137) and results of the analyses was supplied by the Oxidative Research Stress Centre for the characterization of the chemical composition and antioxidant capacity of the above mentioned extract, which is fundamental to determining the underlying mechanisms and properties of this extract and its interaction with our BBB model.

2.9 Statistical analysis

Medcalc (version 11.6.1) was used to statistically analyse the data obtained. Normality was determined using the Kolmogorov-Smirnov. The Student t-test (for normally distributed independent samples) and Mann-Whitney (for not normally distributed independent samples), was applied and the probability of $P<0.05$ was designated as statistically significant in comparison to controls. Consistent with the proposed objectives of this study, statistical differences between results elicited by the experimental compounds to that of untreated bEnd5 cells were investigated.

CHAPTER THREE

Results

3.1.1 Effects of selected concentrations of EtOH on bEnd5 cell viability.

The trypan blue assay is used to routinely to assay the viability status of the cell (Strober, 2001). We exposed bEnd5 cells to 25mM and 100mM EtOH for 24hrs and thereafter evaluated their viability over a period of 96hrs. As illustrated in Fig 3.1.1, cells exposed to 25mM and 100mM EtOH resulted in a significant decrease in viability from 24 to 96hrs ($P \leq 0.05$). It was, however, noted that the cells exposed to 25mM EtOH, displayed a trend of increased in viability between 24 and 96hrs, indicating possible recovery. This is further endorsed statistically, as the viability seen at 96hrs is significantly greater to the viability at 24hrs ($P < 0.05$). Furthermore, there was no statistical differences between the cell viability between cells exposed to 25mM EtOH, and cells exposed to 100mM EtOH, except at 72hrs, whereby cells exposed to 100mM EtOH elicited significantly lower viability than cells exposed to the lower concentration of EtOH.

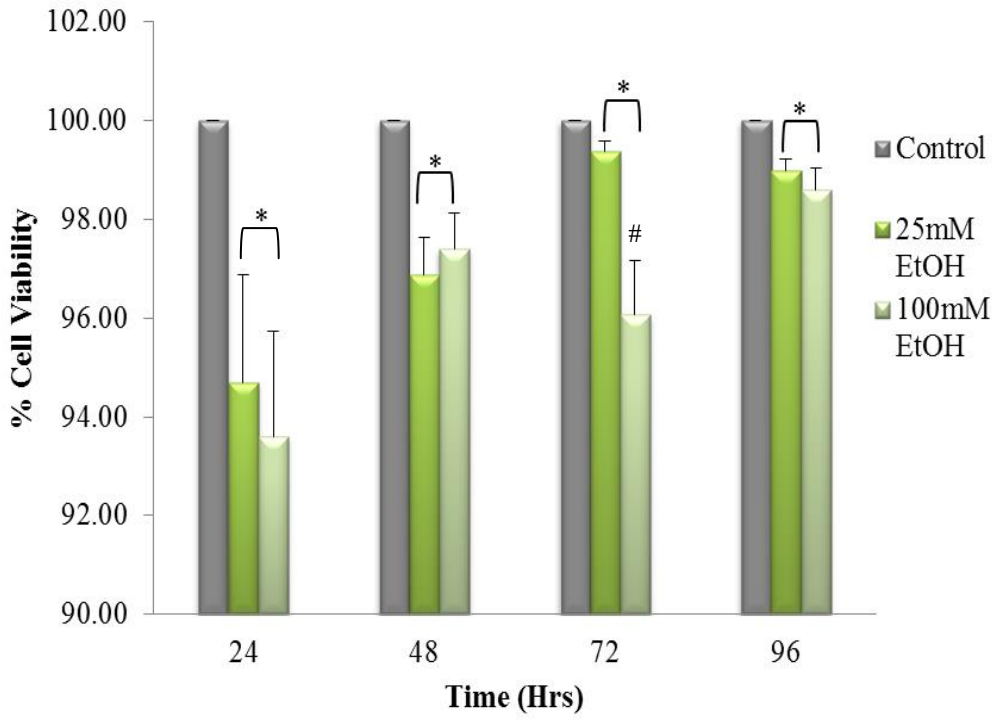

Figure 3.1.1: The above graph represents the effects of EtOH on bEnd5 EC viability as ascertained using the Trypan Blue Assay following a 24hr incubation period. * $P < 0.05$ denotes statistical significance compared to controls, while # displays inter-concentration statistical differences, analysed using the Students *t*-test. Results were displayed as mean ± SEM (n=6).

3.1.2 Effects of a selected concentration of R_f on bEnd5 cell viability.

We investigated the effects of exposing the bEnd5 cells to R_f equivalent to 1.9nM aspalathin, which is approximately equivalent to the plasma concentration after the ingestion of 500ml fermented rooibos tea, to evaluate the effects of R_f derived antioxidants on mouse brain endothelial cell viability, over a period of 96hrs. We observed that R_f exposure resulted in a decrease in bEnd5 viability at 24 and 48hrs, which recovered between 72 and 96hrs ($P \leq 0.05$). Furthermore, the viability of R_f-exposed cells were significantly greater at 96hrs than the viability at 24hrs (P=0.0399), further plausibly indicating that recovery has taken place. This data indicates that R_f-derived antioxidants are detrimental to the viability of brain endothelial cells.

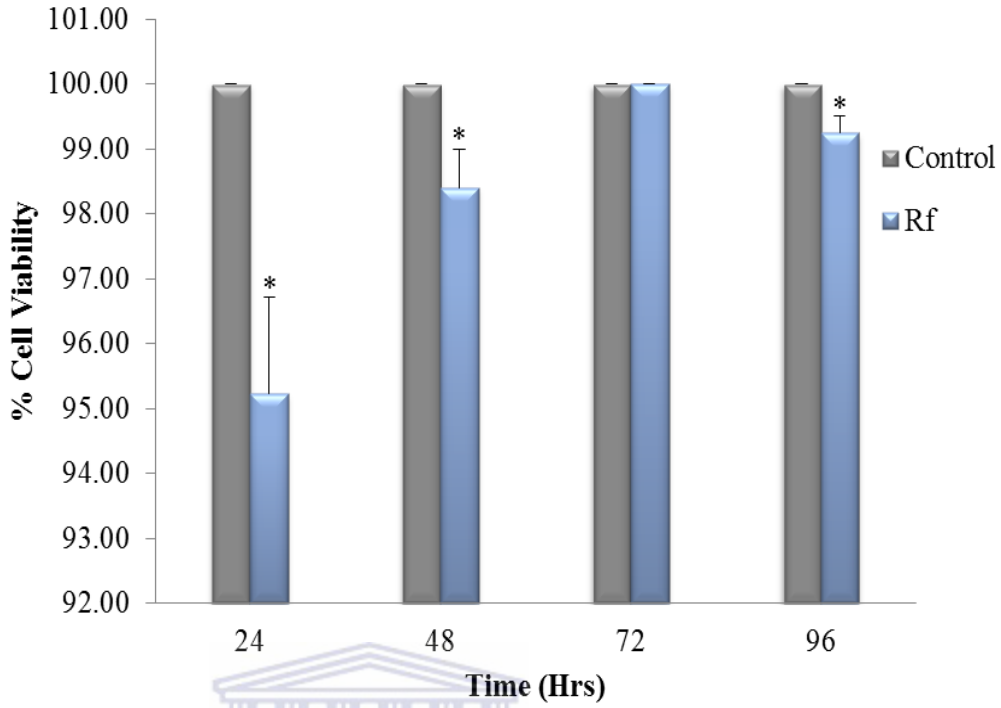

Figure 3.1.2: The graph represents the effects of R_f on bEnd5 EC viability following a 24hr incubation period. * $P < 0.05$ designates statistical significance compared to controls as ascertained using the Students *t*-test. Results were displayed as mean ± SEM (n=6).

3.1.3.1 Effects of R_f on 25mM EtOH exposure on bEnd5 cell viability.

As it is well established that alcohol causes excess amounts of ROS production (Haorah et al., 2005), and since R_f contains copious amounts of antioxidants, we investigated whether the simultaneous exposure of R_f could potentially nullify the effects of alcohol. We therefore exposed bEnd5 cells to the combinations of 25mM EtOH and R_f to evaluate their viability over a period of 96hrs.

As depicted in Fig 3.1.3.1, cells exposed to the simultaneous exposure of 25mM EtOH and R_f, as well as cells exposed only to 25mM EtOH, led to a significant decrease in viability across the 96hr experimental timeframe ($P \leq$

0.05). The trend of ECs exposed to 25mM EtOH and R_f was statistically similar across time. Furthermore, R_f reduced the effects of EtOH on bEnd5 cell viability at 72hrs, but was unable to statistically reverse it.

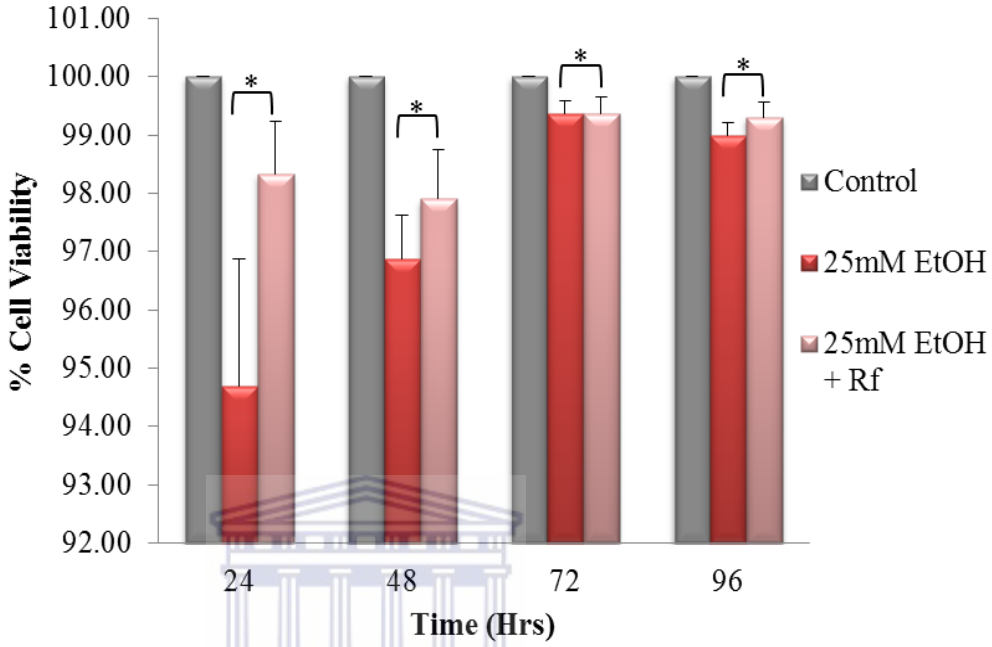

Figure 3.1.3.1: The graph represents the effects of the simultaneous exposure of 25mM EtOH and R_f on bEnd5 EC viability following 24hr exposure. * $P < 0.05$ denotes statistical significance compared to controls as ascertained using the Students *t*-test. Results were displayed as mean ± SEM (n=6).

3.1.3.2 Effects of R_f on 100mM EtOH exposure on bEnd5 cell viability.

We investigated if R_f could possibly nullify the effects of a supraphysiological concentration of EtOH (Fig 3.1.3.2). As previously illustrated and shown in the graph below (refer Fig 3.1.1), exposure to 100mM EtOH resulted in a statistical decrease in bEnd5 cell viability ($P \leq 0.05$). Furthermore, cells exposed simultaneously to 100mM EtOH and R_f diminished bEnd5 viability at 24 and 48hrs ($P \leq 0.05$), while illustrating recovery by 72hrs. More importantly, the effects of a supraphysiological concentration of EtOH, 100mM, were reversed at 72hrs, with the cell

viability of cells exposed to 100mM EtOH being significantly lower than that of 100mM EtOH and R_f.

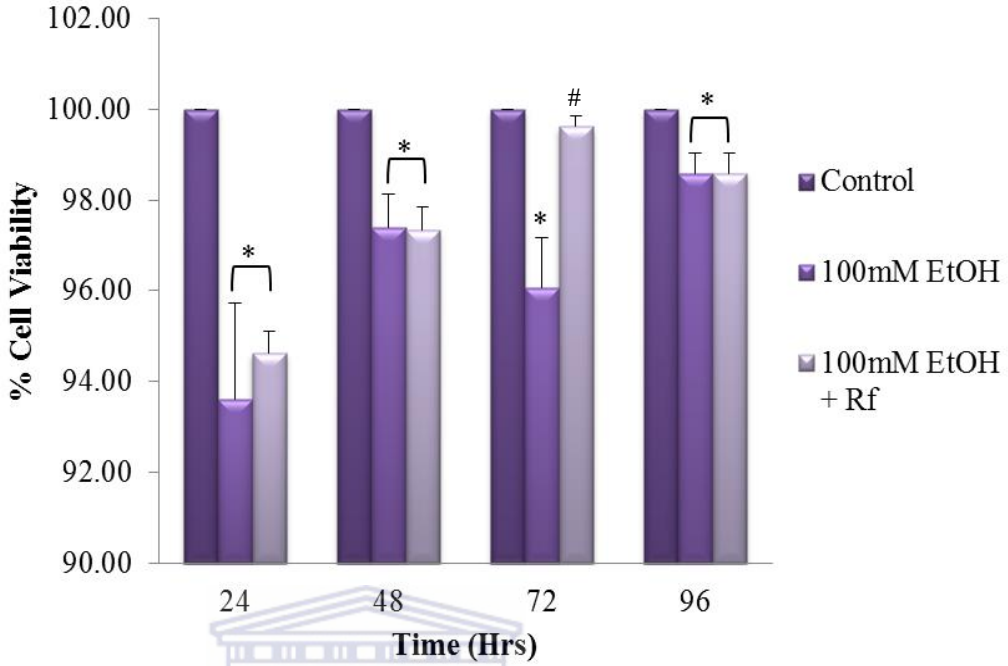

Figure 3.1.3.2: The graph represents the effects of 100mM EtOH and R_f on bEnd5 EC viability following 24hr exposure. * $P < 0.05$ denotes statistical significance compared to controls, while # displays statistical differences between 100mM EtOH and 100mM EtOH + R_f, as ascertained using the Students *t*-test. Results were displayed as mean ± SEM (n=6).

3.1.4 Summary: The effects of EtOH, R_f, and combinations thereof on bEnd5 cell viability

- EtOH decreased viability of mouse brain endothelial cells between 24 and 96hrs.
- R_f decreased viability at 24 and 48hrs, but viability recovered between 72 and 96hrs.

- Cells exposed simultaneously to R_f and 25mM EtOH reduced the effects of 25mM EtOH on bEnd5 cells, however not being able to statistically reverse it.

- The simultaneous exposure of R_f with 100mM EtOH, was able to reverse the effects of 100mM EtOH by 72hrs.

3.2.1 Effects of selected concentrations of EtOH on bEnd5 live cell number.

We exposed bEnd5 cells to 25mM and 100mM EtOH for 24hrs and thereafter evaluated the number of live cells over a period of 96hrs. The live cell number of untreated bEnd5 ECs increased linearly from 24 to 96hrs ($P \leq 0.05$). We established that both concentrations of EtOH resulted in an overall statistical decrease in live cell number until 72hrs ($P \leq 0.05$) (Fig 3.2.1). Comparing the number of EtOH-exposed live cells to the control cells would indicate whether EtOH exposure has an effect on the division of cells. It was interesting to note that the effects of both EtOH concentrations were similar across time and did not exhibit a dose response.

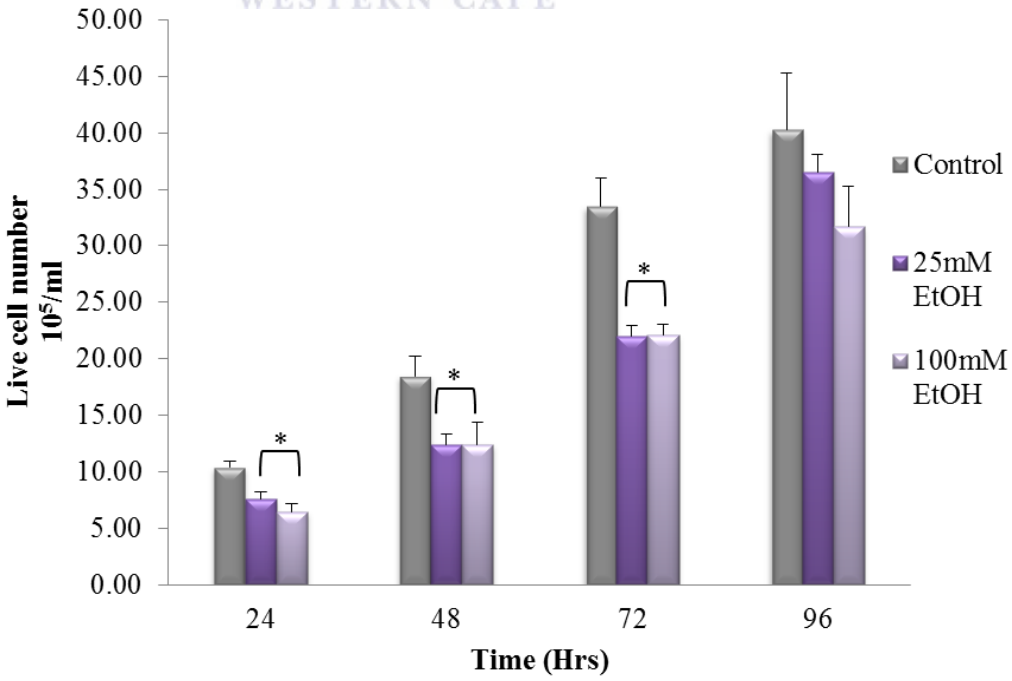

Figure 3.2.1: The graph represents the effects of selected concentrations of EtOH on bEnd5 EC live cell number following 24hr exposure. * $P < 0.05$

designates statistical significance compared to controls ascertained using the Students *t*-test. Results were displayed as mean ± SEM (n=6).

3.2.2 Effects of a selected concentration of R_f on bEnd5 live cell number.

As illustrated in Fig 3.2.2, we investigated the effects of R_f on the live cell number of bEnd5 cells. We found that at 24 and 48hrs, the number of live cells exposed to R_f did not differ statistically to the controls ($P > 0.05$), while at the latter time intervals, 72 and 96hrs, R_f resulted in a significant decline in the live cell number ($P \leq 0.05$) (Fig 3.2.2). This is suggestive that exposure to R_f-antioxidants posed a long term effect on bEnd5 cells.

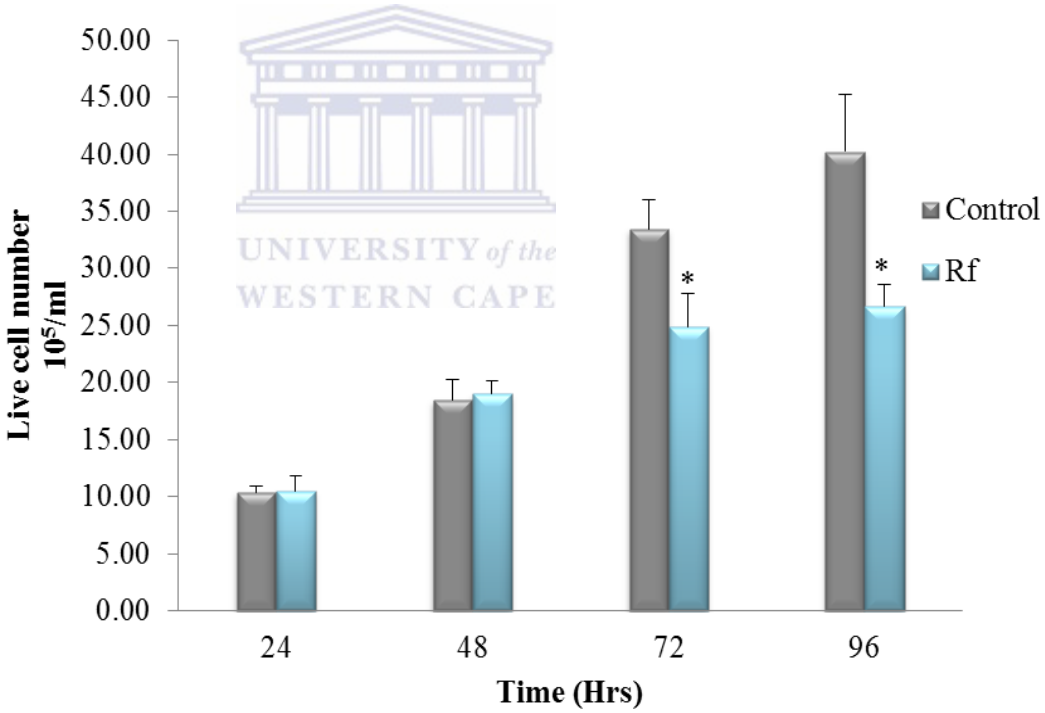

Figure 3.2.2: The graph represents the effects of a selected concentration of R_f on bEnd5 live cell number following a 24hr incubation period. * $P < 0.05$ denotes statistical significance compared to controls analyzed using the Students *t*-test. Results were displayed as mean ± SEM (n=6).

3.2.3 Effects of combinations' exposure on bEnd5 live cell number.

When analyzing the influence of R_f on the EtOH-induced effects on EC live cell number, we observed that with the combinations of 25mM EtOH and R_f; R_f reversed the effects of EtOH at 25mM and also negated the effects of 100mM EtOH statistically over 96hrs, with only the data of 72hrs being significantly different from the control. The subsequent data at 96hrs show a trend of full recovery from 100mM EtOH (Fig 3.2.3).

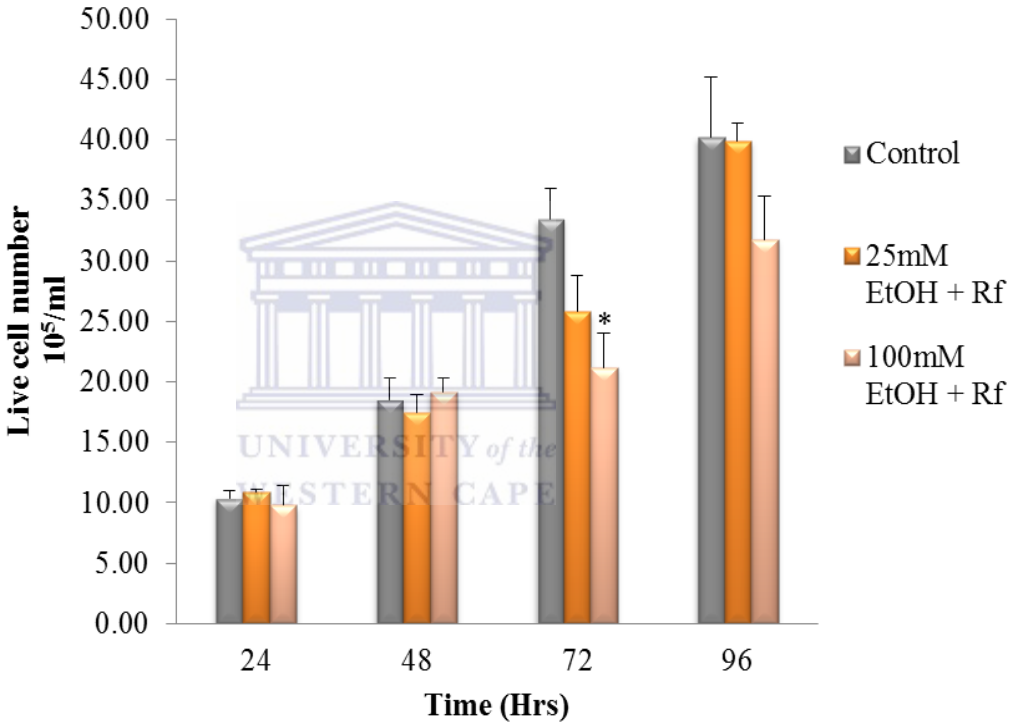

Figure 3.2.3: The graph represents the effects of selected concentrations of 25mM and R_f and 100mM and R_f on bEnd5 live cell number following a 24hr incubation period. * $P < 0.05$ denotes statistical significance compared to controls analyzed using the Students *t*-test. Results were displayed as mean ± SEM (n=6).

3.2.4 Summary: The effects of EtOH, R_f, and combinations' exposure on bEnd5 live cell number.

- Both concentrations of EtOH decreased live cell number of bEnd5 cells across 72hrs.
- The number of live cells exposed to R_f decreased at 72 and 96hrs, indicating a long term effect, showing that R_f-derived antioxidants also has a negative effect on cell division.
- The combination of 25mM EtOH and R_f resulted in live cell numbers that was statistically not different to the controls, indicating that R_f could reverse the effects of EtOH.
- The combinations of 100mM EtOH and R_f resulted in live cell numbers not statistically different to the controls at 24. 48, and 96hrs, while only decreasing statistically at 72hrs. Thus indicating that even at supraphysiological concentrations R_f had been able to reverse the negative effects of alcohol on the ECs of the BBB.

3.3.1 Effects of selected concentrations of EtOH on the rate of cell division.

Based on the differential daily increase of cell numbers we used regression analysis to calculate the straight line equations for controls, EtOH concentrations, and R_f interventions. The slopes of the resultant lines approximate the average rates of cell division for the selected time period. As the data was linear between 24 and 72hrs for all groups we approximated the rate for cell division using the slopes of these lines (Fig 3.3.1). The slope for the control line was 0.4809 cells/hr while that of EtOH was 0.2995 cells/hr and 0.325 cells/hr, respectively for 25mM and 100mM EtOH. The lower slopes of 25mM and 100mM EtOH indicated that the rate for cell division was suppressed relative to the control rates (Table 4).

Table 4: The effects of selected concentrations of EtOH on the rate of cell division.

Control	25mM EtOH	100mM EtOH
y=0.4809x-2.2889 R^2=0.9712	y=0.2995x-0.3611 R^2=0.9643	y=0.325x-1.9278 R^2=0.9809

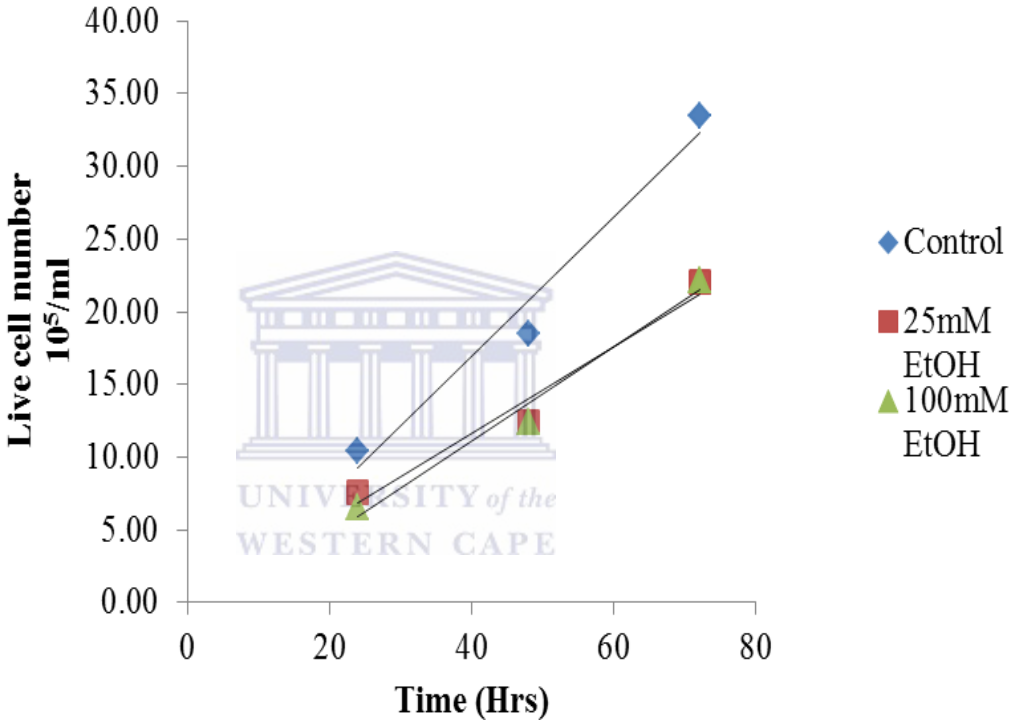

Figure 3.3.1: The graph represents a regression analysis on the effects of selected concentrations of EtOH on bEnd5 live cell number following 24hr exposure.

3.3.2 Effects of a selected concentration of R_f on the rate of cell division.

As illustrated in Fig 3.3.2, the rate of cell division in response to R_f is significantly slower than that of the controls (Fig 3.3.2; Table 5), corroborating the decline observed in the number of live cells (Fig 3.2.2). This is suggestive that exposure to R_f-derived antioxidants posed a long term effect on bEnd5 cells.

Table 5: The effects of a selected concentration of R_f on the rate of cell division.

Control	**R_f**
y=0.435x-0.475 R^2=0.978	y=0.226x+6.687 R^2=0.926

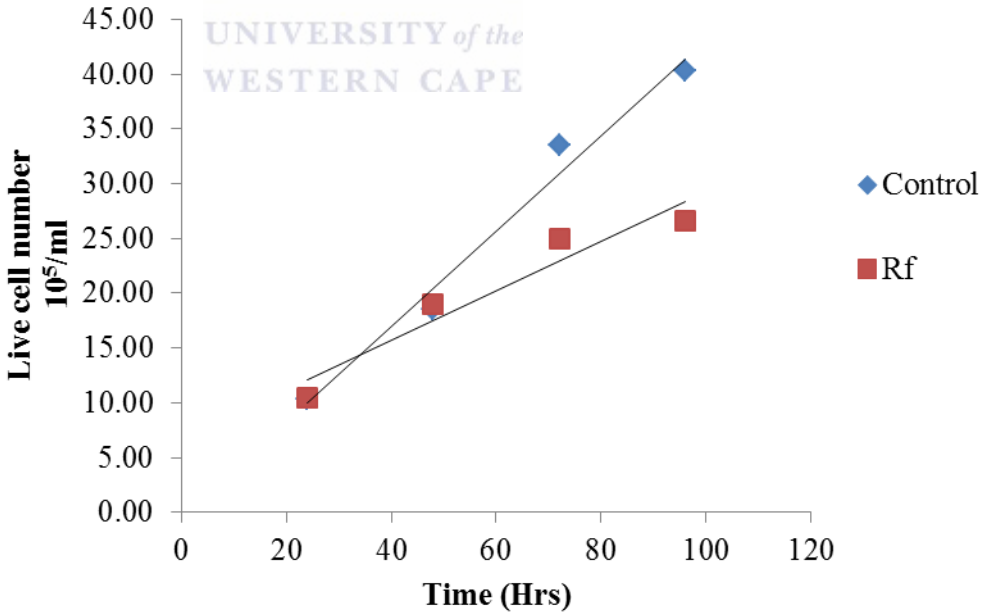

Figure 3.3.2: The graph represents a regression analysis on the effects of a selected concentration of R_f exposure on bEnd5 live cell number following 24hr exposure.

3.3.3 The combinatorial effects of EtOH and R_f on the rate of cell division.

In terms of the rate of cell division, cell division in response to both combinations was significantly slower than the control (Fig 3.3.3; Table 6). When comparing the data of 24hrs to that of 96hrs, R_f significantly contributed to the recovery of cells exposed to 25mM EtOH.

Table 6: The effects of combinations' exposure on the rate of cell division.

Control	**25mM EtOH and R_f**	**100mM EtOH and R_f**
y=0.435x-0.475 R^2=0.978	y=0.397x-0.295 R^2=0.967	y=0.299x+3.514 R^2=0.988

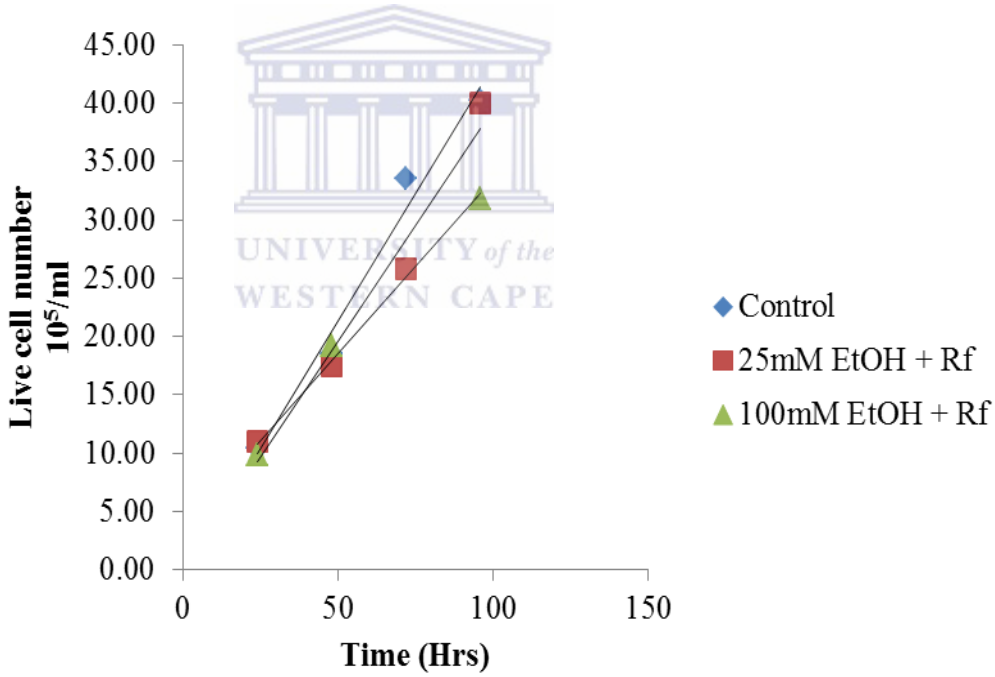

Figure 3.3.3: The graph represents a regression analysis on the effects of selected concentrations of 25mM and R_f and 100mM and R_f on bEnd5 live cell number following a 24hr incubation period.

3.4.1 Effects of EtOH, R_f, and combinations' exposure on bEnd5 cell toxicity.

As illustrated in Fig 3.4.1, we investigated the effects of 25mM EtOH, 100mM EtOH, R_f, as well as the combinations thereof, on cell toxicity using the trypan blue exclusion assay (Avelar-Freitas et al., 2014). Percentage toxicity is scientifically defined as the percentage of dead cells to the total population of cells. Statistically, untreated bEnd5 cells expressed less toxicity ($P \leq 0.05$), than cells exposed to both experimental compounds, EtOH and R_f. However, mouse brain endothelial cells exposed to 25mM and 100mM EtOH, both decreased in toxicity over the 96hr timeframe, indicating recovery between 72 and 96hrs. A similar trend was observed in bEnd5 cells exposed to R_f. To investigate the effects of R_f reversing the toxic effects of EtOH on bEnd5 cells, R_f was applied simultaneously to alcohol exposed cells. R_f treatment with EtOH did not exacerbate any EtOH effect. Furthermore, R_f ameliorated the level of 25mM EtOH toxicity across the 96hrs. The 100mM EtOH groups' toxicity was also decreased by R_f exposure at 24 and 72hrs.

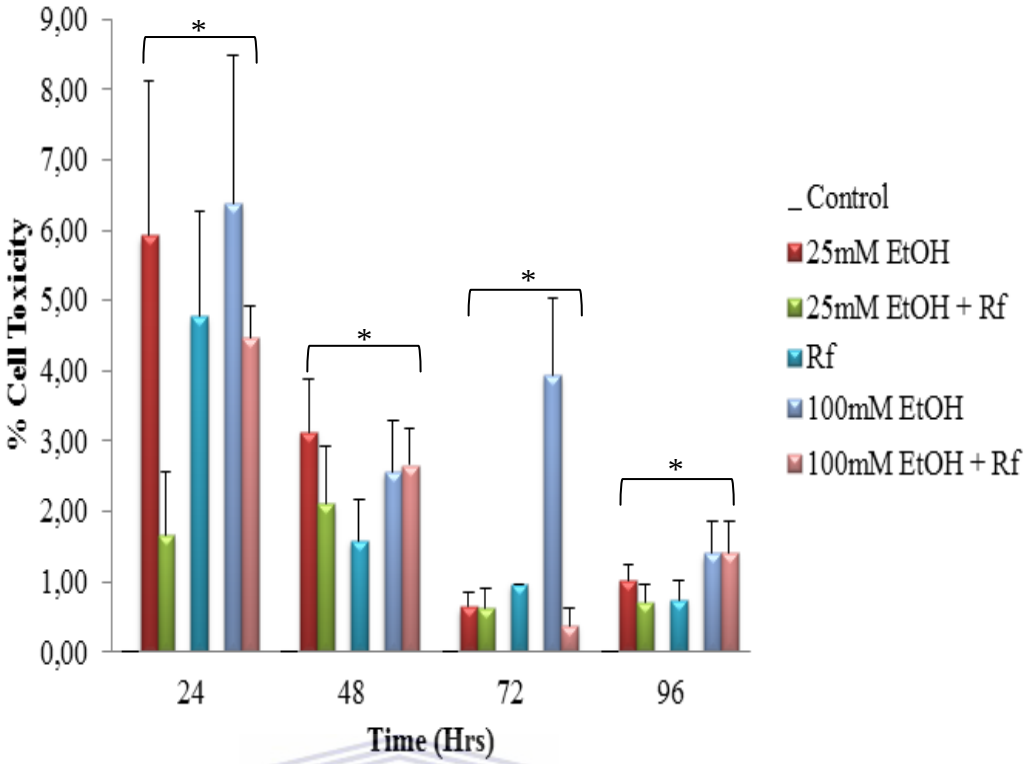

Figure 3.4.1: The graph represents the effects of selected concentrations of EtOH, R_f, and the combinations thereof, respectively on bEnd5 EC toxicity following 24hr exposure. *P < 0.05 denotes statistical significance compared to controls ascertained using the Students *t*-test. Results were displayed as mean ± SEM (n=6).

3.5.1 Effects of selected concentrations of EtOH on the relative transcription of paracellular TJ proteins in bEnd5 cells.

When investigating the effects of the selected concentrations of EtOH on TJ protein transcription, we found that the bEnd5 ECs, as recently reported in the literature (Steiner et al., 2011), did not express occludin and its transcription was not influenced by the exposure to the respective concentrations of EtOH or R_f, hence our focus was primarily shifted to investigate the effects of the EtOH and R_f on one of the critical proteins of BEC TJs, claudin-5. Our data established that the transcription of claudin-5 is not static but changed dramatically over the 96hrs (see Fig 3.5.1). Furthermore, exposure to 25mM EtOH did not affect the transcription of

claudin-5 between 24 and 72hrs ($P \geq 0.05$). EtOH at 100mM induced a sequence of up-regulation of claudin-5 transcription almost 4-fold at 24hrs, followed by suppression at 48hrs, though not statistical ($P \leq 0.05$), and slight up-regulation again at 72hrs. At 96hrs both concentrations of EtOH resulted in suppression of claudin-5 transcription. Furthermore, 100mM EtOH resulted in greater expression of claudin-5 than 25mM EtOH at 24hrs, while at 48hrs, it resulted in significantly lower claudin-5 expression than 25mM EtOH. At 72 and 96hrs, there was no statistical differences between the claudin-5 expression of the two concentrations of EtOH.

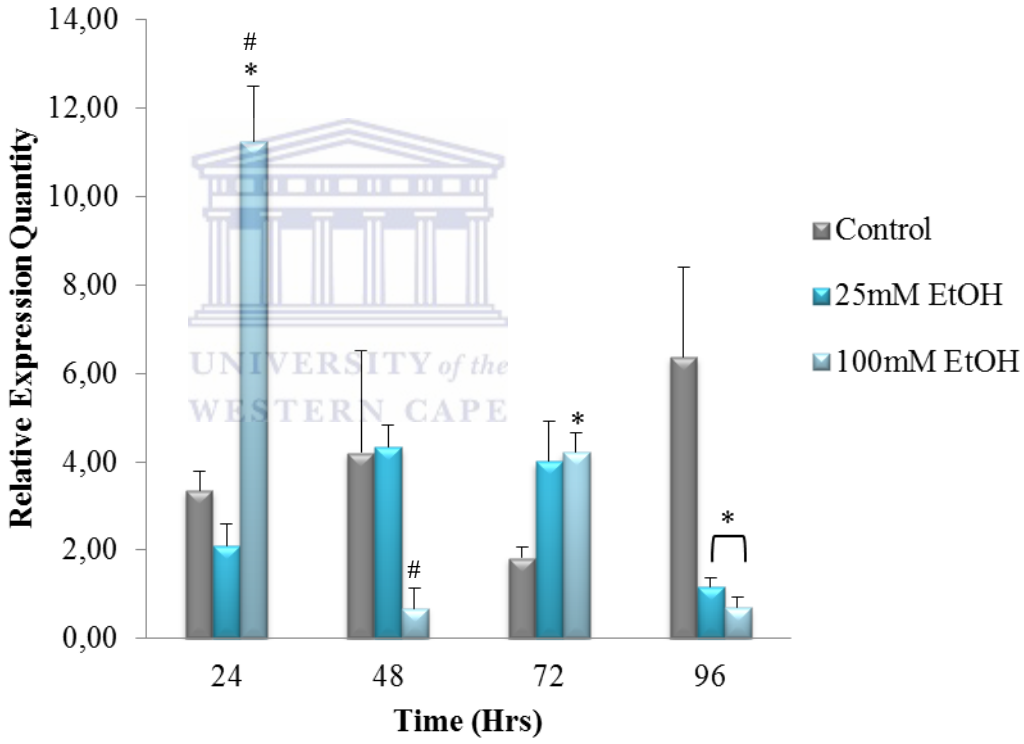

Figure 3.5.1: The graph represents the effects of 25 and 100mM EtOH following 24hr exposure, respectively, on the relative mRNA transcription of claudin-5 after normalization with HPRT and GAPDH. *P < 0.05 denotes statistical significance compared to controls, while # displays inter-concentration statistical differences between 25mM EtOH and 100mM, as analyzed using the Mann-Whitney test. Results were displayed as mean ± SEM (n=6).

3.5.2 Effects of a selected concentration of R_f on the relative transcription of paracellular TJ proteins in bEnd5 cells.

When investigating the effects of R_f on selected TJ expression, we found that similarly to EtOH, R_f did not influence relative mRNA expression of occludin. In addition, the administration of R_f to the bEnd5 ECs resulted in an overall down-regulation of claudin-5 transcription throughout the course of the experiment, except at 72hrs.

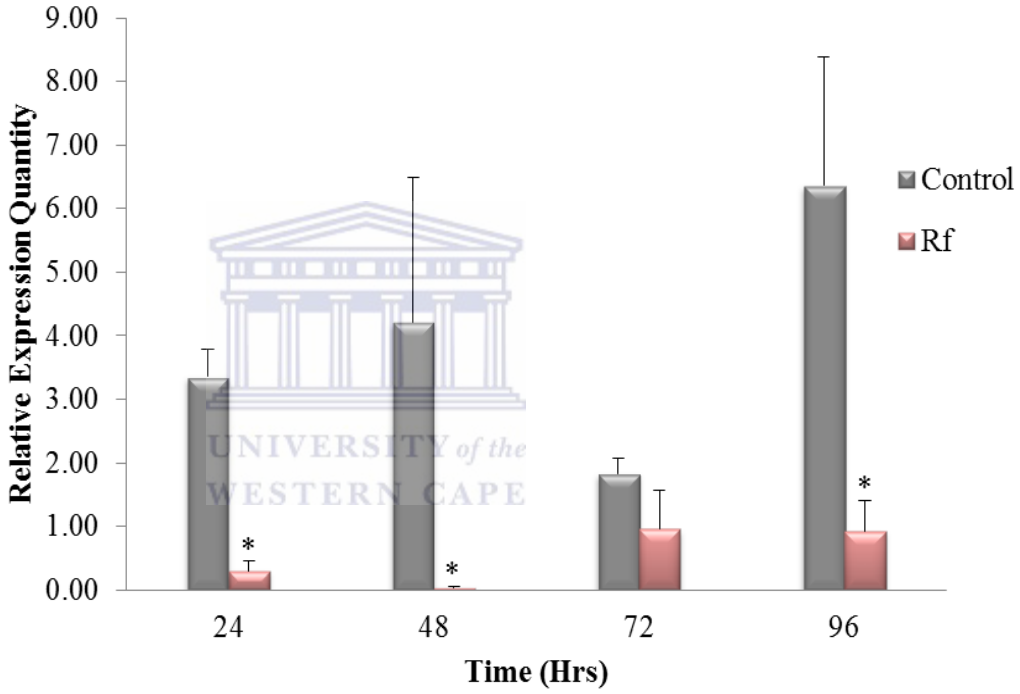

Figure 3.5.2: The graph represents the effects of R_f following 24hr exposure on the relative mRNA transcription of claudin-5 after normalization with HPRT and GAPDH. *P < 0.05 designates statistical significance compared to controls analyzed using the Mann-Whitney test. Results were displayed as mean ± SEM (n=6).

3.5.3 Effects of the combinations' exposure on the relative transcription of claudin-5 in bEnd5 cells.

We investigated the simultaneous effects of EtOH and R_f combinations on the mRNA transcription of claudin-5. Both 25mM and 100mM EtOH, treated together with R_f resulted in a similar effect, generally down-regulating claudin-5 mRNA transcription ($P \leq 0.05$), with the exception of 72hrs ($P \geq 0.05$), whereby it was no different from the controls. In summary, the simultaneous use of EtOH and R_f caused suppression of claudin-5 throughout the course of the experiment, with the exception of 72hrs.

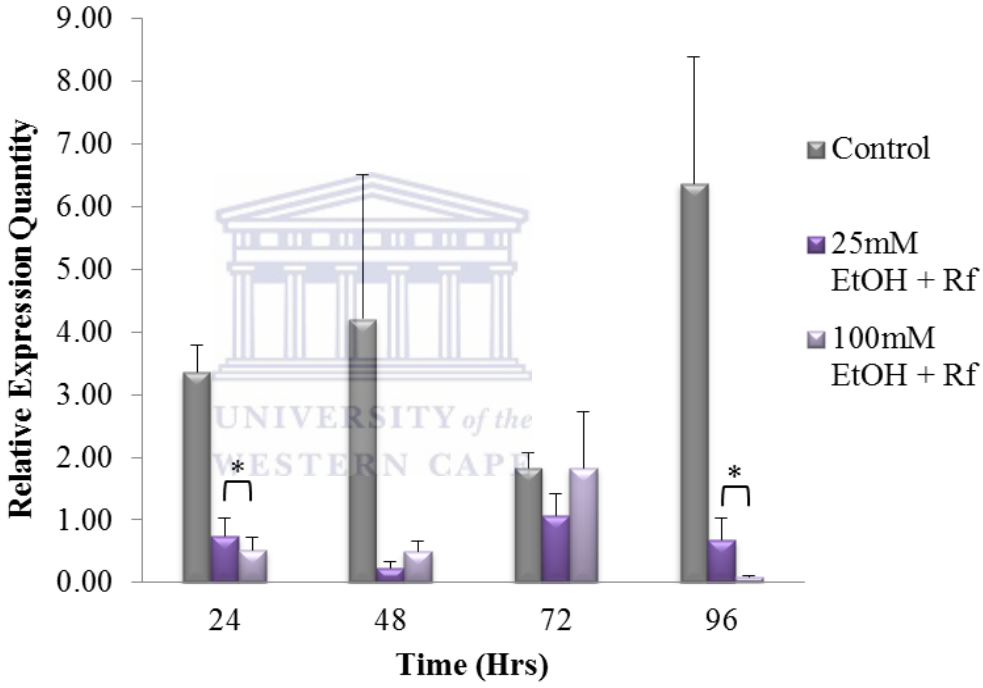

Figure 3.5.3: The graph represents the effects of 24hr combinations' exposure on the relative mRNA transcription of claudin-5 after normalization with HPRT and GAPDH. *P < 0.05 denotes statistical significance compared to controls. Results were displayed as mean ± SEM (n=6).

3.5.4 Summary: Effects of selected concentrations of EtOH, R_f, and the combinations thereof on the relative transcription of paracellular TJ protein: Claudin-5.

- Cells exposed to 25mM EtOH expressed similar claudin-5 transcription to that of the controls between 24 and 72hrs ($P \geq 0.05$), while resulting in the down-regulation of claudin-5 at 96hrs ($P \leq 0.05$).
- The administration of 100mM EtOH up-regulated claudin-5 transcription at 24 and 72hrs significantly ($P \leq 0.05$), while diminishing transcription at 48 and 96hrs, though not all statistical.
- R_f down-regulated claudin-5 transcription across the timeframe of the experiment, particularly between 24 and 48hrs, with the exception of 72hrs.
- The relative mRNA transcription of claudin-5 was lower in response to R_f than EtOH and this was further exacerbated by the combinations, which failed to reverse the effects of EtOH.

3.6.1 Effects of selected concentrations of EtOH on transepithelial electrical resistance of monolayers of bEnd5 ECs.

Tight junctions play an important role in the regulation of permeability. We investigated the permeability across monolayers of bEnd5 cells by measuring the transepithelial electrical resistance (TEER) across the monolayers. ECs exposed to 25mM EtOH resulted in a statistical decrease in TEER measured across the endothelial monolayers from 24 to 96hrs ($P \leq 0.05$). At 25mM EtOH TEER was consistently decreased by 10-15 $\Omega.cm^2$. Cells exposed to 100mM EtOH also resulted in a decrease in TEER across the experimental timeframe. Across the experimental timeframe, TEER of ECs exposed to 25mM EtOH showed no daily statistical difference ($P \geq 0.05$). A cyclic trend was observed with cells incubated with 100mM EtOH, whereby the

resistance at 24hrs (15.04 Ω.cm^2) decreased to 5.66 Ω.cm^2 at 48hrs, followed by an increase to 13.94 Ω.cm^2 at 72hrs, and a decrease again to 9.8 Ω.cm^2 at 96hrs ($P \leq 0.05$). Furthermore, 100mM EtOH resulted in lower TEER readings than 25mM EtOH at 48 and 96hrs, while displaying no differences at 24 and 72hrs.

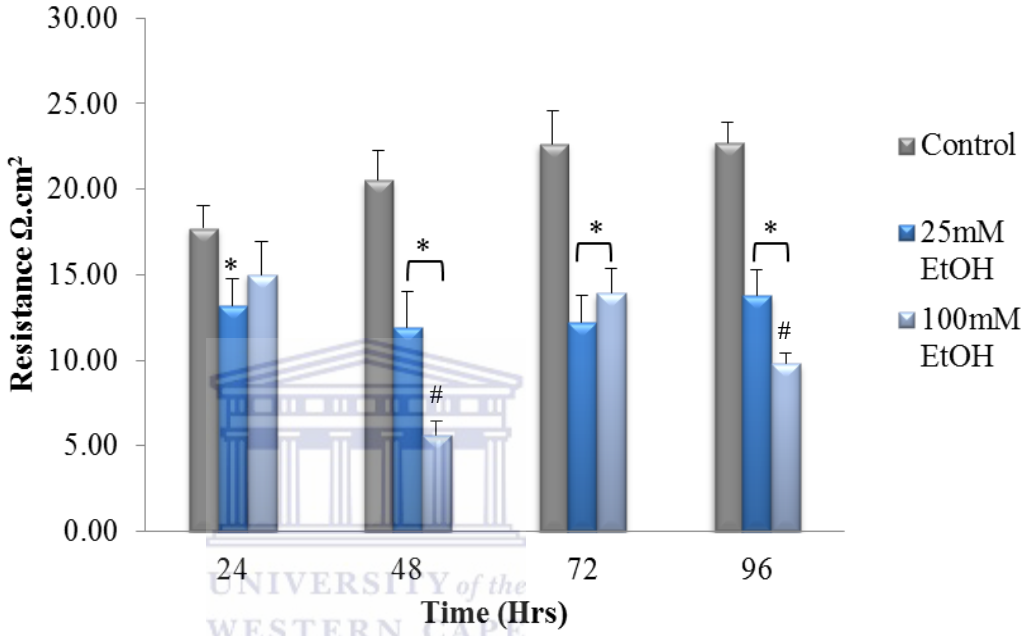

Figure 3.6.1: The graph represents the effects of 25mM and 100mM EtOH, respectively, on TEER following a 24hr exposure. * $P < 0.05$ denotes statistical significance compared to controls, while # displays statistical differences between 25mM and 100mM EtOH, ascertained using the Mann-Whitney Test. Results were displayed as mean ± SEM (n=6).

3.6.2 Effects of a selected concentration of R_f on transepithelial electrical resistance of monolayers of bEnd5 ECs.

In this study, after 24hr exposure, we looked at the effects of R_f on TEER in bEnd5 ECs. As illustrated in the Fig 3.6.2, the incubation of bEnd5 cells with a selected concentration of R_f, resulted in a significant decrease in TEER

across time from 24 to 96hrs ($P \leq 0.05$). The resistance of cells exposed to R_f was averaged at 10.63 $\Omega.cm^2$ across time and displayed no noticeable differences across the 96hrs ($P \geq 0.05$). The implication is that R_f extract may have a long term effect on the permeability of the BBB, as TEER showed no sign of recovery throughout the course of the experiment.

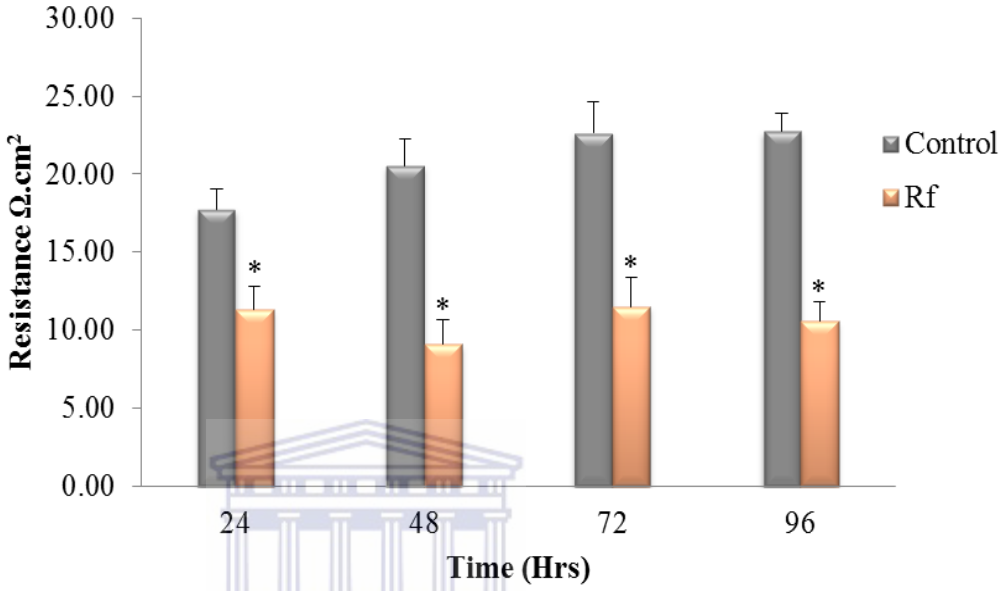

Figure 3.6.2: The graph represents the effects of R_f on TEER following 24hr exposure. * $P < 0.05$ denotes statistical significance as ascertained using the Mann-Whitney Test. Results were displayed as mean ± SEM (n=6).

3.6.3 Effects of combination exposures on transepithelial electrical resistance of monolayers of bEnd5 ECs.

When investigating the simultaneous effects of EtOH and R_f on TEER, we found, that the exposure of both 25mM and 100mM EtOH, treated together with R_f, produced a decrease in TEER of bEnd5 cells from 24 to 96hrs ($P \leq 0.05$). Furthermore, as illustrated in Fig 3.6.3, there was no statistical difference between the daily readings of both the combinations, although not significant, the lowest resistance was observed at 48hrs. Across the

experimental timeframe, 25mM EtOH and R_f, as well as 100mM EtOH and R_f, displayed a decrease in resistance from 24 to 48hrs ($P \leq 0.05$), followed by an increase from 48 to 72hrs ($P \leq 0.05$), and no change between 72 and 96hrs ($P \geq 0.05$). More importantly, the simultaneous exposure of R_f and EtOH exacerbated the EtOH-induced effects on TEER (compare Fig 3.6.1 to Fig 3.6.3).

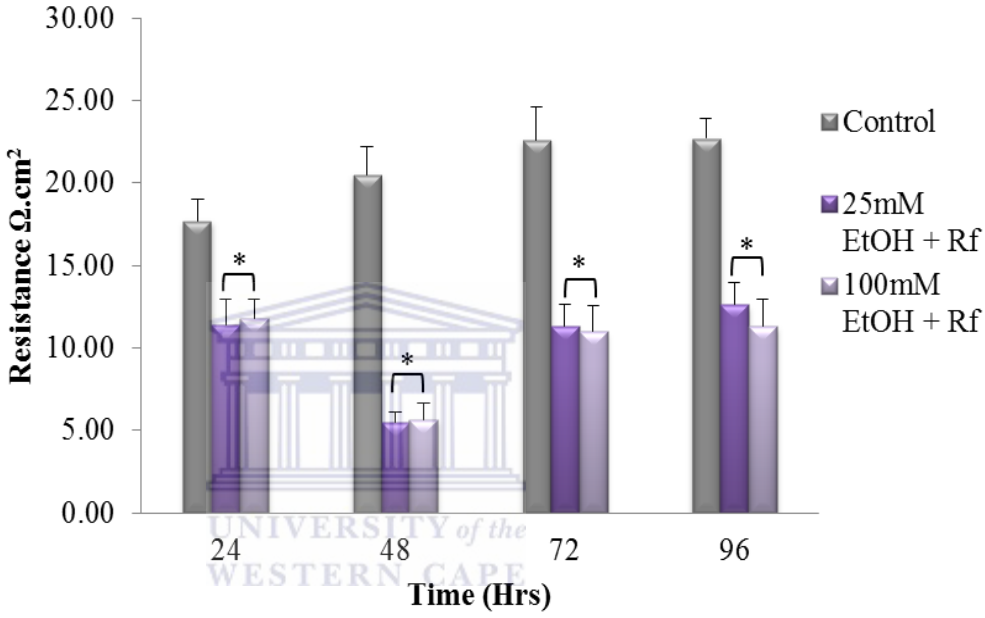

Figure 3.6.3: The graph represents the effects of 25mM EtOH and R_f, and 100mM EtOH and R_f, respectively, on TEER following 24hr exposure. * $P < 0.05$ designates statistical significance compared to controls ascertained using the Mann-Whitney test. Results were displayed as mean ± SEM (n=6).

3.6.4 Summary: Effects of selected concentrations of EtOH, R_f, and combinations' exposure on transepithelial electrical resistance of monolayers of bEnd5 ECs.

- Cells exposed to 25mM EtOH resulted in a decrease in TEER across the 96hr experimental timeframe and statistically did not change from day to day.

- Cells exposed to 100mM EtOH resulted in a decrease in TEER from 48 to 96hrs while showing no difference to the controls at 24hrs.
- TEER values of cells exposed to R_f displayed a decrease from 24 to 96hrs.
- The simultaneous administration of R_f to the EtOH-exposed ECs did not reverse or enhance the effects of EtOH on TEER.

3.7.1 Confluent monolayer of untreated bEnd5 ECs.

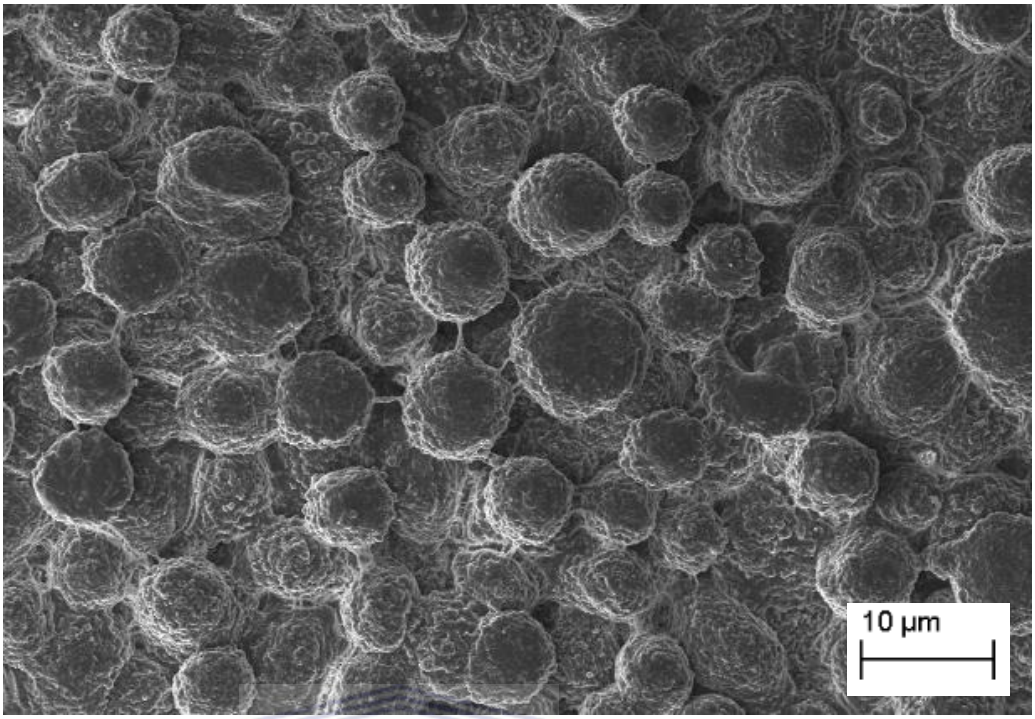

Figure 3.7.1: Ultrastructure of a monolayer of confluent bEnd5 cells at 1000X magnification (96hrs representation).

Tight junction proteins, such as claudin-5 are present on the latero-apical surfaces between adjacent ECs (Cardoso et al., 2010). These junctional proteins form the scaffolding of the BBB which could be compromised by certain exogenous substances and compounds. As illustrated in Fig 3.7.1, there were no noticeable compromised paracellular spaces between adjacent ECs indicating that BBB integrity was present prior to experimental exposure.

3.7.2 Ultrastructure of untreated bEnd5 ECs.

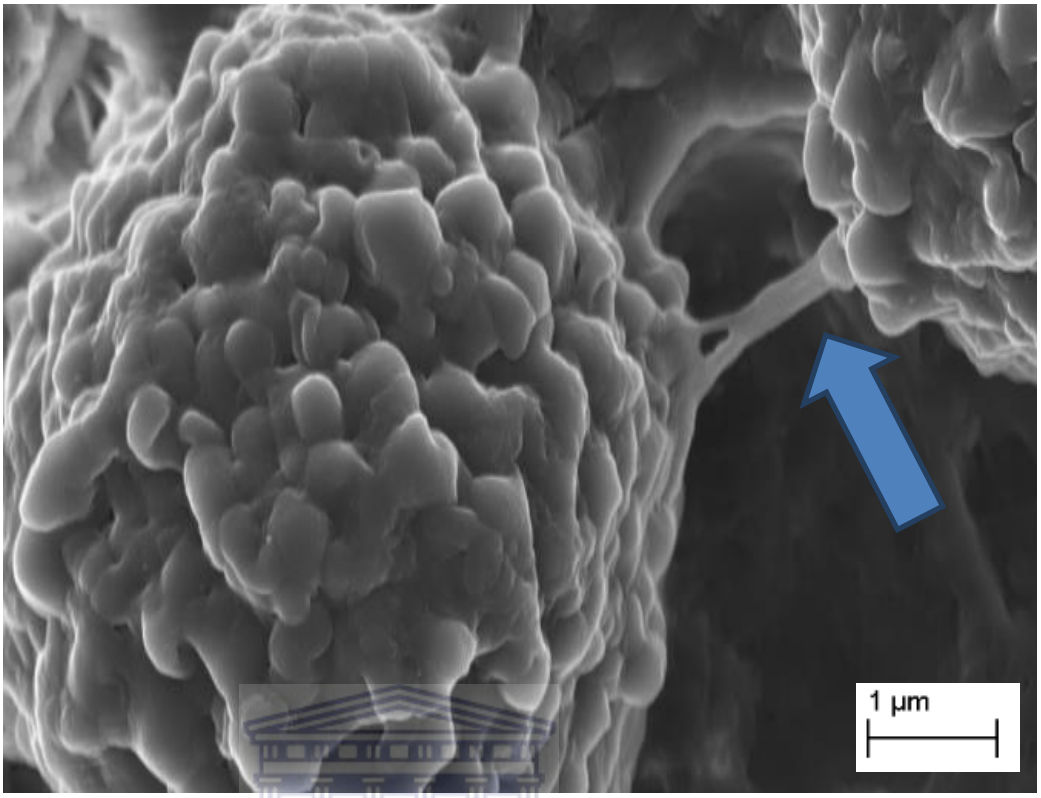

Figure 3.7.2: Ultrastructure of untreated bEnd5 cells at 10000X magnification. The arrow reflects the intact TJ proteins between adjacent ECs (96hrs representation).

Observing the untreated ECs at a 10000X magnification, we found what appeared to be primordial TJs between adjacent cells. The rationale for identifying these strands in Fig.3.7.2 as TJ proteins is the following:

1. It is located at the latero-apical membrane surface of adjacent ECs.
2. It consists of two strands.
3. The extracellular components of the TJ protein, claudin-5 has two extracellular loops (Furuse et al., 1999; Ballabh et al., 2004; Schreibelt et al., 2007). Close examination of the TJ structure in Fig 3.7.2 shows that it consists of two parallel strands.

3.7.3 The effects of 25mM EtOH on the ultrastructure of bEnd5 ECs.

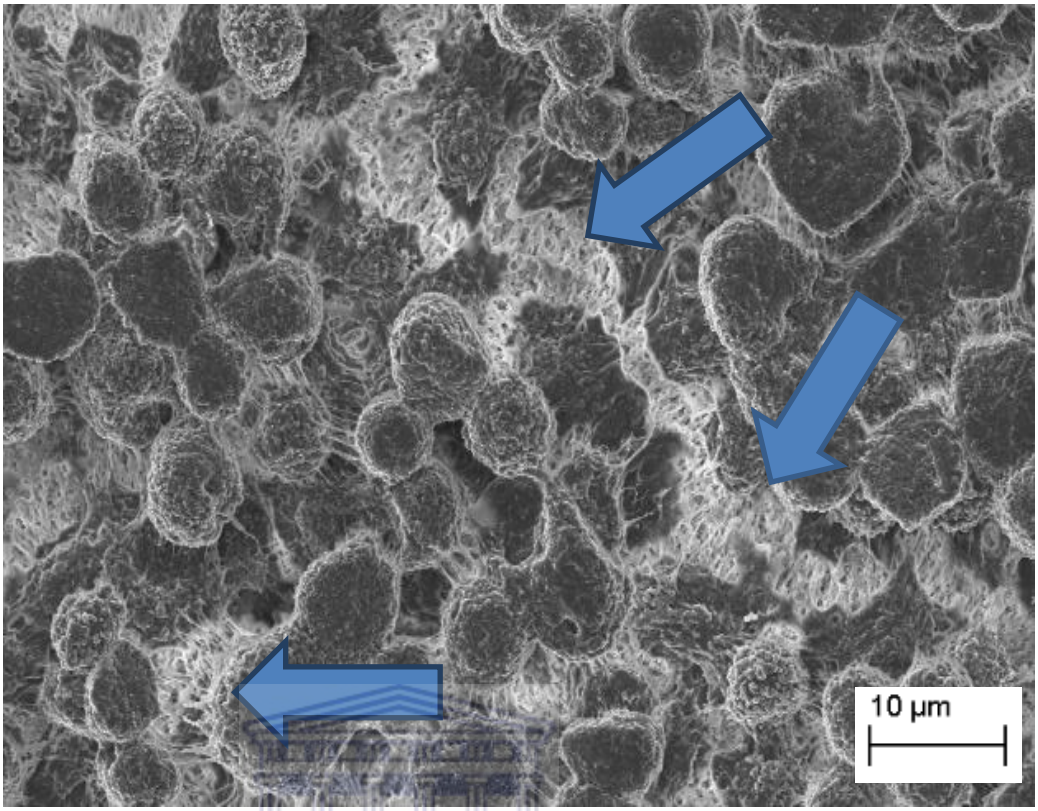

Figure 3.7.3: Ultrastructure of bEnd5 ECs exposed to 25mM EtOH at 1000X magnification. The arrows reflect the compromised paracellular spaces between adjacent ECs (96hrs representation).

Monolayers of bEnd5 cells, exposed to 25mM EtOH, resulted in the prominent appearance of compromised paracellular spaces between adjacent ECs, indicating that the TJs have been implicated impairing the regulation of the transport of substances across the BBB.

3.7.4 The effects of 100mM EtOH on the ultrastructure of bEnd5 ECs.

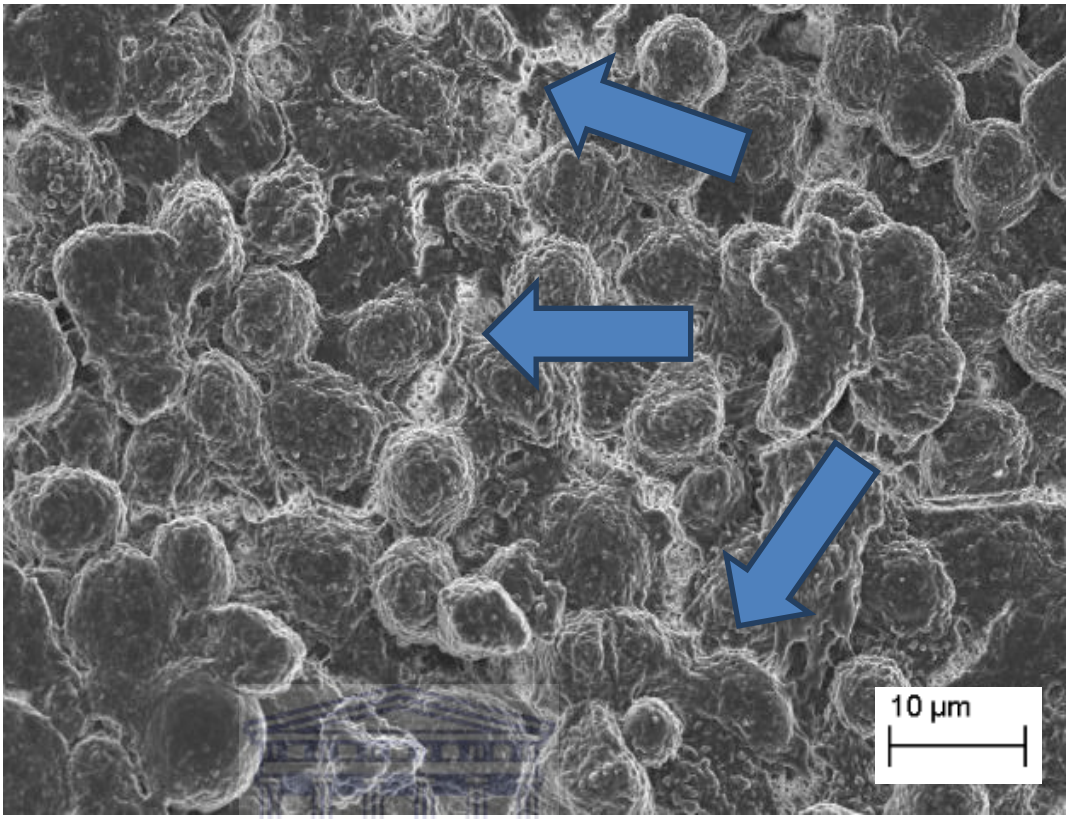

Figure 3.7.4: Ultrastructure of bEnd5 ECs exposed to 100mM EtOH at 1000X magnification. The arrows reflect the compromised paracellular spaces between adjacent ECs (96hrs representation).

We further investigated the exposure of a supraphysiological concentration of EtOH, at 100mM, on the ultrastructure of bEnd5 cells. 100mM EtOH also resulted in noticeably compromised paracellular spaces between adjacent cells (Fig 3.7.4) in comparison to no paracellular spaces as observed with the controls (Fig 3.7.1), signifying severe TJ disruption.

3.7.5 The effects of R_f on the ultrastructure of bEnd5 ECs.

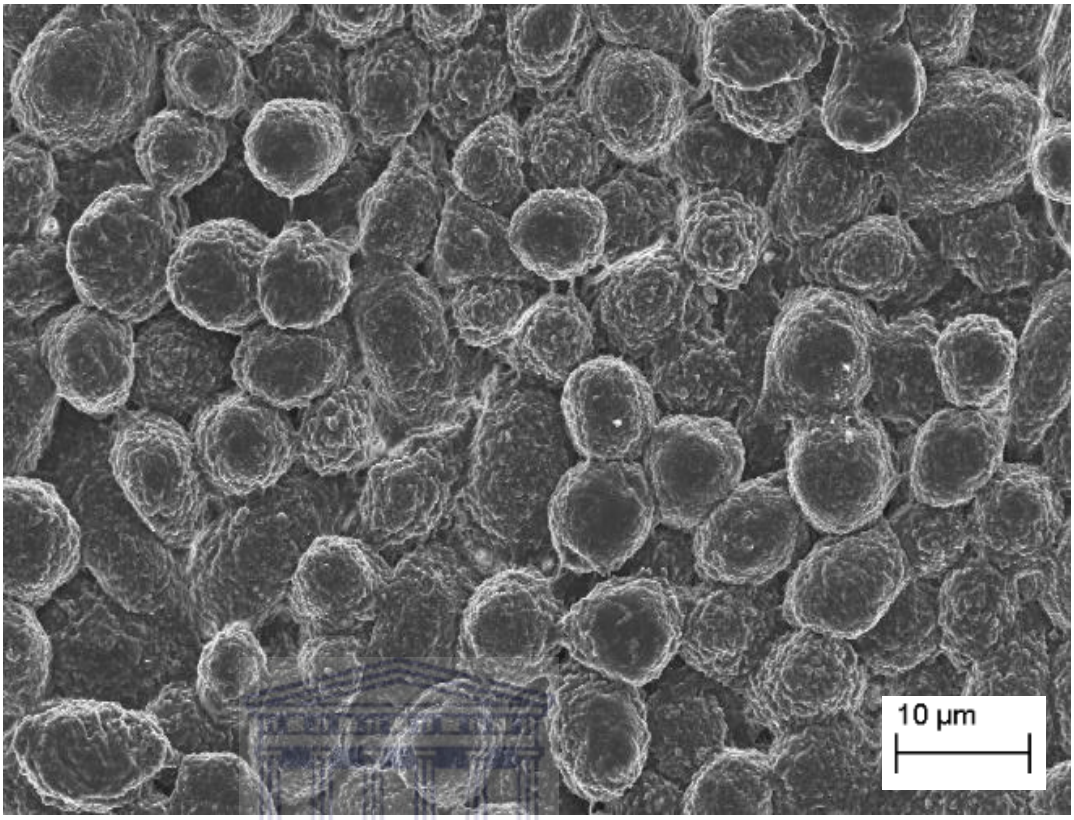

Figure 3.7.5: Ultrastructure of bEnd5 ECs exposed to R_f at 1000X magnification (96hrs representation).

Interestingly, when observed under low magnification as illustrated in Fig 3.7.5, cells exposed to only R_f displayed no noticeable compromised paracellular spaces between adjacent ECs, which was very similar to what was observed in the control cells.

3.7.6 The effects of R_f on the ultrastructure of bEnd5 ECs at 5000X magnification.

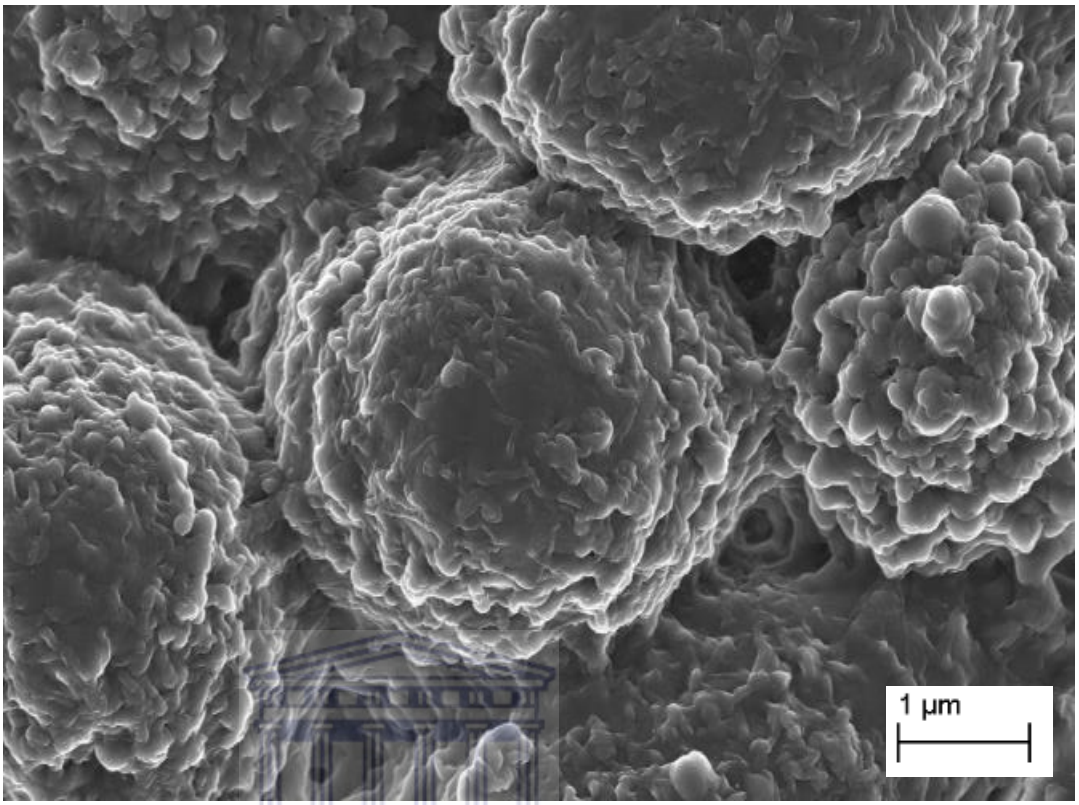

Figure 3.7.6: Ultrastructure of bEnd5 ECs exposed to R_f at 5000X magnification (96hrs representation).

Zooming in and observing the ultrastructure of bEnd5 cells under 5000X magnification in response to R_f, depicted similar results to untreated bEnd5 cells once again, with close associations between adjacent ECs and no apparent compromised paracellular spaces. This indicates that the rooibos extract administered to the cells appear to exert its effects by implicating the transcellular permeability rather than the permeability of the paracellular pathways.

3.7.7 The simultaneous effects of 25mM EtOH and R_f on the ultrastructure of bEnd5 ECs.

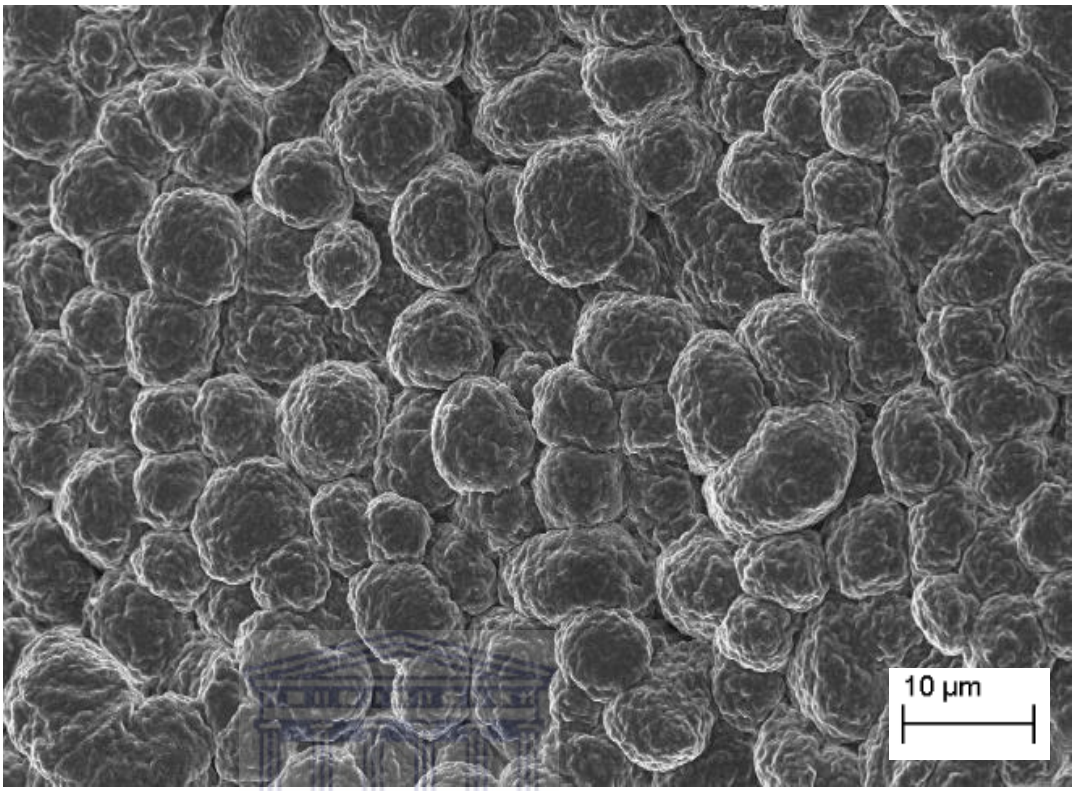

Figure 3.7.7: Ultrastructure of bEnd5 ECs exposed to 25mM EtOH and R_f at 1000X magnification (96hrs representation).

Using SEM, we also investigated the antioxidant properties of R_f in cells simultaneously exposed to a physiological concentration of EtOH, 25mM. We found that the noticeable paracellular spaces observed in cells only exposed to 25mM EtOH (refer Fig 3.7.3) were significantly less, and that the cells rather mimicked the controls (Fig 3.7.7).

3.7.8 The simultaneous effects of 100mM EtOH and R_f on the ultrastructure of bEnd5 ECs.

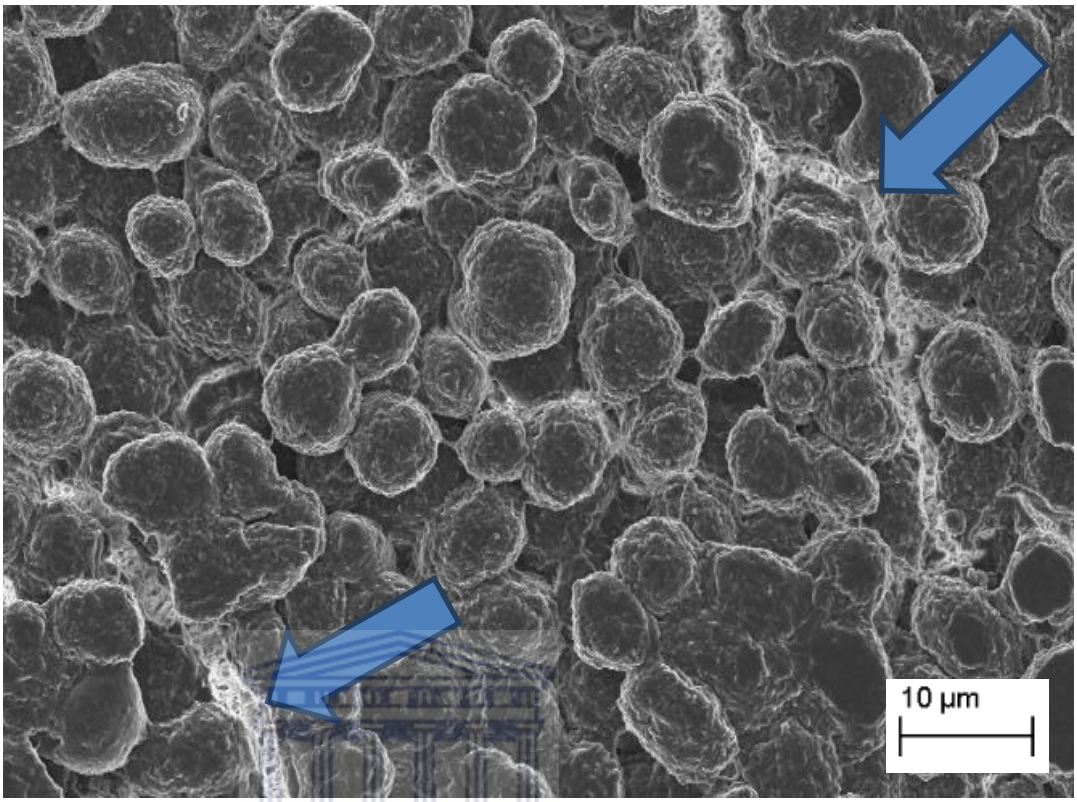

Figure 3.7.8: Ultrastructure of bEnd5 ECs exposed to 100mM EtOH and R_f at 1000X magnification. The arrows reflect the compromised paracellular spaces between adjacent ECs (96hrs representation).

As illustrated in Fig 3.7.8, the combinatorial effect of 100mM EtOH and R_f on bEnd5 cells was similar to the results observed in response to only 100mM EtOH. The prominent display of compromised paracellular spaces indicates that the simultaneous treatment of rooibos extract was not able to reverse or enhance the EtOH induced damage to TJs and paracellular permeability.

3.7.9 The simultaneous effects of 100mM EtOH and R_f on the ultrastructure of bEnd5 ECs at 5000X magnification.

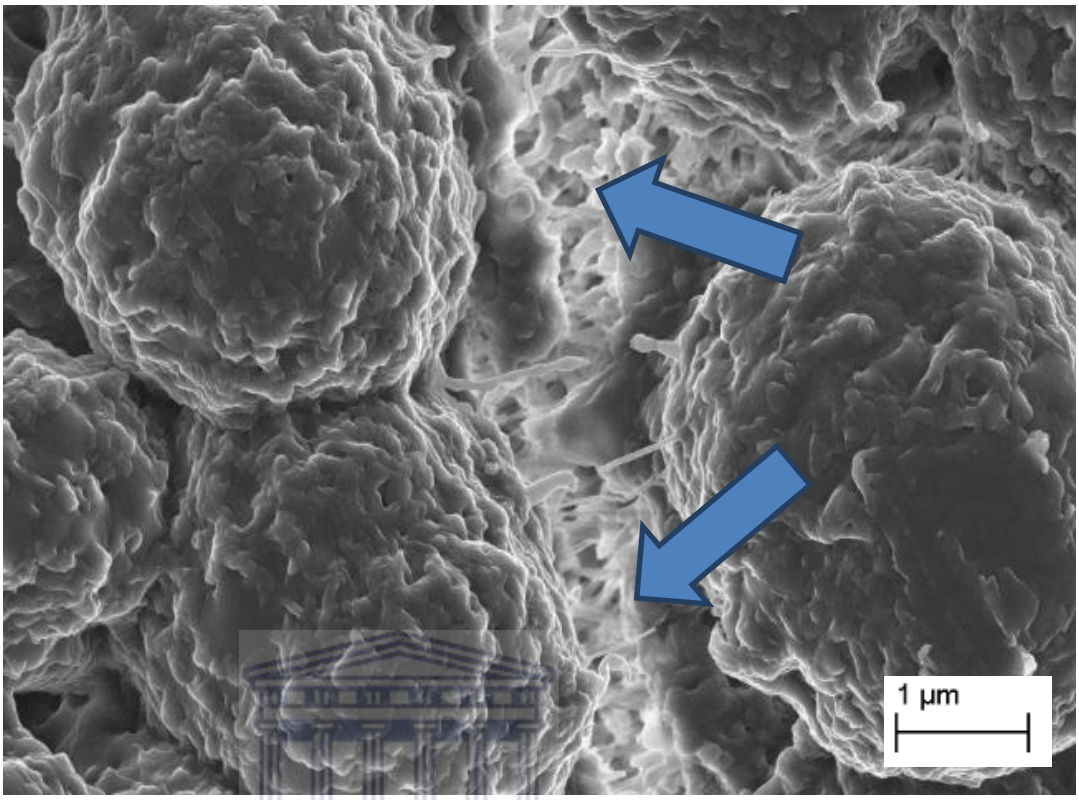

Figure 3.7.9: Ultrastructure of bEnd5 ECs exposed to 100mM EtOH and R_f at 5000X magnification. The arrows reflect the compromised paracellular spaces between adjacent ECs (96hrs representation).

The simultaneous exposure of R_f and 100mM EtOH on the ultrastructure of bEnd5 cells is further validated under 5000X magnification. As illustrated in Fig 3.7.9, the stress fractures between adjacent ECs are more prominent showing the compromised paracellular spaces.

3.7.10 The simultaneous effects of 100mM EtOH and R_f on the ultrastructure of bEnd5 ECs at 10000X magnification.

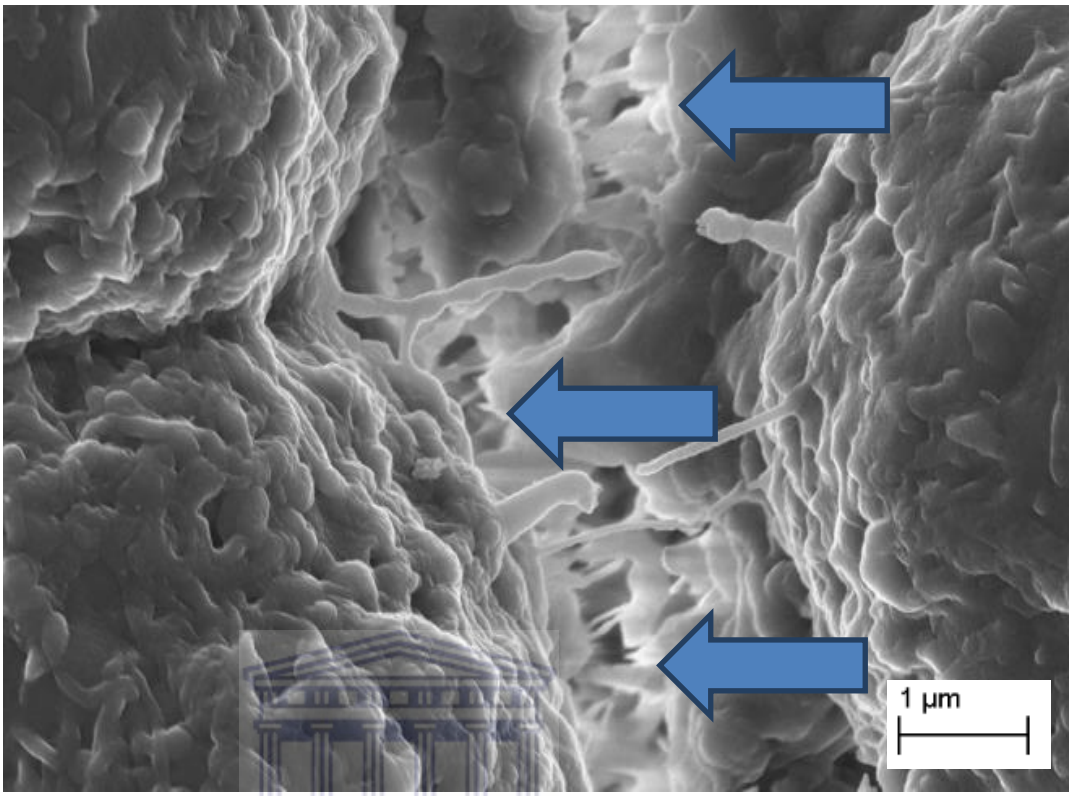

Figure 3.7.10: Ultrastructure of bEnd5 ECs exposed to 100mM EtOH and R_f at 10000X magnification. The arrows reflect the compromised paracellular spaces between adjacent ECs (96hrs representation).

Observing under a higher magnification, we can clearly see the detrimental effects of the simultaneous exposure on the TJs. The integrity of connecting junctions between adjacent ECs is severely compromised as shown in Fig 3.7.10. We can therefore establish that the simultaneous exposure of R_f was not able to reverse nor enhance the resultant EtOH (100mM) effects induced to the paracellular spaces within the EC monolayers.

3.8 Chemical Analysis of R_f (Analysed by the Oxidative Stress Research Centre at CPUT.

The R_f extract used in this study was chemically analysed (see preparation par. 2.1.3, pg. 48-49) to identify and quantify the various antioxidants present in the extract and its antioxidant capacity, as well as the presence of other bioactive molecules. The said chemical analysis was conducted, by Mr R. Rautenbach, under the supervision of Prof J. Marnerwick, from the Oxidative Stress Research Centre at CPUT. The presence of polyphenols, flavonols, flavanols, and most importantly, aspalathin was compared against the antioxidant equivalents, to reflect the antioxidant capacity of R_f. The results presented below were previously reported on by Mentor, S (2015) (thesis). The standards used were gallic acid (GAE), quercetin (QE), and catechin (CE). Furthermore, the antioxidant standards used for the antioxidant assays were ascorbic acid (AAE) and trolox (TE). Gallic acid used as a standard to measure the antioxidant capacity of polyphenols in R_f reacts with any reducing substance and can therefore be used to measure antioxidant capacity *in vitro.*

Table 7: Chemical analysis of R_f sample (Analysed by the Oxidative Stress Research Centre at CPUT). Results are summarized below.

Unit of Concentration	Aspalathin	Poly phenols	Flavonols	Flavanols	FRAP	ORAC	ABTS (TEAC)
100ml	21.3mg	1086.24mg GAE	156.05mg QE	90.96mg CE	7395.24 µmol AAE	21148.92 µmol TE	4905.80µmol TE
g/dry weight	1.065mg	54.34mg GAE	7.80mg QE	4.55mg CE	369.76 µmol AAE	1057.45µmol TE	245.29µmol TE

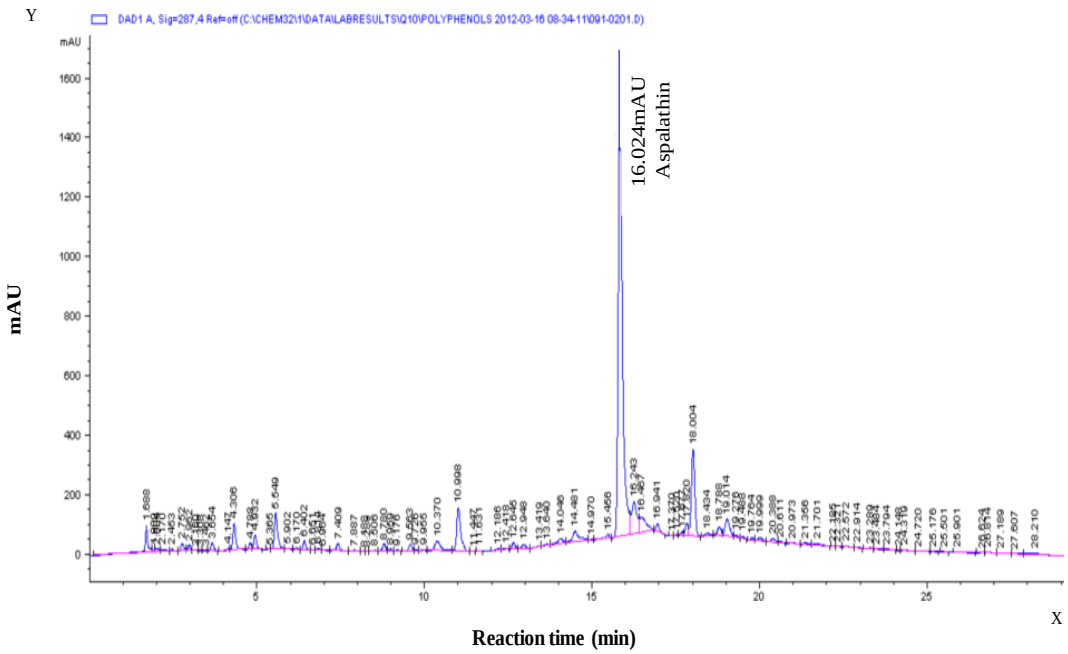

Figure 3.8: Illustration of HPLC (High Pressure Liquid Chromatography) results illustrating polyphenols present in an R_f sample. Chromatographic analysis of the R_f sample generated a prevalent absorbance value of 16.024 mAU, confirming the presence of aspalathin (Analysed by the Oxidative Stress Research Centre at CPUT).

In analysing the R_f extract used in this study, it was established that the total polyphenols present in this extract, measured against GAE, was 1086.24mg/100ml (Table 7). Furthermore, the flavonols and flavanols present in the extract which was measured against quercetin standards reflected 156.05mg/100ml and 96.96mg/100ml, respectively. In addition and not surprisingly, the above table also illustrates that aspalathin is the most prominent of all the polyphenols present in the rooibos extract with 21.3mg/100ml present in this extract. The chromatographic analysis conducted using HPLC, as observed in Fig 3.8, further illustrates that aspalathin is more prominent than the other trace chemicals in the R_f extract used.

Further analysis of the antioxidant assays, with regard to the ORAC assay which is used to measure the peroxyl radical absorbance capacity of antioxidants, indicated that the rooibos extract used reflected an antioxidant capacity of 21148.92µmol/100ml as measured against trolox standards, while the FRAP assay, which assesses the capability of a sample to reduce Fe^{III} to Fe^{II}, revealed this extract's antioxidant capacity to be 7395.24µmol/100ml. The ABTS (TEAC) assay which is suggested to analyse the total antioxidant status revealed that the extract used in this study has an antioxidant status of 4905.80µmol/100ml, also measured against trolox, an antioxidant standard (Table 7).

CHAPTER FOUR

Discussion

4.1.1 Introduction

The BBB is a regulatory boundary between the blood and the CNS. It bars the entry of harmful blood-borne substances into the brain micro-environment (Colgan et al., 2008) and directs the exchanges that take place between the blood and the brain compartments. It is a key component in maintaining brain homeostasis and provides significant ionic stability of the internal parenchyma of the brain. Changes to the ionic environment of the brain would be tantamount to having a stroke. The BBB TJs function to regulate the entry and exit of substances in the brain through the paracellular pathways. For hydrophilic molecules, transport across the BBB is dependent on size and electrical properties of the molecule (Cucullo et al., 2005). However, in contrast, lipid soluble molecules, such as narcotics and alcohol, pass effortlessly through the BBB (Cucullo et al., 2005). Alcohol freely crosses the BBB where it illicits adverse effects on neuronal tissue. It was reported that BBB impairment, as a result of alcohol consumption, is most likely to occur as a result of oxidative stress (Haorah et al., 2005).

Under normal cellular conditions, the formation of ROS occurs during the respiration process through what is known as biological combustion. A surplus of ROS causes oxidative stress which in turn initiates protein, lipid and/or DNA damage. ROS is a contributing factor in numerous diseases (Dudonne et al., 2009), such as ischemic injury and stroke (Colgan et al., 2008). However, ROS is also involved in normal cell functions, and plays an important role in apoptosis, a process that eliminates cancer cells (Joubert et al., 2005). Antioxidants on the other hand, are substances capable of neutralizing excessive quantities of ROS during oxidative stress situations (Dai and Mumper, 2010; Berker et al., 2013). They act as radical scavengers

that disrupt and inhibit ROS-induced radical chain reactions (Huang et al., 2005). Antioxidant compounds such as phenolic molecules are the most active and widely occurring hydrophilic antioxidants, particularly in the diet, such as fruits and vegetables, capable of promoting cellular defenses and inhibiting oxidative damage (Dudonne et al., 2009). Dietary antioxidants are suggested to comprise of radical chain reaction inhibitors, metal chelators, oxidative enzyme inhibitors, and antioxidant enzyme cofactors (Huang et al., 2005). Phenolic antioxidants may also perform as prooxidants under certain circumstances, when the phenoxy radical interacts with oxygen, generating quinones and superoxide anion, instead of reacting with a second radical (Dai and Mumper, 2010). Phenolics, such as quercetin and gallic acid, which are effortlessly oxidized, may display prooxidant actions, while tannins or phenolics with larger molecular weights exhibit little to no prooxidant activity (Dai and Mumper, 2010) depending on the concentration thereof. It has been reported that the different phases in which polyphenols interact with free radical species determines their antioxidant or prooxidant properties (Joubert et al., 2005). For example, antioxidants such as epigallocatechin gallate (EGCG) and gallic acid exhibit effective prooxidant activity during the deoxyribose degradation assay, as they are capable of reducing Fe^{3+} to Fe^{2+}. It has been hypothesized that aspalathin may present prooxidant activity in the same test system as it is a strong antioxidant similar to EGCG (Joubert et al., 2005). This presents a possible mechanism whereby under certain conditions, treatment with antioxidants could present chemical reactions similar to oxidant reactions.

4.1.2 Chemical Analysis

The R_f extract was analysed by the Oxidative Stress Research Centre at CPUT to verify the chemical content and to quantify and characterize the antioxidants in terms of their capacities. The quantity of aspalathin present in the rooibos extract was analysed using HPLC, to establish the antioxidant capacity of R_f. Gallic acid, was used as a standard to measure the antioxidant capacity of polyphenols in R_f, with results being expressed as gallic acid

equivalents (GAE). Furthermore, it reacts with any reducing substance and is therefore suited to measure antioxidant capacity *in vitro*.

The R_f extract used in this study did indeed contain the necessary polyphenols, flavanols, and flavonols (Table 7). More importantly, it validated that aspalathin was present in the R_f extract and that it was the most prominent of all the polyphenols present (Fig 3.8). Furthermore, additional verification that R_f possesses significant antioxidant capacity was measured, and validated using the ORAC and FRAP assays, while the antioxidant status was proven using the ABTS assay (Table 7).

The concentration of aspalathin in the extract was crucial to the determination of the amount of R_f utilized in this study. To our knowledge, this is the first time that the concentration of R_f used to expose cultured cells directly was equated to the concentration of aspalathin found in the plasma following the consumption of 500ml's of R_f tea, which is approximated to display a 1-2 cups of R_f tea. It was also very clear from this study that a concentration of 1.9nM aspalathin had the ability to influence the physiology of bEnd5 cells.

4.1.3 Rationale: EtOH and R_f Concentrations

The concentrations of EtOH used were selected based on extensive data in the published literature (Elamin et al., 2012; Sommer and Spanagel, 2013). The effects of alcohol on ECs have been previously reported on. We repeated respective experimental analyses to establish if the results obtained in previous studies could be repeated. In the absence of establishing negative effects of EtOH on bEnd5 ECs, it would be difficult to test the reversibility of EtOH, using R_f. It was found that in previous studies EtOH plasma concentrations of 10-40mM ensued following moderate EtOH consumption (Elamin et al., 2012), while plasma concentrations of 100mM EtOH be interpreted as a supraphysiological dose of EtOH(Sommer and Spanagel, 2013). The objective for our study was to look at the effects induced by physiological and supraphysiological concentrations of EtOH. We therefore

used two concentrations of EtOH in our study, 25mM EtOH as representation of a physiological dose, and 100mM EtOH as a supraphysiological concentration. The lower concentration of EtOH falls within the plasma concentrations of moderate EtOH drinkers (Elamin et al., 2012). This is particularly significant as most people who consume alcohol fall within this category. Furthermore 100mM EtOH which is regarded as a supraphysiological concentration of EtOH, could be applied to excessive binge drinkers. According to an article by Abdul Muneer et al. (2011), EtOH concentrations 65-100mM resulted in approximately 20% cell death following 48hr exposure, while exposure to 50 and 100mM EtOH, resulted in increased permeability; hence, we investigated the effects of 100mM EtOH as well, to establish if this supraphysiological concentration does lead to cell death and increased permeability.

EtOH metabolism is primary source of excess ROS formation, which is a major contributor of oxidative stress. In addition, ROS-induced TJ disruption, as a result of EtOH, is a leading cause of diminished BBB integrity. Our study corroborated these findings in that EtOH increased permeability (Fig 3.6.1) and displayed a complex mixture of up/down TJ transcription (Fig 3.5.1). However, a shortcoming in this study is that the effects of EtOH on ROS formation and the oxidative stress status of the bEnd5 cell in our study has not been investigated. In addition we found that EtOH decreased cell viability (Fig 3.1.1), decreased cell division (Fig 3.2.1; Fig 3.3.1) and increased cell toxicity (Fig 3.4.1).

We therefore investigated the possible protective effects of R_f, to determine if its potent anti-oxidant potential could reverse or neutralize the ROS-induced effects of EtOH. The concentration of R_f used in this study was based on an article by Breiter et al. (2011) who has shown that following the consumption of 500ml of R_f, the plasma concentration of aspalathin present, peaked at 1.9nM in one of the nine study participants. The administration of 500ml of R_f can generally be equated to two cups of R_f tea. Thus, the rationale for using the selected concentration of R_f in this study is based on the peak

plasma concentration of aspalathin. It is many fold more than the quantity of any other antioxidant present in a R_f extract. The amount of R_f we used to expose our cells in this study was equivalent of 1.9nM of aspalathin. It was the express intention of this study to investigate whether the quantity of antioxidants present in 500ml's of R_f tea would have physiological consequences on the BBB and thus be able to alleviate the ROS-induced effects of EtOH.

4.1.4 Viability

4.1.4.1 The effect of EtOH Treatment on cell viability:

Cells exposed to both concentrations of EtOH, resulted in a decrease in viability across all time-intervals from 24 to 96hrs (Fig 3.1.1). Previous work by Mentor (2015) utilizing similar concentrations of EtOH, showed no to very little changes in viability, however, mimicking the decrease in viability we observe at 48hrs. Metabolized EtOH is a primary contributor of ROS, which is exacerbated by increased CYP2E1 activity following moderate and excessive alcohol consumption (Manzo-Avalos and Saavedra-Molina, 2010). EtOH stimulates the enzymatic activity of cytochrome P450, which enhances excess ROS production as well as diminishes inherent cellular antioxidants which may reduce ROS (Wu and Cederbaum, 2003). Alcohol-induced ROS production impedes the body's natural defense mechanisms .EtOH may also initiate mitochondrial dysfunction and decreased energy conservation; therefore, it is not surprising that both physiological and supraphysiological EtOH concentrations resulted in a detrimental effect on viability. However, we still need to investigate the effects of EtOH on ATP production in our model. Alcohol metabolism produces NO, along with ROS by induction of NADPH/xanthine oxidase and nitric oxide synthase, adding to oxidative stress. Our data showed that the viability at 96hrs was significantly greater in response to EtOH than at 24hrs, indicating recovery of the bEnd5 cells. However, 24hr EtOH exposure induces a 96hr (4 day) negative effect on cell viability.

4.1.4.2 The effect of R_f treatment on cell viability:

A central component of the experimental design was to investigate the effects of R_f-derived antioxidants, equivalent to plasma levels of aspalathin after consuming 500ml's of R_f tea, on cell viability in mouse brain endothelial cells. We do however take cognizance of the fact that the rooibos extract used did not only contain aspalathin, but also other compounds that may work synergistically or antagonistically in our model. Nonetheless it was shown that aspalathin was the most prominent of all the compounds in the rooibos extract (Fig 3.8). We found that exposure to R_f, resulted in a decrease in cell viability between 24 and 48hrs, which recovered between 72 and 96hrs (Fig 3.1.2). Similarly, a study by Mentor (2015), using much higher concentrations also showed decreased viability at 24hrs, and increased viability at 96hrs. Our data indicated that the addition of R_f-derived antioxidants, equivalent of only 1.9nM aspalathin, can induce a physiological effect on the viability of BECs. This was particularly surprising as R_f is generally portrayed to have no adverse effects. Under normal conditions, ROS formation in cells is regulated by innate antioxidant systems, thus the addition of external antioxidants could induce an imbalance in the ROS-antioxidant system of the cell which may be reflected in the results seen in response to R_f. However, the recovery between the latter time intervals, 72 and 96hrs, suggests that the initial adverse effect on EC viability is dependent on inherent cellular mechanisms. Future studies are pivotal in measuring the antioxidant capacity of the bEnd5 cells used in this current study to determine the precise mechanism involved.

4.1.4.3 The effect of EtOH and R_f treatment on cell viability:

When investigating if R_f could negate the effects of EtOH based on its antioxidant potential, we found that exposure to R_f reduced the effects of 25mM EtOH on bEnd5 cell viability at 72hrs, signifying that the EtOH-exposed bEnd5 ECs have significantly benefited as a result of the additional antioxidants. This is particularly important since this is a physiological dose

of EtOH. We further investigated if this was possible at a supraphysiological concentration, and found that the addition of R_f to 100mM EtOH exposed cells reversed the adverse effects of 100mM EtOH on cell viability at 72hrs (Fig 3.1.3.2). Overall, R_f, appeared to reduce and nullify the effects of both concentrations of EtOH at 72hrs, indicating that the alleviating properties of R_f-derived antioxidants requires a timeframe of at least 72hrs to diminish the effects of EtOH-induced ROS. This may be attributed to the metabolism of EtOH. Since its metabolite, acetaldehyde (AA) is equally as toxic; we hypothesize that this may be the reason for the delay in recovery in EtOH induced cells, even with the addition of additional antioxidants.

4.1.5 Cell proliferation

Cell proliferation was determined based on the number of live cells (Cadena-Herrera et al., 2015). The change in cell number between successive 24hr periods over 96hrs was used to calculate the rates of cell division. We compared the rates cell division in control populations of cells to those exposed to EtOH and R_f.

4.1.5.1 The effect of EtOH treatment on cell proliferation:

Cell culture populations exposed to 25mM and 100mM EtOH had a significantly decreased rate of cell division based on the live cell number populations, than that of the untreated bEnd5 cells from 24 to 72hrs (Fig 3.2.1). Previously reported work by Mentor (2015) illustrated that similar concentrations also resulted in decreased cell proliferation at 72hrs, while at the other respective timelines, different findings to ours was noted. This may be attributed to the treatment protocol used, which is vastly different from ours (i.e. the exposure in our study was only for 24hrs). This was affirmed by the slopes of 25mM and 100mM EtOH (Fig 3.3.1), showing that the rates of cell division in EtOH-exposed cells were significantly suppressed in comparison to the control. The EtOH decrease in cell division is supported in

the literature where, Mikami et al. (1997) found that EtOH concentrations (25-200mM), suppressed cell proliferation.

4.1.5.2 The effect of R_f treatment on cell proliferation:

As part of the experimental design, we also investigated the effects of R_f derived antioxidants on the live cell number and cell division of bEnd5 cells. The live cell number was no different from the control at 24 and 48hrs, but resulted in a decrease at 72 and 96hrs. The latter results observed at 72 and 96hrs, respectively resulted in similar results in response to greater concentrations of R_f (Mentor, 2015). When analyzing the rate of cell division in response to R_f, we found that the rate in response to R_f was 0.226 cells/hr, which was significantly slower than the controls (0.435 cells/hr) (Fig 3.3.2). This data suggests that exposure to externally derived R_f antioxidants, may pose a long term detrimental effect to the proliferation of bEnd5 cells, possibly inhibiting or delaying cell proliferation. Since in a balanced cell system, there are equal amounts of oxidants and antioxidants, any addition of excess species that are physiologically not required by the cell may result in physiologically stressing the cell system. Therefore, it comes as no surprise that the additional R_f derived antioxidants displayed such an adverse effect in the bEnd5 ECs.

4.1.5.3 The effect of EtOH and R_f treatment on cell proliferation:

When analyzing the influence of R_f on the EtOH-induced effects on EC live cell number, and rate of cell division, we found that with the combinatorial exposure of EtOH and R_f, the R_f derived antioxidants partially reversed the effects of EtOH on the number of live cells in the experimental timeframe. Simultaneous exposure to R_f and 25mM EtOH, also partially reversed the effects of a physiological concentration of EtOH on the rate of cell division in bEnd5 cells. However, the exposure of R_f together with 100mM EtOH further exacerbated the decrease in the rate of cell division. The effects induced by the simultaneous administration of EtOH and R_f shows that the addition of

R_f-derived antioxidants is able to negate and nullify the EtOH induced ROS damage in the BECs but this imbalance of oxidants and antioxidants in the cell still has a detrimental effect on the cell division of these cells. It is expected that the greater concentration of EtOH will generate much larger concentrations of ROS. Thus, it is conceivable that the R_f concentration used in this study was not sufficient to completely nullify the EtOH-induced ROS.

4.1.6 Cell Toxicity

4.1.6.1 The effect of EtOH treatment on cell toxicity:

EtOH exposure increased cell toxicity in bEnd5 ECs. The production of AA by ADH, during the metabolism of EtOH, in ECs is the most probable explanation for the toxic effects. Not only is AA an extremely mutagenic and carcinogenic molecule, but it has the capacity to generate a large amount of excess ROS species during its metabolism (Sambuy, 2009). However, cell toxicity in response to 25mM and 100mM recovered to normal levels between 72 and 96hrs (Fig 3.4.1), which corroborates with the viability data shown in Fig 3.1.1.

4.1.6.2 The effect of R_f treatment on cell toxicity:

Treatment of bEnd5 cells for 24hrs with R_f resulted in an increase in cell toxicity at all time-intervals (Fig 3.4.1), with decreased toxicity over the 96hr timeframe. This shows that cells exposed to R_f was on a trajectory in recovery and that the adverse effects in response to excess antioxidants is possibly short term. Also the maximum toxicity induced never exceeded 10%. This finding was similar to a study by Mentor (2015), whereby in response to greater concentrations of R_f, bEnd5 cells showed little to no toxicity.

4.1.6.3 The effect of EtOH and R_f treatment on cell toxicity:

When investigating the ability of R_f to reverse or reduce the effects of EtOH, we found that R_f exposure decreased the toxicity in cells exposed to the supraphysiological concentration of EtOH at 24 and 72hrs (Fig 3.4.1). Since EtOH metabolism is a source of ROS, it is believed that R_f may be displaying its antioxidant properties with its metal-chelating abilities and neutralization of singlet oxygen species and thus significantly reducing the oxidant damaging effects of alcohol to the BBB as we have observed by the reversal in cell toxicity, as well as live cell number and viability. The overall low toxicity to all compounds in our study indicates the robustness of bEnd5 cells to toxic insult.

4.1.7 Transcription

It has been premised in the literature that alcohol affects the permeability of the BBB. Haorah et al. (2008) postulated that the alcohol induced changes to BBB permeability was brought about by affecting TJ expression and thus paracellular pathway permeability. In this study, we found that treated and untreated bEnd5 cells did not express the TJ protein occludin. Steiner et al. (2011) also reported that bEnd5 cells lacked the localization of occludin to cellular junctions; however, Findley and Koval (2009) established that occludin-deficient mice are viable and exhibit normal barrier function. Furthermore, the bEnd5 cells used in this study has successfully expressed one of the critical proteins of brain endothelial cell TJs, claudin-5.

4.1.7.1 The effect of EtOH treatment on transcription:

The transcription of claudin-5 in BECs exposed to 25mM and 100mM EtOH changed dramatically across the 96hr timeframe. In addition, as reported, the transcription of claudin-5 in response to the physiological concentration of EtOH was not statistically affected between 24 and 72hrs, but resulted in a decrease at 96hrs. Cells exposed to 100mM EtOH induced an irregular trend

in claudin-5 transcription, with a 4-fold increase in transcription at 24hrs, and statistical suppression at 96hrs (Fig 3.5.1). In addition, Haorah et al. (2008) established in a study using 50mM EtOH that the metabolism of EtOH resulted in the phosphorylation of TJ proteins, thereby altering TJ assembly; ultimately impairing BBB integrity, which is coherent with the suppression in claudin-5 transcription at 96hrs (Fig 3.5.1). Furthermore, it is plausible that the metabolite of EtOH, AA, also strongly contributes to the modifications in the molecular composition of TJs (Elamin et al., 2012).

4.1.7.2 The effect of R_f treatment on transcription:

When investigating the effects of R_f on claudin-5 transcription, we established that R_f resulted in an overall down-regulation of claudin-5 throughout the course of the experiment (Fig 3.5.2). To the best of our knowledge, the effects of R_f on claudin-5 transcription has never before been reported. However, green tea polyphenols (GTPs) was reported to also decrease claudin-5 expression similarly to what was observed in our study (Liu et al., 2013). Excess antioxidants may therefore compromise the paracellular pathway of the BBB.

4.1.7.3 The effect of EtOH and R_f treatment on transcription:

While our study endorsed the data in the literature we further investigated whether this alcohol induced changes to BBB permeability could be reversed or neutralized by co-exposure to R_f. Both the physiological and the supraphysiological concentrations of EtOH on their own and in combination with R_f down-regulated claudin-5 mRNA transcription across the experimental timeframe with the exception of 72hrs. The simultaneous exposure of EtOH and R_f resulted in diminished claudin-5 transcription throughout the course of the experiment (Fig 3.5.3). Based on our hypothesis; we expected reversal or neutralization of the EtOH-induced ROS effects, thus, we were surprised to see that co-exposure led to an increased down-regulation of claudin-5 transcription. This indicated that the ROS and

antioxidant species affected the status of the TJs, by a yet unknown physiological molecular mechanism which exacerbated the suppression of claudin-5.

4.1.8 Permeability

Since TJs play a significant role in the regulation of paracellular permeability, we used the technique of measuring transepithelial electrical resistance (TEER) to approximate changes to monolayer permeability; hence the TEER of confluent monolayers of bEnd5 cells, were recorded in response to exposure of selected concentrations of EtOH, R_f, and the combinations thereof. The measured TEER is inversely proportional to permeability.

4.1.8.1 The effect of EtOH treatment on permeability:

Studies have suggested that the mechanism by which alcohol affects the BBB is through the disruption of the endothelial TJ which then ultimately results in augmented BBB permeability (Haorah et al., 2005; Singh et al., 2007). Our findings have shown that both 25mM and 100mM EtOH decreased the resistance of the bEnd5 cells and increased the monolayer permeability. This decrease observed in response to the selected concentrations of EtOH comes as no surprise, since the overall trend observed in TEER (Fig 3.6.1) relates to events in transcription (Fig 3.5.1), where with the down-regulation of claudin-5 was observed. Interestingly, previous studies have demonstrated that EtOH concentrations of 50 and 100mM decreased TEER of a cell monolayer significantly in a dose dependent manner (Abdul Muneer et al., 2011). Abdul Muneer et al. (2011) also reported that EtOH decreased BBB electrical resistance while increasing BBB permeability, corroborating our findings.

There are two routes for substances to cross the BBB, the paracellular pathway and via the transcellular pathway. Similarly, transepithelial resistance is a function of both transcellular resistance in parallel with

paracellular resistance. Haorah et al. (2005) provided data which implicated alcohol affecting the myosin light chain kinase (MLCK), an enzyme integral to the structure of the intracellular cytoskeleton, which in turn led to compromising the paracellular permeability by phosphorylation of TJs. This provides a plausible explanation of why we observed decreases in TEER across our model of bEnd5 BECs.

4.1.8.2 The effect of R_f treatment on permeability:

Cell monolayers exposed to R_f also resulted in a decrease in TEER across the experimental timeframe of 96hrs (Fig 3.6.2). Given that the bEnd5 cell monolayers were exposed for 24hr before monitoring the permeability, we hypothesized that the R_f-derived antioxidants may pose a long term effect on the permeability of the BBB, as illustrated in the inability of the monolayer to return to control levels of permeability. In addition, the increase in permeability observed (Fig 3.6.2) corroborates the decrease observed in claudin-5 mRNA transcription in response to R_f. However, contrary to this finding, a study by Mentor (2015), illustrated an increase in TEER, which may likely be as a result of the much higher concentrations used.

4.1.8.3 The effect of EtOH and R_f treatment on permeability:

The simultaneous exposure of EtOH and R_f to the bEnd5 cells was not able to reverse the effects of EtOH on TEER. Similarly R_f could not reverse the EtOH induced effects observed in the relative mRNA transcription of claudin-5 (Fig 3.5.3). This further validates the endorsement of the PCR data. Our hypothesis was that the R_f-derived antioxidants would neutralize EtOH-induced ROS, effectively reversing or nullifying, the effects of EtOH. Surprisingly, the addition of R_f exacerbated the effects of alcohol. Also, R_f on its own caused similar effects to alcohol by significantly decreasing the effects on permeability. Since the simultaneous exposure of R_f with EtOH was able to negate the effects of EtOH on the viability and proliferation of bEnd5 cells, we expected that it would produce a similar effect on claudin-5

transcription and bEnd5 permeability. On the contrary, as illustrated (Fig 3.5.3 and Fig 3.6.3), the addition of R_f was not able to reverse or reduce the EtOH-induced effects on these endothelial cells. This may likely be attributed to AA, a toxic metabolite of EtOH. We hypothesize that this highly toxic metabolite of EtOH may be influencing claudin-5 directly, since it has it is speculated that they do interfere with DNA and posttranslational modifications; ultimately signifying that AA may be more toxic than EtOH since it may act directly on proteins as well as via ROS.

4.1.9 Morphology of a monolayer of bEnd5 cells.

The ultrastructure of bEnd5 brain endothelial cells was investigated using high resolution SEM to visualize the fine morphological and molecular detail of the cells growing on cellulose covered inserts, and to compare the morphological effects of EtOH and R_f. Cells were processed for SEM at 96hrs. This enabled the verification of the bEnd5 monolayer and the analysis of the state of confluence of the layer.

SEM is advantageous in the sense that the surface of a specimen is accessible for experimentation at a resolution and depth of field greater than that of the optical microscope (Nixon, 1971), allowing us to visualize structures impossible to see with the naked eye, such as the TJs discussed in our study.

4.1.9.1 Cultural monolayers:

Untreated cells (controls) displayed intact primordial TJs between adjacent ECs, evident by their latero-apical location, and visibility of parallel strands present, while showing no compromised paracellular spaces (Fig 3.7.1 and Fig 3.7.2). The rationale for identifying these structures is based on their theoretical and reported location and morphology. Claudin-5 in particular, is located in the latero-apical membrane surface of adjacent ECs, and the extracellular components of the TJ protein, claudin-5 have two extracellular loops (Furuse et al., 1999; Ballabh et al., 2004; Schreibelt et al., 2007).

Knowing the structural location and morphology assisted in the identification of the paracellular spaces. Generally, the bEnd5 ECs in our study were homogenous, and, round-hexagonal in shape. In addition, intact monolayers displayed marginal folds, which are cell-overlapping areas between adjacent ECs. These findings, as observed in our cultural monolayers, corroborated previous published literature (MacCsallum et al., 1882; Dejana, 2004; Schrot et al., 2005).

4.1.9.2 The effect of EtOH treatment on the ultrastructure of bEnd5 cells:

Contrast to the control cells, bEnd5 monolayers exposed to 25mM EtOH resulted in the prominent appearance of compromised paracellular spaces between adjacent ECs, signifying impaired TJ integrity as well as diminished paracellular regulation of substances traversing the BBB (Fig 3.7.3). Similarly, bEnd5 monolayers exposed to a supraphysiological concentration of EtOH, 100mM, also displayed noticeably compromised paracellular spaces between adjacent ECs (Fig 3.7.4).

4.1.9.3 The effect of R_f treatment on the ultrastructure of bEnd5 cells:

Interestingly, BECs exposed to R_f mimicked the control cells by displaying no prominent compromised paracellular spaces, as well as cell overlapping between adjacent ECs (Fig 3.7.5 and Fig 3.7.6). It may be that the additional antioxidants administered to the BECs exert its effects by implicating the transcellular permeability rather than the paracellular pathways.

4.1.9.4 The effect of EtOH and R_f treatment on the ultrastructure of bEnd5 cells:

Similarly to the controls, cells exposed simultaneously to R_f and 25mM EtOH, displayed no compromised paracellular spaces (Fig 3.7.7), illustrating that the R_f-derived antioxidants were able to reduce the physiological EtOH-induced effects on the paracellular spaces. The combination of 100mM EtOH

together with R_f produced compromised paracellular spaces with stress fractures which resembled the results of exposure to only 100mM EtOH (Fig 3.7.8-3.7.10). This suggests that the simultaneous administration of additional antioxidants failed to reverse or prevent the EtOH-induced damage (at the 100mM level) to the TJs and ultimately paracellular permeability, which is in alignment with results observed in PCR and TEER. This is particularly important since in our study we observed that the effects of R_f treatment resembled data similar to ROS-implicated results.

CHAPTER FIVE

Conclusion

Our findings in this study corroborated previous published literature in that EtOH disrupts TJ protein transcription, in particular, claudin-5, and in doing so led to altered BBB integrity. Furthermore, in alignment with these studies (Abdul Muneer et al., 2011), EtOH adversely affected permeability, by decreasing TEER measurements. This was further validated using high resolution scanning electron microscopy for the observation of paracellular spaces between adjacent BECs. It was also established in this study that both physiological and supraphysiological concentrations of EtOH, both, resulted in adverse effects on cell viability, cell proliferation, cell toxicity, and the rate of cell division. It is well established in the literature, that ROS, may be responsible for the EtOH-induced effects on the bEnd5 ECs. As a result, the underlining hypothesis for this project was that these EtOH-induced ROS effects could be reversed by the simultaneous exposure to R_f, an extract, with an established antioxidant capacity (Berker et al., 2013). Furthermore, the scope of the study limited the use of R_f to a concentration of aspalathin equivalent to that found in the plasma after the intake of 500ml's of R_f tea.

Prior to co-exposure of R_f and EtOH, we investigated the effects of only R_f on the bEnd5 ECs. As observed with SEM, cells exposed to R_f mimicked the controls, illustrating that R_f does not have a detrimental effect on the morphology of ECs and their supporting structures. Exposure to R_f initially resulted in decreased viability but recovered within 96hrs. In terms of live cell numbers, R_f led to diminished numbers of live cells at the later time intervals but remained similar to controls up to 48hrs. The decrease in the number of live cells is corroborated by the rate of cell division in response to R_f, which was significantly slower than untreated bEnd5 ECs. For the first time according to our knowledge, our study established, that similarly to EtOH, R_f administered on its own resulted in

detrimental effects on bEnd5 ECs, as noted when investigating cell toxicity, claudin-5 transcription and permeability across monolayers of bEnd5 ECs.

Overall, we established that EtOH is detrimental to the integrity of bEnd5 ECs, and that the addition of external antioxidants can partially alleviate excess ROS-induced effects. However, morphologically, the addition of R_f derived antioxidants only reversed the effects of a physiological concentration EtOH. Surprisingly, the simultaneous exposure of R_f together with EtOH exacerbated the adverse effects on claudin-5 transcription as well as permeability. The detrimental effects of alcohol exposure may be due to the effects of ROS, as well as the toxic effects of metabolites of EtOH, such as acetaldehyde. These dual effects may have obscured the sole protective effects of R_f against ROS. We therefore hypothesize that this may be a plausible explanation, since the addition of R_f derived antioxidants reversed and reduced the effects of EtOH on cell viability, cell toxicity, and cell proliferation.

Limitations in this study include insufficient analysis on the antioxidant status of the model used in this study, as well as the effects of the experimental compounds on ATP production. To better elucidate the mechanisms underlying the effects of EtOH and R_f on the BBB, future perspectives would include optimizing our bEnd5 model and cell cycle analysis to better analyze cell proliferation and cell division.

REFERENCES

Anonymous (1988) Alcohol drinking. Biological data relevant to the evaluation of carcinogenic risk to humans. *IARC Monogr Eval Carcinog Risks Hum* **44**, 101-52.

Abbott, N.J. (2002) Astrocyte-endothelial interactions and blood-brain barrier permeability. *J Anat* **200**, 629-38.

Abbott, N.J., Ronnback, L. and Hansson, E. (2006) Astrocyte-endothelial interactions at the blood-brain barrier. *Nat Rev Neurosci* **7**, 41-53.

Abdul Muneer, P.M., Alikunju, S., Szlachetka, A.M. and Haorah, J. (2011) Inhibitory effects of alcohol on glucose transport across the blood-brain barrier leads to neurodegeneration: preventive role of acetyl-L: -carnitine. *Psychopharmacology (Berl)* **214**, 707-18.

Al-Nedawi, K., Meehan, B., Kerbel, R.S., Allison, A.C. and Rak, J. (2009) Endothelial expression of autocrine VEGF upon the uptake of tumor-derived microvesicles containing oncogenic EGFR. *Proc Natl Acad Sci USA* **106**, 3794-9.

Anderson, J.M. and Van Itallie, C.M. (2009) Physiology and function of the tight junction. *Cold Spring Harb Perspect Biol* **1**, a002584.

Avelar-Freitas, B.A., Almeida, V.G., Pinto, M.C.X., Mourão, F.A.G., Massensini, A.R., Martins-Filho, O.A., Rocha-Vieira, E. and Brito-Melo, G.E.A. (2014) Trypan blue exclusion assay by flow cytometry. *Bra J Med Biol* **47(4)**, 307-315.

Ballabh, P., Braun, A. and Nedergaard, M. (2004) The blood-brain barrier: an overview: structure, regulation, and clinical implications. *Neurobiol Dis* **16**, 1-13.

Berker, K.I., Ozdemir Olgun, F.A., Ozyurt, D., Demirata, B. and Apak, R. (2013) Modified Folin-Ciocalteu antioxidant capacity assay for measuring lipophilic antioxidants. *J Agric Food Chem* **61**, 4783-91.

Boe, D.M., Vandivier, R.W., Burnham, E.L. and Moss, M. (2009) Alcohol abuse and pulmonary disease. *J Leukoc Biol* **86**, 1097-104.

Bozzola, J.J., and Russel, L.D. (1999) Electron microscopy. In: Chapter 3, Specimen preparation for scanning electron microscopy. *Mississauga, Canada: Jones and Barlett publishers* Inc. **2**, pp 54.

Breiter, T., Laue, C., Kressel, G., Groll, S., Engelhardt, U.H. and Hahn, A. (2011) Bioavailability and antioxidant potential of rooibos flavonoids in humans following the consumption of different rooibos formulations. *Food Chem* **128**, 338-47.

Brooks, T.A., Hawkins, B.T., Huber, J.D., Egleton, R.D. and Davis, T.P. (2005) Chronic inflammatory pain leads to increased blood-brain barrier permeability and tight junction protein alterations. *Am J Physiol Heart Circ Physiol* **289**, H738-43.

Brown, R.C. and Davis, T.P. (2002) Calcium modulation of adherens and tight junction function: a potential mechanism for blood-brain barrier disruption after stroke. *Stroke* **33**, 1706-11.

Burns, E.M., Dobben, G.D., Kruckeberg, T.W. and Gaetano, P.K. (1981) Blood-brain barrier: morphology, physiology, and effects of contrast media. *Adv Neurol* **30**, 159-65.

Cadena-Herrera, D., Esparza-De Lara, J.E., Ramírez-Ibañez, N.D., López-Morales, C.A., Pérez, N.O., Flores-Ortiz, L.F., Medina-Rivero, E. (2015) Validation of three viable-cell counting methods: Manual, semi-automated, and automated. *Biotech Rep* **7**, 9-16.

Capaldo, C.T. and Nusrat, A. (2009) Cytokine regulation of tight junctions. *Biochim Biophys Acta* **1788**, 864-71.

Cardoso, F.L., Brites, D. and Brito, M.A. (2010) Looking at the blood-brain barrier: molecular anatomy and possible investigation approaches. *Brain Res Rev* **64**, 328-63.

Citi, S., Paschoud, S., Pulimeno, P., Timolati, F., De Robertis, F., Jond, L. and Guillemot, L. (2009) The tight junction protein cingulin regulates gene expression and RhoA signaling. *Ann N Y Acad Sci* **1165**, 88-98.

Cobaugh, D.J., Gibbs, M., Shapiro, D.E., Krenzelok, E.P. and Schneider, S.M. (1999) A comparison of the bioavailabilities of oral and intravenous ethanol in healthy male volunteers. *Acad Emerg Med* **6**, 984-8.

Coisne, C., Lyck, R. and Engelhardt, B. (2013) Live cell imaging techniques to study T cell trafficking across the blood-brain barrier *in vitro* and *in vivo*. *Fluids Barriers CNS* **10**, 7.

Colgan, O.C., Collins, N.T., Ferguson, G., Murphy, R.P., Birney, Y.A., Cahill, P.A. and Cummins, P.M. (2008) Influence of basolateral condition on the regulation of brain microvascular endothelial tight junction properties and barrier function. *Brain Res* **1193**, 84-92.

Cucullo, L., Aumayr, B., Rapp, E. and Janigro, D. (2005) Drug delivery and *in vitro* models of the blood-brain barrier. *Curr Opin Drug Discov Devel* **8**, 89-99.

Dai, J. and Mumper, R.J. (2010) Plant phenolics: extraction, analysis and their antioxidant and anticancer properties. *Molecules* **15**, 7313-52.

Dejana, E. (2004) Endothelial cell-cell junctions: happy together. *Nat Rev*

Mol Cell Biol **5**, 261-70.

Deli, M.A., Abraham, C.S., Kataoka, Y. and Niwa, M. (2005) Permeability studies on *in vitro* blood-brain barrier models: physiology, pathology, and pharmacology. *Cell Mol Neurobiol* **25**, 59-127.

Derk, R., Davidson, D.C., Manke, A., Stueckle, T.A., Rojanasakul, Y. and Wang, L. (2015) Potential *in vitro* model for testing the effect of exposure to nanoparticles on the lung alveolar epithelial barrier. *Sensing and Bio-sensing Res* **3,** 38-45.

Dudonne, S., Vitrac, X., Coutiere, P., Woillez, M. and Merillon, J.M. (2009) Comparative study of antioxidant properties and total phenolic content of 30 plant extracts of industrial interest using DPPH, ABTS, FRAP, SOD, and ORAC assays. *J Agric Food Chem* **57**, 1768-74.

Dziegielewska, K.M., Evans, C.A., Malinowska, D.H., Mollgard, K., Reynolds, J.M., Reynolds, M.L. and Saunders, N.R. (1979) Studies of the development of brain barrier systems to lipid insoluble molecules in fetal sheep. *J Physiol* **292**, 207-31.

ElAli, A., Doeppner, T.R., Zechariah, A. and Hermann, D.M. (2011) Increased blood-brain barrier permeability and brain edema after focal cerebral ischemia induced by hyperlipidemia: role of lipid peroxidation and calpain-1/2, matrix metalloproteinase-2/9, and RhoA overactivation. *Stroke* **42**, 3238-44.

Elamin, E., Jonkers, D., Juuti-Uusitalo, K., van Ijzendoorn, S., Troost, F., Duimel, H., Broers, J., Verheyen, F., Dekker, J. and Masclee, A. (2012) Effects of ethanol and acetaldehyde on tight junction integrity: in vitro study in a three dimensional intestinal epithelial cell culture model. *PLoS One* **7**, e35008.

Enciu, A.M., Gherghiceanu, M. and Popescu, B.O. (2013) Triggers and

effectors of oxidative stress at blood-brain barrier level: relevance for brain ageing and neurodegeneration. *Oxid Med Cell Longev* **2013**, 297512.

FASD Prevention Symposium (2008). Fetal Alcohol Spectrum Disorders in Cape Town, South Africa: A huge challenge requiring multi-faceted prevention strategies. *http://research.newsbeat.co.za/projects/FAS.html*.

Faso, L., Trowbridge, R.S., Quan, W., Yao, X.L., Jenkins, E.C., Maciulis, A., Bunch, T.D. and Wisniewski, H.M. (1994) Characterization of a strain of cerebral endothelial cells derived from goat brain which retain their differentiated traits after long-term passage. *In vitro Cell Dev Biol Anim.* **30A**, 226-35.

Findley, M.K. and Koval, M. (2009) Regulation and roles for claudin-family tight junction proteins. *IUBMB Life* **61**, 431-7.

Forster, C., Burek, M., Romero, I.A., Weksler, B., Couraud, P.O. and Drenckhahn, D. (2008) Differential effects of hydrocortisone and TNF alpha on tight junction proteins in an *in vitro* model of the human blood-brain barrier. *J Physiol* **586**, 1937-49.

Furuse, M., Hirase, T., Itoh, M., Nagafuchi, A., Yonemura, S., Tsukita, S. and Tsukita, S. (1993) Occludin: a novel integral membrane protein localizing at tight junctions. *J Cell Biol* **123**, 1777-88.

Furuse, M., Sasaki, H. and Tsukita, S. (1999) Manner of interaction of heterogeneous claudin species within and between tight junction strands. *J Cell Biol* **147**, 891-903.

Furuse, M. and Tsukita, S. (2006) Claudins in occluding junctions of humans and flies. *Trends Cell Biol* **16**, 181-8.

Gabathuler, R. (2010) Approaches to transport therapeutic drugs across the blood-brain barrier to treat brain diseases. *Neurobiol Dis* **37**, 48-57.

Gill, K., France, C. and Amit, Z. (1986) Voluntary ethanol consumption in rats: an examination of blood/brain ethanol levels and behavior. *Alcohol Clin Exp Res* **10**, 457-62.

Grant, G.A., Abbott, N.J. and Janigro, D. (1998) Understanding the Physiology of the Blood-Brain Barrier: *In Vitro* Models. *News Physiol Sci* **13**, 287-293.

Gumbleton, M. and Audus, K.L. (2001) Progress and limitations in the use of *in vitro* cell cultures to serve as a permeability screen for the blood-brain barrier. *J Pharm Sci* **90**, 1681-98.

Hanhineva, K., Torronen, R., Bondia-Pons, I., Pekkinen, J., Kolehmainen, M., Mykkanen, H. and Poutanen, K. (2010) Impact of dietary polyphenols on carbohydrate metabolism. *Int J Mol Sci* **11**, 1365-402.

Haorah, J., Heilman, D., Knipe, B., Chrastil, J., Leibhart, J., Ghorpade, A., Miller, D.W. and Persidsky, Y. (2005) Ethanol-induced activation of myosin light chain kinase leads to dysfunction of tight junctions and blood-brain barrier compromise. *Alcohol Clin Exp Res* **29**, 999-1009.

Haorah, J., Ramirez, S.H., Floreani, N., Gorantla, S., Morsey, B. and Persidsky, Y. (2008) Mechanism of alcohol-induced oxidative stress and neuronal injury. *Free Radic Biol Med* **45**, 1542-50.

Harper, C. (1998) The neuropathology of alcohol-specific brain damage, or does alcohol damage the brain? *J Neuropathol Exp Neurol* **57**, 101-10.

Harper, C. and Matsumoto, I. (2005) Ethanol and brain damage. *Curr Opin*

Pharmacol **5**, 73-8.

Hommer, D.W. (2003) Male and female sensitivity to alcohol-induced brain damage. *Alcohol Res Health* **27**, 181-5.

Hong, I.S., Lee, H.Y. and Kim, H.P. (2014) Anti-oxidative effects of Rooibos tea (*Aspalathus linearis*) on immobilization-induced oxidative stress in rat brain. *PLoS One* **9**, e87061

http://www.marshall.edu/bms/2012/08/30/richard-egleton-ph-d/ [Accessed 20 June 2015].

http://www.pharmadirections.com/_blog/Formulation_Development_Blog/post/Biopharmaceutics_Classification_System_and_In-vitro_membrane_models/ [Accessed 13 March 2015].

Huang, D., Ou, B. and Prior, R.L. (2005) The chemistry behind antioxidant capacity assays. *J Agric Food Chem* **53**, 1841-56.

Huber, J.D., Hau, V.S., Borg, L., Campos, C.R., Egleton, R.D. and Davis, T.P. (2002) Blood-brain barrier tight junctions are altered during a 72-h exposure to lambda-carrageenan-induced inflammatory pain. *Am J Physiol Heart Circ Physiol* **283**, H1531-7.

Huber, J.D., Witt, K.A., Hom, S., Egleton, R.D., Mark, K.S. and Davis, T.P. (2001) Inflammatory pain alters blood-brain barrier permeability and tight junctional protein expression. *Am J Physiol Heart Circ Physiol* **280**, H1241-8.

Israel, Y., Rivera-Meza, M., Karahanian, E., Quintanilla, M.E., Tampier, L., Morales, P. and Herrera-Marschitz, M. (2013) Gene specific modifications unravel ethanol and acetaldehyde actions. *Front Behav Neurosci* **7**, 80.

Jaffe, E.A., Nachman, R.L., Becker, C.G. and Minick, C.R. (1973) Culture of human endothelial cells derived from umbilical veins. Identification by morphologic and immunologic criteria. *J Clin Invest* **52**, 2745-56.

Joubert, E. and Ferreira, D. (1996) Antioxidants of Rooibos tea- a possible explanation for its health promoting properties? *SA J Food Sci Nutr* **8(3)**, 79-83.

Joubert, E. and Schulz, H. (2006) Production and quality aspects of rooibos tea and related products. A review. *J App Bot Food Qual* **80**, 138-144.

Joubert, E., Winterton, P., Britz, T.J. and Gelderblom, W.C. (2005) Antioxidant and pro-oxidant activities of aqueous extracts and crude polyphenolic fractions of rooibos (*Aspalathus linearis*). *J Agric Food Chem* **53**, 10260-7.

Kawano, A., Nakamura, H., Hata, S., Minakawa, M., Miura, Y. and Yagasaki, K. (2009) Hypoglycemic effect of aspalathin, a rooibos tea component from *Aspalathus linearis*, in type 2 diabetic model db/db mice. *Phytomedicine* **16** , 437-43.

Koob, G.F. (2013) Theoretical frameworks and mechanistic aspects of alcohol addiction: alcohol addiction as a reward deficit disorder. *Curr Top Behav Neurosci* **13**, 3-30.

Koval, M., Fan, X., Fernandez, A.L., Johnson, L.N., Joshi, P.C. and Guidot, D.M (2008) Effects of alcohol and GM-CSF on alveolar tight junctions. *Proc Am Thorac Soc* **5**.

Kreuz, S., Joubert, E., Waldmann, K.H. and Ternes, W. (2008) Aspalathin, a flavonoid in *Aspalathus linearis* (rooibos), is absorbed by pig intestine as a C-glycoside. *Nutr Res* **28**, 690-701.

Li, J., Ye, L., Wang, X., Liu, J., Wang, Y., Zhou, Y. and Ho, W. (2012) (-)-Epigallocatechin gallate inhibits endotoxin-induced expression of inflammatory cytokines in human cerebral microvascular endothelial cells. *J Neuroinflammation* **9**, 161.

Lippmann, E.S., Azarin, S.M., Kay, J.E., Nessler, R.A., Wilson, H.K., Al-Ahmad, A., Palecek, S.P. and Shusta, E.V. (2012) Derivation of blood-brain barrier endothelial cells from human pluripotent stem cells. *Nat Biotechnol* **30**, 783-91.

Liu, X., Wang, Z., Wang, P., Yu, B., Liu, Y. and Xue, Y. (2013) Green tea polyphenols alleviate early BBB damage during experimental focal cerebral ischemia through regulating tight junctions and PKC alpha signaling. *BMC Complement Altern Med* **13**, 187.

Lovinger, D.M. and Roberto, M. (2013) Synaptic effects induced by alcohol. *Curr Top Behav Neurosci* **13**, 31-86.

Luissint, A.C., Artus, C., Glacial, F., Ganeshamoorthy, K. and Couraud, P.O. (2012) Tight junctions at the blood brain barrier: physiological architecture and disease-associated dysregulation. *Fluids Barriers CNS* **9**, 23.

Lund-Andersen, H., Kjeldsen, C.S., Hertz, L. and Brondsted, H.E. (1976) Uptake of glucose analogues by rat brain cortex slices: Na^+-independent membrane transport. *J Neurochem* **27**, 369-73.

MacCallum, D.K., Lillie, J.H., Scaletta, L.J., Occhino, J.C., Frederick, W.G. and Ledbetter, S.R. (1982) Bovine corneal endothelium *in vitro*. Elaboration and organization and of a basement membrane. *Exp Cell Res* **139**, 1-13.

Malaeb, S.N., Cohen, S.S., Virgintino, D. and Stonestreet, B.S. (2012) Core

Concepts: Development of the Blood-Brain Barrier. *NeoReviews* **13 (4)**, e241.

Mallikarjuna, K., Shanmugam, K.R., Nishanth, K., Wu, M.C., Hou, C.W., Kuo, C.H. and Reddy, K.S. (2010) Alcohol-induced deterioration in primary antioxidant and glutathione family enzymes reversed by exercise training in the liver of old rats. *Alcohol* **44**, 523-9.

Manzo-Avalos, S. and Saavedra-Molina, A. (2010) Cellular and mitochondrial effects of alcohol consumption. *Int J Environ Res Public Health* **7**, 4281-304.

Marnewick, J., Joubert, E., Joseph, S., Swanevelder, S., Swart, P. and Gelderblom, W. (2005) Inhibition of tumour promotion in mouse skin by extracts of rooibos (*Aspalathus linearis*) and honeybush (*Cyclopia intermedia*), unique South African herbal teas. *Cancer Lett* **224**, 193-202.

Marnewick, J.L., Joubert, E., Swart, P., Van Der Westhuizen, F. and Gelderblom, W.C. (2003) Modulation of hepatic drug metabolizing enzymes and oxidative status by rooibos (*Aspalathus linearis*) and Honeybush (*Cyclopia intermedia*), green and black (*Camellia sinensis*) teas in rats. *J Agric Food Chem* **51**, 8113-9.

Marnewick, J.L., Rautenbach, F., Venter, I., Neethling, H., Blackhurst, D.M., Wolmarans, P. and Macharia, M. (2011) Effects of rooibos (*Aspalathus linearis*) on oxidative stress and biochemical parameters in adults at risk for cardiovascular disease. *J Ethnopharmacol* **133**, 46-52.

Mascotti, K., McCullough, J. and Burger, S.R. (2000) HPC viability measurement: trypan blue versus acridine orange and propidium iodide. *Transfusion* **40**, 693-6.

Masters, J.R., and Stacey, G.N. (2007) Changing medium and passenging lines. *Nat Protoc*. **2**, 2276-2284.

Matter, K. and Balda, M.S. (2003) Signalling to and from tight junctions. *Nat Rev Mol Cell Biol* **4**, 225-36.

Mentor, S. (2015) *In vitro* modulatory effects of fermented rooibos extract (*Aspalathus linearis*) against ethanol-induced effects on the mouse blood-brain barrier.
http://etd.uwc.ac.za.

Mikami, K., Haseba, T. and Ohno, Y. (1997) Ethanol induces transient arrest of cell division (G2 + M block) followed by G0/G1 block: dose effects of short- and longer-term ethanol exposure on cell cycle and cell functions. *Alcohol* **32**, 145-52.

Nitta, T., Hata, M., Gotoh, S., Seo, Y., Sasaki, H., Hashimoto, N., Furuse, M. and Tsukita, S. (2003) Size-selective loosening of the blood-brain barrier in claudin-5-deficient mice. *J Cell Biol* **161**, 653-60.

Nixon, W.C. (1971) The general principles of scanning electron microscopy. *Biol Sc*i **261,** 45-50.

Opuwari, C.S. and Monsees, T.K. (2014) *In vivo* effects of Aspalathus linearis (rooibos) on male rat reproductive functions. *Andrologia* **46**, 867-77.

Oscar-Berman, M. and Marinkovic, K. (2003) Alcoholism and the brain: an overview. *Alcohol Res Health* **27**, 125-33.

Panickar, K.S. and Anderson, R.A. (2011) Effect of polyphenols on oxidative stress and mitochondrial dysfunction in neuronal death and brain edema in cerebral ischemia. *Int J Mol Sci* **12**, 8181-207.

Pardridge, W.M. (2003) Blood-brain barrier drug targeting: the future of brain drug development. *Mol Interv* **3**, 90-105, 51.

Pardridge, W.M. (1995) Transport of small molecules through the blood–brain barrier: biology and methodology. *Adv Drug Deliv **15***, 5–36.

Parsons, O.A. (1996) Alcohol abuse and alcoholism. *Neuropsych Clin Prac* 175–201.

Pawan, G.L. (1972) Metabolism of alcohol (ethanol) in man. *Proc Nutr Soc* **31**, 83-9.

Perez, M., Redondo, J.F., Gallardom A., Aranaz, I. (2014) Chitin and chitosan derivatives. Advances in drug discovery and developments. In: Preparation of chitin and chitosan derivatives having mercapto groups. *Boca Raton: CRC Press Taylor and Francis Group*, pp 132.

Pfeiffer, F., Schafer, J., Lyck, R., Makrides, V., Brunner, S., Schaeren-Wiemers, N., Deutsch, U. and Engelhardt, B. (2011) Claudin-1 induced sealing of blood-brain barrier tight junctions ameliorates chronic experimental autoimmune encephalomyelitis. *Acta Neuropathol* **122**, 601-14.

Pruznak, A.M., Nystrom, J. and Lang, C.H. (2013) Direct central nervous system effect of alcohol alters synthesis and degradation of skeletal muscle protein. *Alcohol* **48**, 138-45.

Raj Narayana, K., Reddy, M.S., Chaluvadi, M.R. and Krishna, D.R. (2001) Bioflavonoids classification, pharmacological, biochemical effects and therapeutic potential. *Ind J Pharm* **33,** 2-16.

Ross, J.A. and Kasum, C.M. (2002) Dietary flavonoids: bioavailability, metabolic effects, and safety. *Annu Rev Nutr* **22**, 19-34.

Ron, D. and Messing, R.O. (2013) Signaling pathways mediating alcohol effects. *Curr Top Behav Neurosci* **13**, 87-126.

Sambuy, Y. (2009) A sideways glance. Alcoholic breakdown of barriers: how ethanol can initiate a landslide towards disease. *Genes Nutr* **4**, 77-81.

Sameer, A.S., Nissar, S., Qadri, Q., Alam, S., Baba, S.M. and Siddiqi, M.A. (2011) Role of CYP2E1 genotypes in susceptibility to colorectal cancer in the Kashmiri population. *Hum Genomics* **5**, 530-7.

Schaffer, S., Eckert, G.P., Schmitt-Schillig, S. and Muller, W.E. (2006) Plant foods and brain aging: a critical appraisal. *Forum Nutr* **59**, 86-115.

Schaffer, S. and Halliwell, B. (2012) Do polyphenols enter the brain and does it matter? Some theoretical and practical considerations. *Genes Nutr* **7**, 99-109.

Schreibelt, G., Kooij, G., Reijerkerk, A., van Doorn, R., Gringhuis, S.I., van der Pol, S., Weksler, B.B., Romero, I.A., Couraud, P.O., Piontek, J., Blasig, I.E., Dijkstra, C.D., Ronken, E. and de Vries, H.E. (2007) Reactive oxygen species alter brain endothelial tight junction dynamics via RhoA, PI3 kinase, and PKB signaling. *FASEB J* **21**, 3666-76.

Schrot, S., Weidenfeller, C., Schaffer, T.E., Robenek, H. and Galla, H.J. (2005) Influence of hydrocortisone on the mechanical properties of the cerebral endothelium *in vitro*. *Biophys J* **89**, 3904-10.

Sharma, R., Gentry, R.T., Lim, R.T. Jr and Lieber, C.S. (1995) First-pass metabolism of alcohol. Absence of diurnal variation and its inhibition by cimetidine after evening meal. *Dig Dis Sci* **40**, 2091-7.

Shin, J.Y., Sohn, J. and Park, K.H. (2013) Chlorogenic acid decreases retinal

vascular hyperpermeability in diabetic rat model. *J Korean Med Sci* **28**, 608-13.

Sommer, W. and Spanagel, R. (2013) Behavioral neurobiology of alcohol addiction. Preface. *Curr Top Behav Neurosci* **13**, v-vii.

Stalmach, A., Mullen, W., Pecorari, M., Serafini, M. and Crozier, A. (2009) Bioavailability of C-linked dihydrochalcone and flavanone glucosides in humans following ingestion of unfermented and fermented rooibos teas. *J Agric Food Chem* **57**, 7104-11.

Steiner, O., Coisne, C., Engelhardt, B. and Lyck, R. (2011) Comparison of immortalized bEnd5 and primary mouse brain microvascular endothelial cells as *in vitro* blood-brain barrier models for the study of T cell extravasation. *J Cereb Blood Flow Metab* **31**, 315-27.

Stenesh, J. (1989) Dictionary of biochemistry and molecular biology. *Wiley and Sons*.

Stevenson, B.R. and Begg, D.A. (1994) Concentration-dependent effects of cytochalasin D on tight junctions and actin filaments in MDCK epithelial cells. *J Cell Sci* **107 (Pt 3)**, 367-75.

Strober, W. (2001) Trypan blue exclusion test of cell viability. *Curr Protoc Immunol* **3**, Appendix 3B.

Tanobe, K., Nishikawa, K., Hinohara, H., Okamoto, T., Saito, S. and Goto, F. (2003) Blood-brain barrier and general anesthetics. *Masui* **52**, 840-5.

Taraboletti, G., D'Ascenzo, S., Borsotti, P., Giavazzi, R., Pavan, A. and Dolo, V. (2002) Shedding of the matrix metalloproteinases MMP-2, MMP-9, and MT1-MMP as membrane vesicle-associated components by endothelial cells. *Am J Pathol* **160**, 673-80.

Thiberge, S., Nechushtan, A., Sprinzak, D., Gileadi, O., Behar, V., Zik, O., Chowers, Y., Michaeli, S., Schlessinger, J. and Moses, E. (2004) Scanning electron microscopy of cells and tissues under fully hydrated conditions. *Proc Natl Acad Sci USA* **101**, 3346-51.

Tiffany, S.T., Carter, B.L. and Singleton, E.G. (2000) Challenges in the manipulation, assessment and interpretation of craving relevant variables. *Addiction* **95 Suppl 2**, S177-87.

Tiwari, V., Kuhad, A. and Chopra, K. (2009) Suppression of neuro-inflammatory signaling cascade by tocotrienol can prevent chronic alcohol-induced cognitive dysfunction in rats. *Behav Brain Res* **203**, 296-303.

Tong, J., Wang, Y., Chang, B., Zhang, D. and Wang, B. (2013) Evidence for the Involvement of RhoA Signaling in the Ethanol-Induced Increase in Intestinal Epithelial Barrier Permeability. *Int J Mol Sci* **14**, 3946-60.

Ulicna, O., Greksak, M., Vancova, O., Zlatos, L., Galbavy, S., Bozek, P. and Nakano, M. (2003) Hepatoprotective effect of rooibos tea (*Aspalathus linearis*) on CCl4-induced liver damage in rats. *Physiol Res* **52**, 461-6.

van Heerden, M.S., Grimsrud, A.T., Seedat, S., Myer, L., Williams, D.R. and Stein, D.J. (2009) Patterns of substance use in South Africa: results from the South African Stress and Health study. *S Afr Med J* **99**, 358-66.

Vauzour, D., Vafeiadou, K., Rodriguez-Mateos, A., Rendeiro, C. and Spencer, J.P. (2008) The neuroprotective potential of flavonoids: a multiplicity of effects. *Genes Nutr* **3**, 115-26.

Vengeliene, V., Bilbao, A., Molander, A. and Spanagel, R. (2008)

Neuropharmacology of alcohol addiction. *Br J Pharmacol* **154**, 299-315.

Villano, D., Pecorari, M., Testa, M.F., Raguzzini, A., Stalmach, A., Crozier, A., Tubili, C. and Serafini, M. (2010) Unfermented and fermented rooibos teas (*Aspalathus linearis*) increase plasma total antioxidant capacity in healthy humans. *Food Chem* **123**, 679-683.

von Wedel-Parlow, M. and Galla, H.J. (2010) A microscopic *in vitro* study of neutrophil diapedesis across the blood-brain barrier. *Micro: Sci, Tech, App Edu, 1161-1167.*

Wegener, J., Sieber, M. and Galla, H.J. (1996) Impedance analysis of epithelial and endothelial cell monolayers cultured on gold surfaces. *J Biochem Biophys Methods* **32**, 151-70.

Wilhelm, I., Molnar, J., Fazakas, C., Hasko, J. and Krizbai, I.A. (2013) Role of the blood-brain barrier in the formation of brain metastases. *Int J Mol Sci* **14**, 1383-411.

World Health Organization (2011) Global Status Report on Alcohol and Health. *Geneva: World Health Organization, 2011*. http://www.who.int/substance_abuse/publications/global_alcohol_report/en/index.html (accessed 25 April 2012).

Wu, D. and Cederbaum, A.I. (2003) Alcohol, oxidative stress, and free radical damage. *Alcohol Res Health* **27**, 277-84.

Yamamoto, M., Ramirez, S.H., Sato, S., Kiyota, T., Cerny, R.L., Kaibuchi, K., Persidsky, Y. and Ikezu, T. (2008) Phosphorylation of claudin-5 and occludin by rho kinase in brain endothelial cells. *Am J Pathol* **172**, 521-33.

Yang, T., Roder, K.E. and Abbruscato, T.J. (2007) Evaluation of bEnd5 cell line as an in vitro model for the blood-brain barrier under normal and hypoxic/aglycemic conditions. *J Pharm Sci* **96**, 3196-213.

Youdim, K.A., Dobbie, M.S., Kuhnle, G., Proteggente, A.R., Abbott, N.J. and Rice-Evans, C. (2003) Interaction between flavonoids and the blood-brain barrier: *in vitro* studies. *J Neurochem* **85**, 180-92.

Youdim, K.A., Shukitt-Hale, B. and Joseph, J.A. (2004) Flavonoids and the brain: interactions at the blood-brain barrier and their physiological effects on the central nervous system. *Free Radic Biol Med* **37**, 1683-93.

APPENDICES

APPENDIX A

Measurement of flavanols (Analysed by the Oxidative Stress Research Centre at CPUT)

Principle of flavanol measurements

The Flavanol analysis was conducted using 4-dimethylaminocinnamaldehyde (DMACA). DMACA reacts with flavanols to generate a significant blue colour, which is interpreted at a wavelength of 640nm.

Chemical preparation

For the quantification of flavanols, chemicals used were: 32% hydrogen chloride-methanol (HCl-MeOH), and 250ml HCl (Saarchem, Cat no.100319 LP) which was added to 750ml MeOH (Saarchem, Cat no.4164080 LC) and thoroughly combined. A total of 0.25g DMACA (Merck, Cat no.822034) was weighed and added to a 500ml HCl-MeOH mixture, and further mixed until dissolved. The standard, catechin, was employed for the measurement of flavanols. Furthermore, 1mM of catechin hydrate standard (Sigma-Aldrich, Cat no.C1251) was set by allowing 0.0145g of catechin hydrate to dissolve in 50ml MeOH. In preparation of the control, 0.0029g catechin hydrate was dissolved in 50ml of MeOH. All solutions were prepared daily for the respective analysis, and subsequently stored at -40°C.

Sample analysis

50µl of the standard catechin, control, and sample was added to the designated wells of a clear 96-well plate. To initiate the reactions, 250µl DMACA was added to all the wells. Subsequently, the plate incubated for 30

min at RT and the resulting absorbance was analysed at a wavelength of 640nm using a Multiskan^{TM} spectrum plate reader.

APPENDIX B

Measurement of flavonols (Analysed by the Oxidative Stress Research Centre at CPUT)

Principle of flavonol measurements

Quercetin was employed in the flavonol analysis as the standard for determining total phenolic content at a wavelength of 360nm.

Chemical preparation

Chemicals utilized for the measurement of flavonols were as follows: 10% EtOH, 95% EtOH, and 0.1% HCl (Saarchem, Cat no.100319 LP) combined in 95% EtOH and 2% HCl. The standard solution was prepared by dissolving 4mg quercetin (Sigma-Aldrich, Cat no.Q0125) in 50ml of 95% EtOH, while for the control sample, a total of 1.5mg quercetin was dissolved in 50ml 95% EtOH. Intermittently, the samples were stored at -40°C.

Samples analysis

12.5µl of the standard quercetin, controls and samples was added to the designated wells of a clear 96-well plate. Furthermore, a 12.5µl solution comprising of 0.1% HCl and 95% EtOH was added to each well. Subsequently, 225µl of 2% HCl was added to each. The plate incubated for 30 min at RT, after which, the Multiskan^{TM} spectrum plate reader was used to measure the absorbance at the wavelength of 360nm.

APPENDIX C

Measurement of phenolics (Analysed by the Oxidative Stress Research Centre at CPUT)

Principle of polyphenolic measurements

This analysis employs the Folin Ciocalteu reagent using gallic acid as the standard in measuring total polyphenols in a sample.

Chemical preparation

Chemicals employed in the quantification of polyphenolic content comprised of: 10% EtOH and Folin Reagent (Merck, Cat no.109001) and 7.5% sodium carbonate ($NaCO_3$) (Sigma-Aldrich, Cat no.223530), kept at RT. In preparation of gallic acid (Sigma-Aldrich, Cat no.G7384), 40mg was dissolved in 50ml of 10% EtOH to generate a 800mg/L stock concentration. In preparing the control, 10mg of the gallic acid was dissolved in 50ml of 10% EtOH solution to generate a final concentration of 200mg/L. Solutions were prepared daily on the respective day of analysis and stored at -40^{o}C.

Sample analysis

25µl of the standard gallic acid, controls, as well as the samples (in triplicate) was added to the designated wells of a clear 96-well plate (Lasec SA, Cat no.PGRE655180). A total of 125µl Folin reagent was added to all wells. The plate incubated for 5 min at RT, before 100µl Na_2CO_3 was added to each well. This was followed by further 2hr incubation in the dark at RT before measuring absorbance with a Multiskan^{TM} plate reader at 760-765nm.

APPENDIX D

Oxygen radical absorbance capacity assay (ORAC) (Analysed by the Oxidative Stress Research Centre at CPUT)

Principle of the ORAC assay

The results signify the ORAC value, which refers to the net protection area under the quenching curve of β-PE (fluorescein) in the presence of an antioxidant. Furthermore, the ORAC value is determined by dividing the area under the sample curve by the area under the trolox curve, with both areas being amended by subtracting the area under the blank curve. A single ORAC unit is allocated as the net protection area provided by 1μM Trolox in final concentration.

Chemical preparation

Chemicals utilized in the ORAC assay were namely: hexane (Saarchem, Cat no.2868040 LC) kept at RT, acetone/water/acetic acid (AWA) solution, which was made up of 700ml acetone (Saarchem, Cat no.1022040 LC), 295ml dH_20 and 5ml glacial acetic acid. A 75mM phosphate buffer with a pH 7.4 was prepared and consisted of two solutions.

For the preparation of solution 1, 1.035g sodium di-hydrogen orthophosphate-1-hydrate ($NaH_2PO_4.H_2O$) (Sigma-Aldrich, Cat no.S9638) was weighed and mixed in 100ml double distilled water (ddH_2O). For the preparation of solution 2, 1.335g di-sodium hydrogen orthophosphate dehydrate ($Na_2HPO_4.2H_2O$), (Merck, Cat no.5822880EM) was weighed and mixed in 100ml of ddH_2O. An amount of 18ml (solution 1) was combined with 82ml (solution 2), to obtain a 75mM, pH 7.4 phosphate buffer. The fluorescein sodium salt stock solution ($C_{20}H_{10}Na_2O_5$) was kept in the dark at 4°C (Sigma-Aldrich, Cat no.F6377). Of the $C_{20}H_{10}Na_2O_5$ solution, 0.0225g was weighed and left to dissolve in 50ml phosphate buffer. 25mg/ml AAPH (2, 2'-Azobis (2-methylpropionamidine) dihydrochloride (Sigma-Aldrich, Cat

no.440914) .0.5M Perchloric acid (PCA) (Saarchem, Cat no.494612), comprised of 195ml dH_20 mixed with 15ml 70% PCA. Trolox (Sigma-Aldrich, Cat no.238831) was utilized as a standard in the measurement of ORAC., whereby 500µM of Trolox standard concentration was generated by mixing 0.00625g of 6-Hydroxy-2,5,7,8-tetra-methylchroman-2-carboxylic acid (Sigma-Aldrich, Cat no.238831) in a 50ml phosphate buffer thoroughly. In preparing the Trolox control (250µM), 0.00312g of 6-Hydroxy-2,5,7,8-tetra-methylchroman-2-carboxylic acid was dissolved in 50ml phosphate buffer. The samples were prepared on ice daily, and stored at -40^{o}C on the day of analysis.

Sample analysis

12ul of the standard Gallic acid, controls and samples (triplicate) was added to the designated wells of a clear 96-well plate. 10µl was added to a volume of 2ml phosphate buffer before being diluted. The final volume of the assay was 200ul. The Multiskan^{TM} plate reader was employed to measure results utilizing an excitation wavelength of 485nm and emission wavelength of 530nm.

APPENDIX E

Ferric reducing antioxidant power assay (FRAP) (Analysed by the Oxidative Stress Research Centre at CPUT)

Principle of the FRAP assay

The FRAP assay utilizes an oxidation/reduction reaction to evaluate the ability of a sample to reduce Fe^{III} to Fe^{II}. Antioxidants give electrons the same way as reductants in oxidation/reduction reactions, thus it is proposed that the FRAP assay is an optimal assay for assessing antioxidant capacity. On the other hand, it does not directly calculate the antioxidant capacity of potential antioxidants, and as there are no free radicals introduced into the system, it lacks methods for comparing antioxidant capacities towards different types of radicals.

Chemical preparation

For the chemical preparation of the FRAP assay, the following was used: 300mM acetate buffer, pH 3.6 containing 1.627g sodium acetate and 16ml glacial acetic acid (Saarchem, Cat no.1021000), as well as distilled water (dH_20), to a final volume of 1L. 40mM HCl and 10mM TPTZ (2, 4, 6-tri [2-pyridyl]-s-triazine) (Sigma-Aldrich, Cat no.T1253) containing 0.0093g TPTZ and 3ml of 40mM HCl. In addition, a 20mM iron (III) chloride hexahydrate (Sigma-Aldrich, Cat no.F2877) solution was produced with 0.054g $FeCl_3.6H_2O$ and 10ml dH_20. L-ascorbic acid (Sigma-Aldrich, Cat no.A5960) was utilized as a standard for this assay. The stock solution of this standard comprised of 1mM L-ascorbic which was attained by dissolving 0.0088g of ascorbic acid in 50ml dH_20. The solutions were prepared daily for the chemical analyses.

Sample analysis

The FRAP solution was prepared by combining the following reagents: 30ml acetate buffer, 3ml TPTZ solution, 3ml $FeCl_3$ solution, and 6.6ml dH_20. 10µl of the standard ascorbic acid, controls and samples (triplicate) was added to the designated wells of a clear 96-well plate. Subsequently, a volume of 300µl FRAP reagent was added to all wells, generating a final volume of 310µl. The plate was placed in the incubating oven for 30 min, set at 37°C and analysed using a Multiskan^{TM} plate reader at a wavelength of 593nm.

APPENDIX F

ABTS (2, 2'-azino-di-3-ethylbenzthialozine sulphonate) Trolox equivalent antioxidant capacity (TEAC) assay (Analysed by the Oxidative Stress Research Centre at CPUT)

Principle of the ABTS (TEAC) assay

ABTS radical cation scavenging assay was established for the determination of the total antioxidant status (TAS) of body fluids. $ABTS^{\bullet+}$, a stable and long-lived cation comes about when methymyoglobin, activated to its ferryl state by hydrogen peroxide incubated with ABTS. Antioxidants are suggested to either scavenge the $ABTS^{\bullet+}$ or impede the radical generating process.

Chemical preparation

7mM ABTS diammonium salt, prepared 24hrs prior to assay (Sigma-Aldrich, Cat no.A1888) and 140mM potassium-peroxodisulphate, freshly prepared (Merck, Cat no.105091) were required for this assay. Incubation was in the dark at RT. The standard utilized in the ABTS assay was Trolox. The standard (1mM) was prepared by combining 0.0125g Trolox (Sigma-Aldrich, Cat no.238831) to 50ml EtOH. In addition, 200µM of the control was prepared by mixing 0.0025g Trolox with 50ml of EtOH. Samples were set up on ice and stored at -40°C.

Sample analysis

25µl of the standard Trolox, controls and samples (triplicate) was added to the designated wells of a clear 96-well plate. EtOH was used to dilute the ABTS solution, 1ml of ABTS to 20ml of EtOH. Furthermore, the absorbance was read at approximately 2 (±0.1). 300µl taken from the ABTS solution, was added to each well. The plate incubated at RT for 30 min, using a Multiskan™ plate reader with a wavelength of 734nm and temperature of 25°C.